IDENTIFYING HIGHER-ORDER NEURONS INVOLVED IN THE TASTE CIRCUITRY IN *DROSOPHILA MELANOGASTER* VIA AN OPTOGENETICS SCREEN

by

Celia Kit Si Lau

B.Sc., The University of British Columbia, 2017

A THESIS SUBMITTED IN PARTIAL FULFILLMENT OF

THE REQUIREMENTS FOR THE DEGREE OF

MASTER OF SCIENCE

in

THE FACULTY OF GRADUATE AND POSTDOCTORAL STUDIES

(Zoology)

THE UNIVERSITY OF BRITISH COLUMBIA

(Vancouver)

April 2020

The following individuals certify that they have read, and recommend to the Faculty of Graduate and Postdoctoral Studies for acceptance, the thesis entitled:

Identifying higher-order neurons involved in the taste circuitry in *Drosophila melanogaster* via an optogenetics screen

submitted by Celia Kit Si Lau in partial fulfillment of the requirements for

the degree of Master of Science

in Zoology

Examining Committee:

Dr. Michael Gordon, Zoology
Supervisor

Dr. Elizabeth Rideout, Cellular and Physiological Sciences
Supervisory Committee Member

Dr. Ben Matthews, Zoology
Additional Examiner

Additional Supervisory Committee Members:

Dr. Vanessa Auld, Zoology
Supervisory Committee Member

Abstract

The ability to detect various tastes greatly enhances survivorship. The detection of nutritious or toxic foods leads to a promotion or inhibition of feeding. Although the characterization of taste-detection at the periphery is extensive, their connection to second-order taste neurons is only beginning to be elucidated. In *Drosophila melanogaster*, we can harness powerful genetic tools to help map out the neuronal circuitry that translates the sensory inputs of taste to the motor commands of feeding. Our objective is to identify higher-order neurons that bridge this sensorimotor circuitry. Understanding how taste information is processed in fruit flies may shed light on how its mammalian counterparts do so, as well.

To accomplish this, we exploit the Sip-Triggered Optogenetic Behaviour Enclosure (STROBE) for its high-efficiency and biological relevance to screen for potential taste neurons. In total, 123 driver lines were selected and screened through optogenetic neuronal activation. One line, in particular, *R70C07-GAL4*, was chosen for the further characterization of its role in feeding inhibition. It predominantly labels two clusters of cell bodies that are bilateral to the brain's primary taste center, the subesophageal zone (SEZ). It is predicted to be responsible for aversive feeding behaviour. To test this, we created split-GAL4 lines to narrow down this population before GRASP and additional optogenetic activation experiments were performed to confirm the identity of neurons that are responsible for altering feeding behaviour. Upon activation, one subset of the lateral SEZ population was revealed to induce significantly aversive feeding behaviour, while another induced appetitive feeding. Surprisingly, both subsets show a positive GRASP signal with both sweet and bitter gustatory receptor neurons (GRNs).

The evidence presented here demonstrates that clear feeding preferences can be made even by activating a population of neurons that communicates with GRNs of opposing valence. This

raises the question of whether feeding decisions are instigated by the relative activity between pathways of opposing taste valences, and if this ratio of activity is already encoded at the level of second-order taste neurons, possibly challenging the extension of the labelled-lines theory into higher-order neurons.

Lay Summary

Making the correct feeding decisions is crucial for survival. Our taste system has evolved to enable us to distinguish between potentially toxic and nutritious foods based on palatability. Thus, our nutrients intake is reliant on the communication between our taste system and motor coordination, yet we know very little about this circuitry. Here, we utilize the common fruit fly, which possesses a taste palette similar to mammals, to help us understand this connection. Like mammals, flies have cells that specialize in the detection of different tastes. Cells that detect sweetness signal to the brain to promote feeding, whereas cells that detect bitterness inhibits feeding. We discovered a novel set of cells that appear to communicate with both sweet- and bitter-sensing cells and are capable of regulating feeding. We suspect that these cells help propagate opposing taste signals in the brain, questioning whether taste information is integrated early in the circuitry.

Preface

This work was executed at UBC's Life Sciences Institute by Celia Kit Si Lau and Dr. Michael Gordon. Dr. Gordon designed and supervised the project. All questions and project directions were constructed in collaboration between Dr. Gordon and I. I performed all the experiments, as well as the quantification and analysis of data using Microsoft Excel, ImageJ and GraphPad Prism6. Pierre-Yves Musso and Pierre Junca were responsible for the shortlisting of hemidrivers used to isolate the lateral SEZ neurons. The immunohistochemistry of gustatory receptor neuron projections in Chapter 1 (Figure 1-2) was reproduced and adapted from Pierre Junca. I used Adobe Illustrator to create all the other figures for the experiments I conducted.

Table of Contents

Abstract ..... **iii**

Lay Summary ..... **v**

Preface ..... **vi**

Table of Contents ..... **vii**

List of Figures ..... **x**

List of Abbreviations ..... **xi**

Acknowledgements ..... **xiii**

Chapter 1: Introduction **1**

1.1 The fly gustatory system 1

1.2 Gustatory organs of the adult fly 2

1.2.1 Peripheral fly taste 2

1.2.2 Post-ingestion fly taste 3

1.3 Taste receptors 3

1.3.1 Bitter and sweet GRs 4

1.3.2 Other classes of taste receptors 5

1.4 Taste projections in the adult fly brain 5

1.5 Modulation of GRN activity 6

1.5.1 Bitter and sweet mixtures 6

1.5.2 Starvation 8

1.6 Higher-order taste processing 9

1.7 Motor coordination of the PER 10

1.8 Fly neurogenetics 12

1.8.1 The GAL4/UAS binary expression system 12
1.8.2 Using the GAL4/UAS system to manipulate neuronal activity 12
1.8.3 Split-GAL4: Achieving sparse labelling of neurons 13
1.8.4 Detecting synaptic connections with GRASP 14
1.9 Real-time monitoring of food interactions in freely moving flies 14
1.9.1 Sip-triggered optogenetic behavior enclosure 16
1.10 Project overview 17
Chapter 2: Materials and methods 24
2.1 Fly stocks 24
2.2 Fly preparation and STROBE experiments 24
2.3 Immunohistochemistry 25
2.4 Statistical analysis 26
Chapter 3: Results 27
3.1 Optogenetic screening of driver lines with the STROBE 27
3.2 The neuronal activation of *R70C07-GAL4* suppresses feeding 28
3.3 *R70C07-GAL4* expression pattern includes leg but not labellar or pharyngeal GRN projections 29
3.4 Split-GAL4s refine the lateral SEZ neuron population 30
3.4.1 Lateral SEZ neuronal subsets are sufficient to inhibit or promote feeding 30
3.4.2 Not all neurons of the lateral SEZ population are sufficient to alter feeding behaviours 30
3.4.3 Two distinct neuronal groups make up the lateral SEZ population 31
3.4.4 Bitter and sweet sensory neurons GRASP with lateral SEZ neurons 32

Chapter 4: Discussion **41**

4.1 Using the STROBE to identify novel taste neurons 41

4.1.1 The targeted efficiency for screening purposes 41

4.1.2 False positives 41

4.2 The dual-modal connectivity of the lateral SEZ neurons 44

4.2.1 Lateral SEZ neurons as interneurons that modulate GRNs 44

4.2.2 Lateral SEZ neurons as part of bitter- and sweet-exclusive pathways 46

4.3 Future directions and experiments 47

Chapter 5: Conclusion **49**

References **51**

Appendices **63**

Appendix A 63

List of Figures

Figure 1-1. Areas of taste detection on the adult *Drosophila*. 19

Figure 1-2. GRNs of opposing valence project to partially distinct regions of the SEZ. 20

Figure 1-3. The orchestration of muscles for PER and ingestion. 21

Figure 1-4. Fly neurogenetic tools. 22

Figure 3-1. Neuronal activation screen using the STROBE. 33

Figure 3-2. Neurons of *R70C07-GAL4* are sufficient in suppressing feeding. 34

Figure 3-3. Subsets of the lateral SEZ population are sufficient in altering feeding. 35

Figure 3-4. Not all lateral SEZ neurons are sufficient in altering feeding. 36

Figure 3-5. Two distinct neuronal groups make up the lateral SEZ population. 38

Figure 3-6. The lateral SEZ population contains neurons proximal to sweet and bitter GRNs. .. 40

Figure 4-1. Model: Lateral SEZ neurons receive GRN input to inform feeding decisions. 48

List of Abbreviations

AD	Activating domain
AKH	Adipokinetic hormone
AMMC	Antennal mechanosensory and motor center
bGLNs	Bitter gustatory local neurons
CAFE	Capillary feeder
DBD	DNA (deoxyribonucleic acid) binding domain
DCSO	Dorsal cibarial sense organ
DEET	Diethyltoluamide
dNPF	*Drosophila* neuropeptide F
DopEc	Dopamine/ ecdysteroid
DSOG1	Descending subesophageal neurons 1
Fdg	Feeding neurons
FlyPAD	Fly proboscis and activity detector
G2N-1	Gustatory second-order neuron 1
$GABA_BRs$	Gamma aminobutyrate B receptors
GFP	Green fluorescent protein
GR	Gustatory receptor
GRASP	GFP reconstitution across synaptic partners
GRNs	Gustatory receptor neurons
GtACR1	Guillardia theta anion channel receptor 1
IN1	Ingestion neurons 1
IR	Ionotropic receptor
MN	Motoneurons
OA	Octopamine
OA-VL	Octopaminergic/ tyraminergic ventral lateral neurons
OA-VPM4	Octopaminergic ventral paired medial 4 neurons
Obp	Odorant binding protein
OptoFLIC	Optogenetic fly liquid-food interaction counter
PER	Proboscis extension response

PI	Preference index
Ppk	Pickpocket
SEZ	Subesophageal zone
sGPN	Sweet gustatory projection neurons
sNPF	Short neuropeptide F
SO	Sense organ
STROBE	Sip-triggered optogenetic behaviour enclosure
t-GRASP	Targeted GFP reconstitution across synaptic partners
TH	Tyrosine-hydroxylase
TH-VUM	Ventral unpaired medial neurons expressing tyrosine hydroxylase
TPN	Taste projection neuron
UAS	Upstream activating sequence
VCSO	Ventral cibarial sense organ
VNC	Ventral nerve cord
7004	*R70C07-p65.AD; VT044519-GAL4.*DBD
7010	*R70C07-p65.AD; R10E08-GAL4.DBD*
7037	*R70C07-p65.AD; R37H08-GAL4.DBD*
7038	*R70C07-p65.AD; R38E08-GAL4.DBD*
7053	*R70C07-p65.AD; R53C05-GAL4.DBD*

Acknowledgements

I wish to express my deepest gratitude to my supervisor Dr. Michael Gordon, who first took me under his wing as an undergraduate volunteer in his lab. His kind support and belief in me have undeniably propelled my academic journey beyond what I could have imagined for myself a few years back. Thank you for your patience and willingness to share your vast wealth of knowledge with me. Thank you also to my supervisory and examining committee, Dr. Vanessa Auld, Dr. Elizabeth Rideout, and Dr. Ben Matthews for all your time and constructive feedback that helped better my research.

Thank you to the past and present members of the Gordon Lab for mentoring and encouraging me. I am so grateful to have worked alongside such amazing scientists. I want to especially thank Meghan, who I can always count on to listen to my troubles and answer my endless questions. I also want to thank Pym and Pierre for always looking out for me and constantly enlightening me. I will truly miss the Gordon Lab family.

Finally, I want to thank my friends and family for their continued love and support- I wouldn't have made it this far without them by my side. Importantly, I would like to recognize the unconditional and selfless care my parents have provided me over the years— your emotional and financial support means everything to me. Thank you for being understanding and never giving up on me. Last but not least, thank you to Herman who I have shared most of my ups and downs with. You believed in my capabilities when I doubted it myself and always pushed me to achieve greater things. Thank you.

Chapter 1: Introduction

1.1 The fly gustatory system

Gustation is a sense that is vitally conserved across the animal kingdom. It determines individual fitness, allowing animals to distinguish between potentially nutritious foods and those that may be toxic. Generally, the sweetness of a substance acts as a cue for the presence of caloric content. Therefore, the detection of sweetness attracts animals to approach and consume (Vosshall et al., 2007). On the contrary, harmful substances in nature are often bitter, triggering avoidance behaviour when it is detected (Glendinning, 2007; Vosshall et al., 2007). However, the exact details of how gustatory information gets relayed through the brain to evoke the corresponding behaviours are still largely unknown. The common fruit fly, *Drosophila melanogaster*, is an excellent model organism for studying these mechanisms since flies detect and utilize mostly the same few taste modalities as humans to form feeding decisions (Singh, 1997). Studying the basic taste circuitry in fruit flies will provide the foundation for building our understanding of how sensory input translates into the proper motor output.

There are about 78,000 neurons in the fruit fly brain, compared to the estimated 86 billion in humans (Azevedo et al., 2009). In addition to their numerically simpler brain with generally stereotyped neural identity and connectivity, the availability of powerful tools catered to genetically manipulating flies has allowed for the discovery of numerous neuronal circuits (Simpson, 2009). Amongst these efforts, the characterization of the peripheral taste detection system in fruit flies has been met with great success.

Taste is detected by bristle structures called sensilla. The presence of sensilla on the legs, proboscis, wing margins, ovipositor (Figure 1-1A) and in the pharynx (Figure 1-1B) allows a fly

to taste with various external and internal body parts (Stocker, 1994). Taste sensilla are similar to mammalian taste buds (Adler et al., 2000); each harbours multiple cells that respond to different taste modalities (Figure 1-1C). Fly sensilla contain several gustatory receptor neurons (GRNs) and one mechanosensory neuron (Stocker, 1994). Each sensillum generally possesses one sweet, one water, and one bitter- and high salt-sensing GRN, along with a fourth GRN of variable tuning (Cameron et al., 2010; Dahanukar et al., 2007; Jaeger et al., 2018; Meunier et al., 2003; Nakamura et al., 2002; Vosshall et al., 2007). Tastants from the external environment travel through the terminal pore of a sensillum and make contact with GRN dendrites. The GRNs then send projections to the brain, with arborizations terminating in the subesophageal zone (SEZ). This compartment of the brain is referred to as the primary taste center, acting as the first point of taste signal relay (Ito et al., 2014; Rajashekhar et al., 1994; Thorne et al., 2004; Wang et al., 2004).

1.2 Gustatory organs of the adult fly

1.2.1 Peripheral fly taste

Due to their small size, flies often walk on their food source. With every step, they can assess the palatability of the substance beneath them. This is made possible by the many taste sensilla that exist on their tarsi, their most distal leg segments (Ling et al., 2014). Additionally, the forelegs have more taste sensilla than the other legs, providing the fly with a clearer idea of the food quality near the mouth (Ling et al., 2014). After receiving attractive taste signals from their legs, a fly will extend its feeding structure, the proboscis, towards the food source. The first point of contact with the food occurs at the labellum, a structure at the distal tip of the proboscis that is most densely decorated with taste sensilla. The labellum consists of two labial palps that are

analogous to the mammalian tongue. This is the last site of taste confirmation before the food is taken up.

1.2.2 Post-ingestion fly taste

If peripheral taste signals indicate palatability, ingestion commences by the separation of the labial palps to expose the entrance of the pharynx. The consumed substance passes by the labral sense organ (LSO) first, then the ventral and dorsal cibarial sense organs (VCSO; DCSO), which are positioned in the pharynx in a bilaterally symmetrical manner (Gendre et al., 2004). Taste sensilla are found within these SOs, suggesting that taste signals are collected after ingestion as well. Indeed, a subset of pharyngeal taste neurons was found to be responsive to sweetness and is capable of driving consumption (LeDue et al., 2015). Interestingly, the number of GRNs present in the SOs decreases with increasing depth into the pharynx. One reason for having more sensitive taste detection early is to prevent harmful substances from travelling farther into the digestive system. Indeed, a recent study suggests that pharyngeal GRNs communicate with neurons that are sufficient in causing regurgitation (Chen et al., 2019).

1.3 Taste receptors

The repertoire of taste receptors expressed in a GRN determines that neuron's tuning to different stimuli (Marella et al., 2006). Originally, a family of gustatory receptor (GR) genes was identified via a bioinformatics approach whereby proteins were grouped based on their structure (Clyne et al., 2000). Although GRs share the same seven-transmembrane domain, this family is quite divergent in regards to tissue-specific expression. This can be attributed to the low amino acid sequence similarity found amongst GRs. The GR gene family currently consists of 60 identified members, encoding 68 proteins that are also expressed in places other than the labellum

(Dunipace et al., 2001; Robertson et al., 2003; Scott et al., 2001). The diversity of this family allows GRNs to detect a variety of tastants.

1.3.1 Bitter and sweet GRs

Since many bitter compounds are toxic, it is crucial to detect them. The receptor requirements appear complex and dependent on the ligand (Lee et al., 2010; Moon et al., 2006). Some GRs, namely Gr66a, Gr32a, Gr33a, Gr89a and Gr39a are broadly required for bitter responses and are thus considered to be the core bitter GRs, while others are more narrowly tuned (Weiss et al., 2011). Caffeine and DEET detection for example, both require Gr66a but the former also requires Gr93a and the latter also requires Gr32a and Gr33a (Lee et al., 2009; 2010). It is hypothesized that the core bitter GRs encode for receptor subunits, required in different combinations to detect an array of bitter compounds.

While Gr66a is expressed in all bitter-sensing neurons, the presence of Gr5a receptors marks another major GRN population, with no overlap between the two (Thorne et al., 2004; Wang et al., 2004). Gr5a-positive neurons are responsive to a variety of sweet compounds (Thorne et al., 2004), but the Gr5a receptor itself is only necessary for the detection of trehalose (Dahanukar et al., 2001). This points to the existence of other receptors that are required for a more complete range of sweetness detection. A set of "sweet GRs" was identified to include the phylogenetically related receptors Gr5a, Gr61a, and Gr64a-f, as well as the more distantly related Gr43a (Dahanukar et al., 2007; Fujii et al., 2015; Jiao et al., 2007, 2008; Robertson et al., 2003; Slone et al., 2007). The sweet GRs are found in subsets of Gr5a-positive neurons, with Gr64f expressed in most, if not all the sugar-responsive GRNs (Dahanukar et al., 2007; Jiao et al., 2007, 2008; Ling et al., 2014).

1.3.2 Other classes of taste receptors

Aside from sweet and bitter neurons, a sensillum can harbour two other GRNs. One of them is a low osmolarity/ water-sensor that expresses Ppk28 (Cameron et al., 2010; Chen et al., 2010) . This receptor is a member of the Pickpocket gene family, encoding a Degenerin/ Epithelial sodium channel (Cameron et al., 2010). Of the 31 Ppks found in fruit flies, some are known to possess other functions. For example, Ppk23 , Ppk25 and Ppk29 are in pheromone-sensing neurons on the legs, helping shape courtship behaviour (Lu et al., 2012; Liu et al., 2012; Starostina et al., 2012; Thistle et al., 2012; Toda et al., 2012).

While the valence of bitter and sweet compounds remains constant regardless of concentration, this is not true for salt. Low concentrations are appetitive, whereas high concentrations are aversive for both fruit flies and mammals, such that salt homeostasis can be maintained (Chandrashekar et al., 2010; Oka et al., 2013). An ionotropic receptor, IR76b is responsible for low- and high-salt detection in distinct GRNs (Hiroi et al., 2004; Lee et al., 2017; Zhang et al., 2013). In particular, the presence of IR76b in Gr64f-positive neurons is required for most low-salt attraction, demonstrating that sweet neurons can be recruited to convey non-sweet appetitive signals. Similarly, Gr66a-positive neurons are recruited for high-salt responses along with a set of glutamatergic GRNs that express Ppk23 (Jaeger et al., 2018).

1.4 Taste projections in the adult fly brain

Following the detection of taste at the periphery, the signals get relayed to the SEZ, a ventral compartment in the fly brain, where most GRN axons terminate. This region is innervated by 3 afferent taste nerves, grouping the axons that come from the same taste organ. Pharyngeal inputs arborize in the anterior dorsal SEZ (Figure 1-2A-C), whereas inputs from the legs (Figure

1-2H-J) run narrowly along the brain's midline, in the back of the brain. Stacked in between these are the taste peg projections and the discrete bitter and sweet projections from the labellum (Figure 1-2D-G; Kwon et al., 2014; Wang et al., 2004). The GRN projection patterns (Figure 1-2K-N) in the SEZ reflect not only which taste organs the signals originate from, but also the taste modality being represented. Grossly, the characteristic projection patterns in the SEZ can be organized into 10 categories, made up of combinations of the five different types of projections (Kwon et al., 2014). The core bitter GRs have distinct leg, pharyngeal and bitter labellar projections (Kwon et al., 2014). Gr5a and Gr64f GRNs have similar sweet labellar arborizations but the latter has additional inputs from the legs and pharynx (Kwon et al., 2014). It is important to note that leg projections have to go through the ventral nerve cord (VNC) first, before reaching the termination point at the SEZ. The projection from each leg targets a designated neuromere of the thoracico-abdominal ganglia. The patterning of VNC projections depends on which GRs are present and from which legs the neurons originate. An extensive and systematic characterization of taste projections in the brain and VNC has been performed by Kwon and colleagues (2014) by comparing the GFP expression of many GR driver lines. This information provides the groundwork for further mapping the taste circuitry in flies.

1.5 Modulation of GRN activity

1.5.1 Bitter and sweet mixtures

In nature, most compounds exist in mixtures. If a sweet substance is tainted with something bitter, it may be more beneficial for the fly to override the sweet attraction and follow the bitter-avoidance behaviour. Indeed, mixtures of sweet and bitter substances can inhibit feeding behaviours (Chu et al., 2014; French et al., 2015; LeDue et al., 2016; Meunier et al., 2003).

Mechanistically, this can occur in two ways: either the bitter compounds directly activate bitter-sensing cells, and/or the bitter compounds inhibit sweet GRNs that can impede the feeding pathway. Both may occur, depending on which bitter compound the fly encounters (French et al., 2015). The detection of L-canavanine is solely reliant on bitter GRN activation, whereas the detection of strychnine in sweet mixtures likely affects the sweet pathway as well. It is hypothesized that bitter compounds interfere with the sugar molecules or with sugar transduction pathways because the presentation of strychnine to flies was not able to suppress artificially-activated sweet GRNs. A candidate modulator of this mechanism is the odorant-binding protein 49a (Obp49a) since it is closely located to the Gr64a sweet receptors and is capable of binding to select bitter compounds. Additionally, Obp49a mutants lack both the usual avoidance of bitter-sweet mixtures and the inhibition of sugar-induced nerve firings (Jeong et al., 2013).

Although the Obp49a pathway has not been fully elucidated, an alternate pathway involving lateral inhibition has been described (Chu et al., 2014). The observation that $GABA_B$ receptors ($GABA_BRs$) are present in sweet-sensing but absent in bitter-sensing taste neurons prompted Chu et al. (2014) to hypothesize that $GABA_BRs$ play a role in taste discrimination. Indeed, when exposed to sucrose and L-canavanine mixtures, flies with chemically blocked or genetically downregulated $GABA_BRs$ have a heightened sensitivity to sucrose and alleviated bitter-suppression on sweet GRN activity (Chu et al., 2014). Importantly, the use of L-canavanine in these experiments allow the results to be attributed to the involvement of a neural circuit-specific modulation of sweet GRNs through $GABA_BRs$, not Obp49a. Moreover, these GABAergic neurons were found to have synaptic connections with both sweet- and bitter-sensing GRN axonal arbours, solidifying the fact that GABAergic interneurons also facilitate the discrimination of sweet and

bitter mixtures (Chu et al., 2014). Although it is important to avoid consuming less-than-optimal food, it may be beneficial to sometimes tolerate these foods during modes of starvation.

1.5.2 Starvation

The satiety and internal state of animals also influence GRN responses. During starvation, sensitivity towards sweetness increases, while sensitivity towards bitterness decreases (Inagaki et al., 2012; Inagaki et al., 2014; Ledue et al., 2016). The former is produced by *Drosophila* neuropeptide F (dNPF) neurons and the release of dopamine onto sweet-sensing, Gr5a GRNs that express the dopamine/ ecdysteroid, DopEc receptor (Inagaki et al., 2012; Srivastava et al., 2005). Possibly acting as a mediator between the dNPF neurons and the Gr5a GRNs is the TH-VUM neuron, which is described as a ventral unpaired medial neuron (VUM) that expresses tyrosine-hydroxylase (TH). Effectively, this is a dopaminergic neuron that increases activity upon food deprivation, which in turn promotes the attraction towards sucrose (Marella et al., 2012).

A more recent paper (Youn et al., 2018) demonstrates a similar phenomenon, but involves a subset of octopaminergic (OA) neurons, called the OA-VPM4 (ventral paired medial) neurons (Busch et al., 2009). Meanwhile, the decreases in bitter sensitivity in starved individuals have been ascribed to a cluster of ventrolateral octopaminergic/ tyraminergic neurons (OA-VLs; Ledue et al., 2016). Starvation reduces the activity of OA-VLs, decreasing its release of octopamine and tyramine onto bitter GRNs, leading to the depotentiation of bitter GRNs. Possible upstream activators of this pathway are short NPF (sNPF) –releasing neurons and adipokinetic hormone (AKH)-releasing neurons, with the latter acting further upstream (Inagaki et al., 2014). Evidence for this model comes from the observation that sNPF mutants and flies with ablated AKH cells lose the starvation-induced reduction of bitter sensitivity and that activating AKH cells did not rescue sNPF mutants (Inagaki et al., 2014). The results agree with previous studies that also link

dNPF and sNPF to internal state-influenced feeding behaviours (Krashes et al., 2009; Wu et al., 2005). Finally, it is interesting to note that, over time, a shift in the reliance on appetitive gustatory cues to internal nutritional feedback occurs. This is critical since the nutritional value and palatability of foods do not always correlate faithfully, as in the case with sugars (Stafford et al., 2012).

1.6 Higher-order taste processing

GRNs are very well characterized, but only a handful of studies have identified downstream neurons. With the help of a large phenotypic screen, the first set of second-order neurons were identified in 2015 (Kain et al). The activation of these neurons was sufficient in triggering the proboscis extension response (PER; Kain et al., 2015). These neurons were named the sweet gustatory projection neurons (sGPNs) because they come into contact with Gr5a (sweet) sensory neurons, and can be activated either by sugar stimulation at the proboscis or by artificial activation of sweet GRNs. The axons of sGPNs terminate in the antennal mechanosensory and motor center (AMMC), suggesting for the first time that the AMMC is part of the higher-order taste processing pathway. Moreover, sGPNs also integrate internal state signals, since sucrose stimulation evokes greater activity in sGPNs of starved flies than compared to sated flies. Interestingly, the large change in activity can occur even without comparable changes in Gr5a neuronal activity. The authors propose that starvation may be causing an amplification of signal in the sGPNs or that starvation alters other signalling pathways that may stimulate the sGPNs (Kain et al., 2015). Another pair of second-order neurons identified were denoted the gustatory second-order neurons (G2N-1s; Miyazaki et al., 2015). These also receive synaptic input from Gr5a GRNs, but unlike sGPNs, the G2N-1s locally arborize and terminate within the ventral SEZ. A third set

of distinct second-order neurons activated by sucrose appear to be specific to pharyngeal inputs (Yapici et al., 2016). These cholinergic neurons were named the ingestion neurons (IN1), and their activation is sufficient to prolong ingestion. With the progression of feeding, flies become sated and the IN1s become insensitive to sucrose stimulation. As a consequence, the drive for sustained ingestion is reduced, demonstrating the ability of IN1 neurons to be modulated by starvation signals (Yapici et al., 2016). More recently, a single pair of bilaterally symmetrical interneurons called bitter gustatory local neurons (bGLNs) was characterized to be activated by bitter tastants and is sufficient in inhibiting attractive behaviour upon receiving signals from bitter GRNs (Bohra et al., 2018). Aside from second-order taste neurons that reside locally in the SEZ, long-range taste projection neurons (TPNs) also exist to relay taste input to regions of the higher brain, specifically the mushroom body, the learning and memory complex of the brain (Kim et al., 2017). Notably, the valence of signals appears to remain consistent and segregated at the level of second-order taste neurons.

1.7 Motor coordination of the PER

Ultimately, taste detection influences feeding decisions. To feed, fruit flies need to extend their feeding structure, the proboscis, to contact and subsequently draw up food with a sipping motion. This motor program is coined the proboscis extension response, PER (Chabaud et al., 2006; Dethier, 1976). Labellar or leg stimulation with a palatable substance triggers the PER, whereas stimulation with a non-palatable substance reduces the PER probability. The robustness of this discreet motor program creates for a good quantitative readout for experiments that aim to identify the mechanisms and neuronal players within the taste circuitry.

PER can be characterized by a series of subprograms, orchestrated by the movement of different feeding muscles located in the head and proboscis of the fly (Figure 1-3). There are two groups of motoneurons (MNs) from the SEZ that control the feeding muscles: those with axons that either run through the labial nerve or the pharyngeal nerve (Rajashekhar & Singh, 1994; Schwarz et al., 2017). Importantly, experiments that separately activated different MNs have demonstrated that execution of the prior subprogram is not necessary for the propagation of the next (Gordon et al., 2009; Schwarz et al., 2017). However, the silencing of different MNs has shown that failure of any individual subprograms leads to an overall failure of PER, with notable temporal interruptions (Gordon et al., 2009; Schwarz et al., 2017). This suggests that the motoneurons directly innervating the muscles responsible for PER are not command neurons themselves but are rather passive effectors that are situated downstream of such neurons.

A potential candidate for command neurons are the feeding (fdg) neurons, a pair of interneurons also located in the SEZ, that upon artificial activation, is sufficient in producing the whole feeding motor program (Flood et al., 2013). Although the fdg neurons do not have overlapping arbours with sweet-sensing GRNs, they do however show neuronal activity when stimulated with sucrose. This was not observed in satiated flies, suggesting that fgd neurons not only integrate gustatory signals but also their metabolic state. Meanwhile, working in the opposite direction of fdg neurons are the descending subesophageal neurons (DSOG1), which help regulate the cessation of consumption through an indirect modulation of proboscis muscles. These neurons are different from fdg neurons however, being non-responsive to gustatory stimulation and satiety. Thus, it was proposed that DSOG1 neurons act as the gate for the translation of taste and satiety signals into motor output. Ultimately, the discovery of these second-order taste neurons brings us

closer to understanding the pathways in which peripheral taste can be translated to produce the proper motor response.

1.8 Fly neurogenetics

The rapid expansion of genetic tools and machinery designed for fruit flies and the broadening use of this organism in more fields of research has dynamically propelled the advancement of both.

1.8.1 The GAL4/UAS binary expression system

One of the most powerful gene manipulation tools used in *Drosophila* is the GAL4/UAS binary expression system (Figure 1-4). The technique borrows two interacting genetic elements from yeast and places it into the fruit fly system (Brand et al., 1993; Duffy, 2002; Fischer et al., 1988). One element is a yeast transcription factor, GAL4. It actively binds to an upstream activating sequence (*UAS*), allowing the transcription of downstream genes (Figure 1-4A). By placing known promoters/ enhancers in front of the *GAL4* gene, one can restrict the location of GAL4 expression to specific cell types. Meanwhile, genes of interest can be inserted downstream of *UAS*, such that the GAL4 protein can drive expression of the effector gene only in the restricted cell types. Further restriction of effector gene transcription can be achieved by introducing a repressor of GAL4 protein, GAL80 (Figure 1-4B, Lee et al., 1999; Lohr et al., 1995). It attaches to GAL4 proteins and physically blocks GAL4-UAS interactions. This system can be used for genetic silencing experiments.

1.8.2 Using the GAL4/UAS system to manipulate neuronal activity

The creation of an extensive collection of GAL4 promotor lines that are under the control of different promotors enabled the labelling of distinct subsets of neurons in the fly brain (Pfieffer

et al., 2008). With large GAL4 driver line collections such as those offered by Janelia Farms and Vienna Drosophila Resource Center, researchers can use different *UAS* effector lines to visualize and directly manipulate neuronal activity. Many studies screen through these large libraries of GAL4 drivers by using specific *UAS* effector lines, such as *UAS-GFP* to examine the expression pattern, or *UAS-Kir2.1* and *UAS-CsChrimson* to silence and activate neuron populations, in order to look for gain- or loss-of-function phenotypes (Baines et al., 2001; Klapoetke et al., 2014). This methodology was used to initially identify candidates in all the aforementioned studies that identified second-order taste neurons. It is worth noting that a more direct way of finding higher-order taste neurons is now available via a genetic tool that can label the post-synaptic partners of neurons (Talay et al., 2017). For this technique to be successful however, a clean and sparse labelling of the presynaptic neuron population must be achieved first. If not, then the labelling of its post-synaptic partners will be muddled with noise. Similarly, it is difficult to identify the exact neurons required for a specific phenotype when broad-expression GAL4 lines are being used. Thus, it is critical to have techniques that can selectively isolate and manipulate neurons within the GAL4 driver lines.

1.8.3 Split-GAL4: Achieving sparse labelling of neurons

The split-GAL4 system is an intersectional genetic tool that allows for the spatial refinement of GAL4 expression (Luan et al., 2006). As the name suggests, the GAL4 protein is divided into two. Only cells that co-express the two parts will have functional GAL4 that allows for effector gene transcription (Figure 1-4C). To accomplish this, the two functionally distinct parts of the GAL4 protein, the DNA-binding domain (DBD) and the activating domain (AD) are separately fused to complementary segments of a leucine zipper and placed under the control of different promoters (Figure 1-4C). These constructs are called hemidrivers. The Zip^{-} and Zip^{+} are

attached at the N-terminus of the *GAL4DBD* and C-terminus of the *GAL4AD*, respectively. The heterodimerizing property of the zip sequences means that the *DBD* and *AD* domains can rejoin in cells where both promoters are active. Thus, the split-GAL4 system is useful for obtaining a sparser labelling of neurons by combining different *GAL4DBD*s and *GAL4AD*s that have partially overlapping expression patterns. This allows for more precise manipulations of neurons in a multitude of ways by using different *UAS-effector* constructs.

1.8.4 Detecting synaptic connections with GRASP

Another frequently used method that also employs split proteins is called GRASP, GFP reconstitution across synaptic partners. It enables the visual detection of cell-cell contact points by expressing complementary halves of membrane-tethered GFP under the control of two different promoters. Individually, these GFP halves do not fluoresce, but when cells expressing the complementary halves are close enough in proximity, GFP will be reconstituted and reporter signal can be visualized. To allow for this concurrent expression of 4 different transgenes, the two functionally similar GAL4/UAS and LexA/LexAop systems were used in parallel (Feinberg et al., 2008; Gordon et al, 2009; Lai et al., 2006). The larger GFP fragment is under the control of *GAL4* and the much smaller fragment is controlled by the *LexA* promoter. Many studies searching for secondary taste neurons use this method to confirm the connection between the candidate neurons and GRNs (Bohra et al. 2018; Kain et al., 2015; Miyazaki et al, 2015).

1.9 Real-time monitoring of food interactions in freely moving flies

Conducting behavioural tests is an indispensable step to identifying novel neurons within the taste circuitry. Common ways to evaluate feeding and tasting behaviour in flies is by examining PER probability and performing two-choice preference tests and CAFE (Capillary Feeder) assays.

There are caveats to these assays however: PER tests require the physical-restraint of the flies, which may alter their natural taste-evoked behaviours; two-choice assays result in only the qualitative assessment of consumption preferences based on colour- or radioactive-labelled tastants which could be excreted before taking measurements; and CAFE assays provide volumetric measurements of food consumption by relying on the use of liquid tastants stored in capillaries, a food context and consistency that is not generally found in a fly's natural diet. In particular, the latter two methods have low resolution, capturing only end-point behaviour data (Ja et al., 2007; Meunier et al., 2003; Moon et al., 2006; Wong et al., 2009). The limitations of these existing assays prompted the development of the flyPAD (fly Proboscis and Activity Detector), which can record the way freely-moving fly interact with non-liquid food in a multiplex setup (Itskov et al., 2014). Individual flies are tested in arenas where food is placed on top of one electrode and is surrounded by another; together, it is referred to as a "channel." The small scale and proximity of the two connected electrodes mean that when the fly touches the food with its proboscis, it will be simultaneously standing on the second electrode. These channels act as a sensor because when the connection is made, there is a change in capacitance between the electrodes and is digitally recorded as a food-interaction event. The flyPAD measures three different parameters: number and duration of food interactions and number of activity bouts (representing how frequent the fly approaches the food). It is important to mention that the two former parameters strongly correlate to the amount of food ingested, and can represent actual feeding events. With two different food choices presented in each arena, the FlyPAD can determine a fly's preference for either food. As such, this device can be used to measure the effects of genetic manipulations on feeding behaviour. For example, quantifying feeding preferences in flies with

silenced neurons can help researchers identify its necessity in producing feeding behaviours (Steck et al., 2018).

1.9.1 Sip-triggered optogenetic behavior enclosure

While neuronal silencing experiments can simulate the natural situation where a fly does not encounter a stimulus, artificial activation experiments are more difficult to interpret since they often lack behavioural relevancy. Therefore, to more accurately evaluate the sufficiency of candidate taste neurons in affecting feeding, the coupling of physical food interaction and neuronal activation is crucial. A few devices have been designed to address this: the optoFLIC (optogenetic Fly Liquid-Food Interaction Counter), optoPAD (optogenetic Proboscis Activity Detector) and STROBE (Sip-Triggered Optogenetic Behaviour Enclosure) (Klapoetke et al., 2014; May et al., 2019; Musso et al., 2019; Steck et al., 2018). Both the optoPAD and STROBE operate on the existing flyPAD hardware, while the STROBE utilizes a different algorithm for tracking food interactions. With specified promoters driving the expression of either anion channelrhodopsin (GtACR1) or red-shifted channelrhodopsin (CsChrimson), the flies being tested will be able to receive neuronal inhibition or activation through light illumination (Klapoetke et al., 2014; Mohammad et al., 2016). Particularly in the STROBE, detected food interactions trigger the onset of light illumination, with latencies down to tens of milliseconds. Thus, activation by the STROBE should mimic activation by chemical taste detection.

Similar to the flyPAD, food interactions recorded by the STROBE are capable of representing consumption behaviour, as the results can be confirmed with dye-consumption assays (Musso et. al., 2019). However, because conventional consumption assays are less sensitive than the STROBE, it is expected that only results with a greater deviation from being preference-neutral can be replicated with consumption assays.

A typical STROBE activation experiment involves having two food sources placed on two distinct channels, with only one of those channels being paired to the onset of light (Musso et al., 2019). When flies are given the choice between two identical foods (e.g. tasteless agar), their preference for the food on the light-paired channel provides a measure of the valence of the neurons being activated. Upon activating sweet GRNs in flies, a strong attraction towards the light-paired option is produced, quantified as a positive preference index (PI; Musso et al., 2019; Jaeger et al., 2018). Conversely, activation of bitter GRNs produces strong avoidance (negative PI). The STROBE has also been used to measure the effects of mushroom body neurons on feeding, demonstrating its efficacy in activating higher-order circuits (Musso et al., 2018). Importantly, these experiments relay general information about the valence of signals from activated neuron populations that can be used to quickly screen through and select candidate taste neurons. Activated neuron populations that evoke an avoidance of the light-paired choice may naturally play a role inhibiting feeding, while those that evoke an attraction towards the light-paired choice may promote feeding. Since the STROBE can test multiple flies in parallel, it offers relatively high-throughput readout for screens that are searching for novel taste neurons, as compared to other labour-intensive screens that rely on immunohistochemistry or PER quantification (Kain et al., 2015; LeDue et al., 2016).

1.10 Project overview

The characterization of taste-detection at the periphery is extensive, but their connection to second-order taste neurons is only starting to be elucidated. Our objective is to identify higher-order neurons that take part in the taste sensorimotor circuitry. We hypothesize that optogenetically

activating small populations of neurons in the *Drosophila melanogaster* brain will reveal neurons that increase or decrease feeding behaviour.

To accomplish this, we exploit the STROBE for its high efficiency and biological relevance to screen for potential taste neurons. In total, 123 driver lines were selected and screened through optogenetic neuronal activation. One line, in particular, *R70C07-GAL4*, was chosen for the further characterization of its role in feeding inhibition. It predominantly labels two clusters of cell bodies in the brain that are bilateral to the SEZ, predicted to be responsible for aversive feeding behaviour. To test this, we created split-GAL4 lines to narrow down this population. GRASP and optogenetic activation experiments were then performed on these sparsely labelled lines. Upon activation, one subset of the lateral SEZ population was revealed to induce significantly aversive feeding behaviour, while another induced appetitive feeding. Surprisingly, both showed positive GRASP signal both bitter and sweet GRNs. The evidence presented here points to the existence of functional connections between these local lateral SEZ neurons and both sweet and bitter GRNs. Moreover, it demonstrates that clear feeding preferences can made even by activating a population that communicates with GRNs of opposing valence. Genetic silencing, calcium imaging and pre-synaptic labelling experiments will answer remaining questions on these neurons' necessity for feeding, level of activity in response to palatable and non-palatable foods, as well as the directionality of its communication with GRNs.

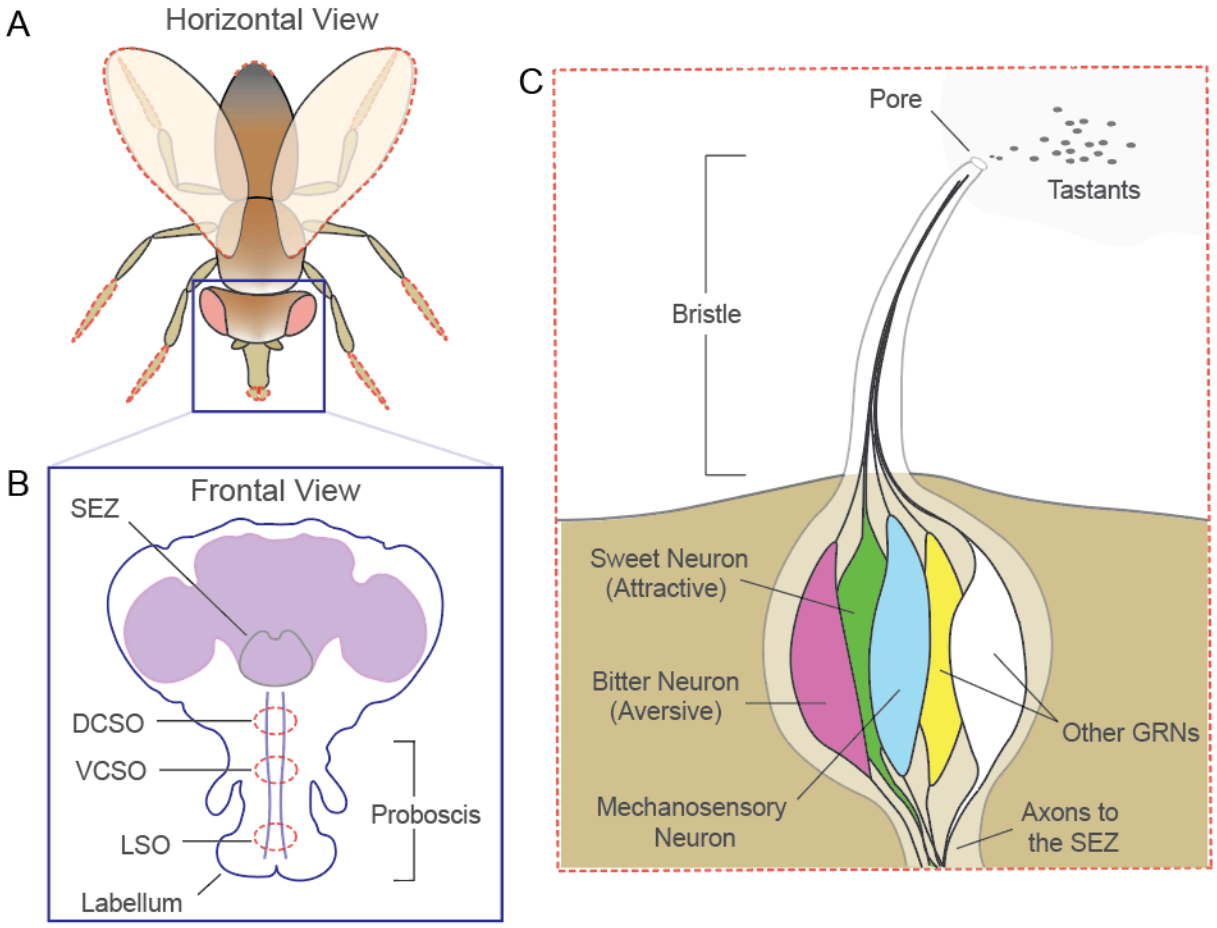

Figure 1-1. Areas of taste detection on the adult *Drosophila*.

(**A**) Schematic of a fruit fly, outlining areas of taste detection at the periphery (dotted red outline). (**B**) Taste detection also occurs within the three pharyngeal sense organs (SO; dotted red outline), the dorsal cibarial (DCSO), ventral cibarial (VCSO) and labral sense organ (LSO). Taste detection signals are first relayed to the brain (purple) to a region called the subesophageal zone (SEZ; grey outline). (**C**) Schematic of a taste sensillum that typically houses a mechanosensory neuron and a few GRNs, depending on the sensillum-type. Sweet-responsive GRNs can induce attractive behaviour, whereas bitter-responsive GRNs can induce aversive behaviour in fruit flies.

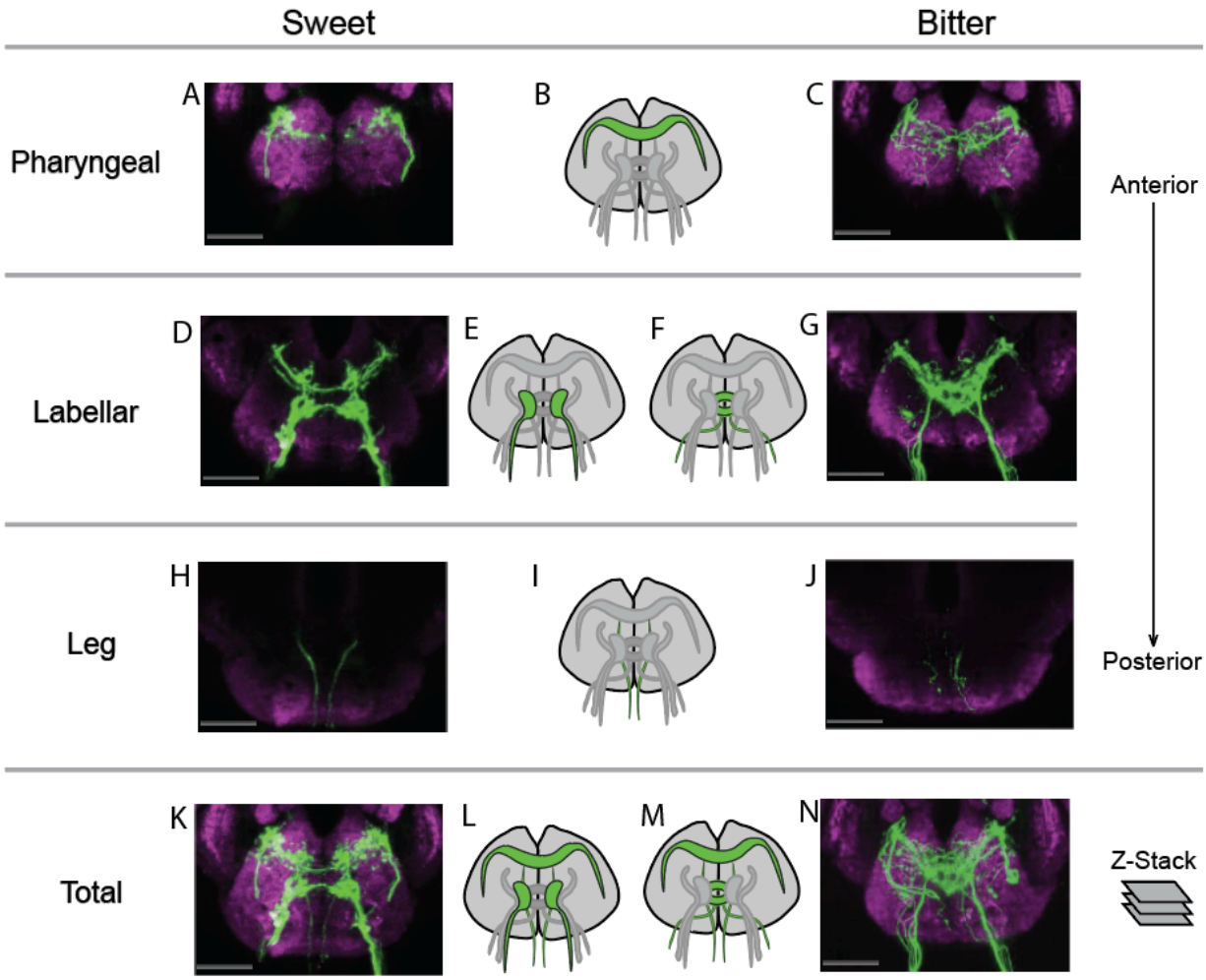

Figure 1-2. GRNs of opposing valence project to partially distinct regions of the SEZ.
Confocal images and schematics of GRN projections to the SEZ. Brains are stained to detect GFP expressed in GRNs (green) and the neuropil (nc82 in magenta). Different focal planes show projections from the pharynx (**A-C**), labellum (**D-G**), legs (**H-J**) and total projections (**K-N**). Sweet neurons express GFP driven by *Gr64f-GAL4* (**A, D, H, K**). Bitter neurons express GFP driven by *Gr66a-GAL4* (**C, G, J, N**). The total Z-stack of sweet (**K, L**) and bitter (**M, N**) projections are distinct due to differences in the labellar projections. All scale bars, 50 µm. (Adapted from Pierre Junca and Kwon et al., 2007).

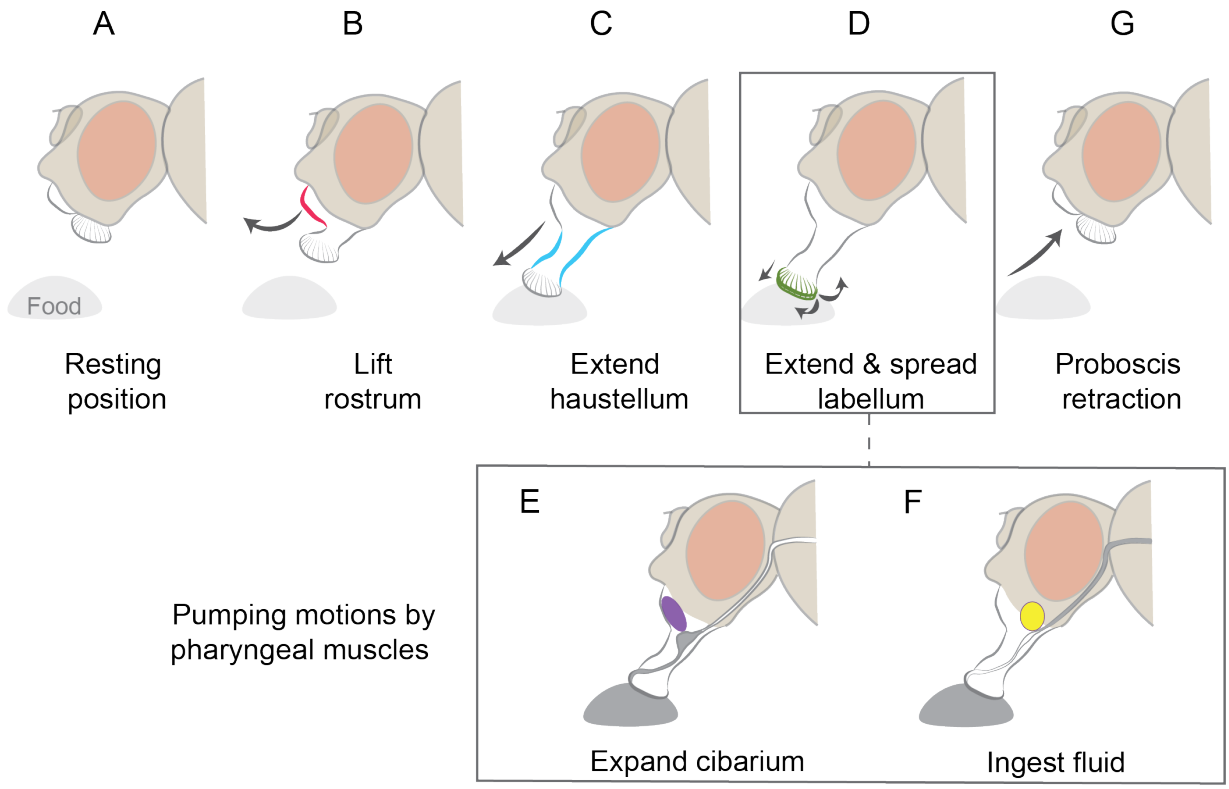

Figure 1-3. The orchestration of muscles for PER and ingestion.

(**A**) The resting position of a fly's head before the onset of the proboscis extension response (PER). Upon the detection of food, the PER commences with (**B**) the lifting of the rostrum**,** followed by (**C**) an extension of the haustellum. Then, (**D**) the labellum extends and spreads apart to allow for food intake. (**E**) Pharyngeal muscles (purple and yellow) expand the cibarium, draw up food and (**F**) usher the food to the esophagus. (**G**) The proboscis fully retracts, marking the completion of a feeding event. (Adapted from Flood et al., 2013; Gordon et al., 2009; Manzo et al., 2012).

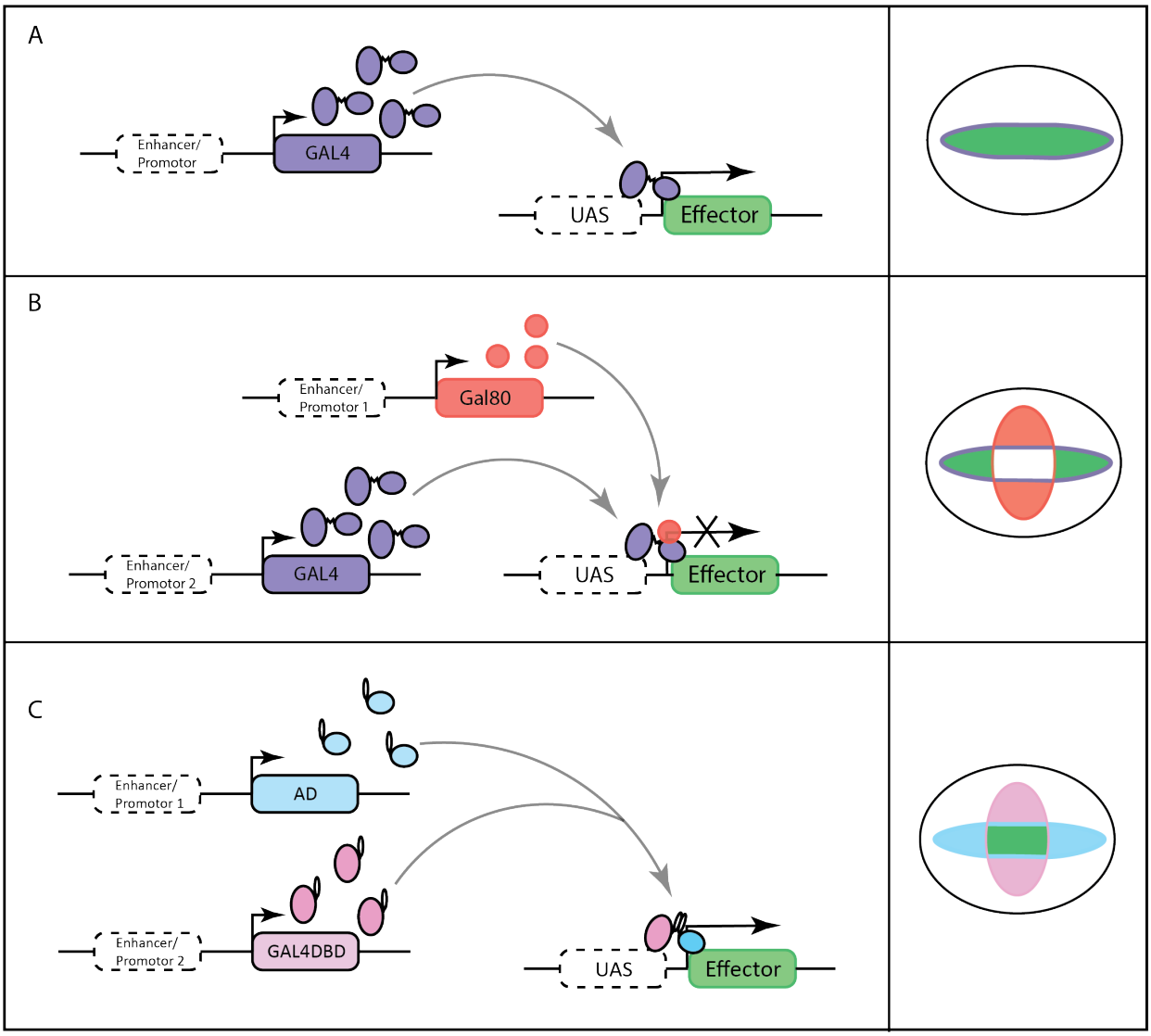

Figure 1-4. Fly neurogenetic tools.

(**A**) GAL4/UAS: The GAL4 transcription factor (TF) is placed under the control of a promoter that specifies its location of expression. Wherever the GAL4 TF is expressed, it can bind and initiate transcription of the *effector* gene in those cells only. (**B**) GAL80 repression: Restriction of the transcription of the *effector* is conferred in cells where GAL80, a GAL4 repressor protein is also expressed. A temperature-sensitive version is also available, $GAL80^{ts}$, where the repression of GAL80 on the GAL4 TFs can be relieved at around 30° Celsius. (**C**) Split-GAL4: The GAL4 protein can be divided into its DNA-binding domain and activating domain, and individually driven by different promoters. These constructs are called hemidrivers. Each domain is engineered with a complementary side of a leucine zipper, such that when both hemidrivers are present, the

domains can rejoin and create functional GAL4s. Schematics on the right represent the outcome of expression pattern using the respective genetic tools. Coloured patches represent the presence of the corresponding proteins. Green represents the expression of the *effector* as a result.

Chapter 2: Materials and methods

2.1 Fly stocks

Fly stocks were raised on standard cornmeal fly food at 25°C in 70% humidity. For optogenetic activation experiments, we used *20XUAS-IVS-CsChrimson.mVenus* (in attP40 insertion site) from the Bloomington Drosophila Stock Center (BDSC, stock number: 55135). The full list of enhancer/trap lines used for the optogenetic activation screen is listed in Appendix A. To create the split-GAL4 lines, the following hemidrivers were used: *R10E08-GAL4.DBD* (69792); *R37H08-GAL4.DBD* (68786); *R38E08-GAL4.DBD* (69427); *R53C05-GAL4.DBD* (69451); *R70C07-p65.AD* (71122); *VT044519-GAL4.DBD* (75123). For GRASP experiments, we used *Gr5a-LexA::VP16, UAS-CD4::spGFP1-10, LexAop-CD4::spGFP11* (Gordon and Scott, 2009) and *Gr66a-LexA::VP16* (Thistle et al., 2012).

2.2 Fly preparation and STROBE experiments

For the preparation and duration of the experiments, flies were maintained at 25°C in 70% humidity. Female flies were collected 2-5 days after eclosion and allowed to recover in fresh vials containing standard medium for at least 1 day before transferring into aluminum foil-covered vials containing 1 ml standard medium with either 1 mM of all-*trans*-retinal (retinal-fed flies) or supplemented with 99% ethanol (the solvent for the all-*trans*-retinal reconstitution) at the same volume (non-retinal-fed control) for 2 days. Afterwards, flies were starved for 20-24 hours in similar conditions, except the standard medium was replaced by 1% agar, such that their ± all-*trans*-retinal diets are maintained throughout the 3 days.

Immediately prior to the start of the STROBE assays, all flies were subjected to 1 hour of water-deprivation to promote food interaction. Loaded into both channels of each arena are 4 µl of 1% agar with sucrose (for the activation of split-GAL4 lines to promote food interactions) or without sucrose (for the activation screen). To initiate each experiment, the acquisition on the STROBE software is initiated before flies are individually placed in each arena via mouth aspiration. Experiments were continued for 1 hour and the preference index were calculated as: (Interactions with Food 1 – Interactions with Food 2)/ (Interactions with Food 1 + Interactions with Food 2). The red LED is always associated to the left channel, with Food 1. Details of the STROBE system, including the design and programming can be found in Musso and colleagues' paper (2019).

The sucrose (S7903-1KG), agar (A1296-1KG) and all-*trans*-retinal (R2500-1G) used for these experiments were purchased from Sigma-Aldrich.

2.3 Immunohistochemistry

Brain immunohistochemistry was performed following a previously described method (Chu et al., 2014). To stain flies with the *UAS-CsChrimson* transgene, the primary antibodies used are: mouse anti-brp (1:50, Developmental Studies Hybridoma Bank #nc82) and rabbit anti-GFP (1:1000, Invitrogen), with secondary antibodies: goat anti-rabbit Alexa-488 (A11008, Invitrogen) and goat anti-mouse Alexa-546 (A11030, Invitrogen). For GRASP experiments, the following were used as primary antibodies: mouse anti-GFP (1:100, Sigma-Aldrich, G6539), rat anti-DN-cadherin (1:25, DSHB DNEX#8), and rabbit anti-DsRed (1:1000, Clontech #632496) with secondary antibodies: goat anti-mouse Alexa-488 (A11029, Invitrogen), goat anti-rat Alexa-568 (A11077, Invitrogen) and goat anti-rabbit Alexa-647 (A21245, Invitrogen).

All images were acquired using a Leica SP5 II Confocal microscope. All images were taken sequentially with a line-scanning speed of 200 Hz and a resolution of 1024 × 1024 pixels. Images with a magnification of 25x was with a water immersion objective with a Z-stack step size of 1 μm, while 63x was with an oil immersion lens and a step size of 0.5 μm.

2.4 Statistical analysis

Statistical tests were performed using GraphPad Prism six software. Descriptions and results of each test are provided in the figure legends, along with sample sizes.

All replicates within each condition are different fly individuals that are genetic replicates. The behavioural data shown are from at least two experiments, where the control and test flies were always tested together. In cases where the minimum number of interactions (10) was not met, the individual fly's data were removed.

Chapter 3: Results

3.1 Optogenetic screening of driver lines with the STROBE

By artificially activating and silencing parts of the feeding circuit in flies and observing their behaviour, we can understand how feeding is regulated and which neurons may be involved. The STROBE, which temporally couples optogenetic activation with fly feeding, can mimic the natural neuronal activation a fly would experience as they would normally taste and feed (Musso et al., 2019). The experimental setup is simple yet highly versatile in manipulating neurons at both sensory and higher-order levels. This allows the STROBE to be exploited for high-throughput screens searching for novel players in the taste circuitry. Since there is a lack of knowledge on how taste information is relayed beyond GRNs, we sought to elucidate this pathway by using the STROBE to screen different neuron populations for their sufficiency in altering feeding behaviour.

To start, thousands of split-GAL4 driver lines were visually assessed based on the expression pattern of their GAL4 counterparts. The availability of split-GAL4 versions makes it easier to gain refined control over neuronal subsets later on. In total, 123 driver lines that label neurons not yet implicated in taste were shortlisted and screened in the STROBE (Figure 3-1A). Flies expressing CsChrimson under the control of those GAL4 drivers were fed with all-*trans*-retinal 3 days prior to the experiment to make CsChrimson functional, whereas control flies of the same genotype were not fed with all-*trans*-retinal. Flies were individually introduced into STROBE arenas that contain two choices of identical plain agar (1%), where only the interaction with one of the choices triggers a red LED light that excites neurons with functional CsChrimson (Figure 3-1B). Since control flies do not have photoactivation capability, the food choices should be effectively the same to them. Therefore, a neutral preference index, where flies interact

relatively equally on either food choices is expected. Meanwhile, a fly exhibiting a positive PI means it preferred to interact with the food option that is paired with light activation, suggestive of an appetitive response (Figure 3-1A). Conversely, a negative PI means the fly avoided the neuronal-activating option, suggestive of an aversive behaviour (Figure 3-1A). It is considered the avoidance of the light-triggering choice rather than attraction to the other because the decreased interactions with the light-triggering choice is not generally accompanied by increased interactions with the non-light-triggering choice.

In total, 6 of the GAL4s significantly promoted feeding behavior upon neuronal activation, and 34 significantly inhibited feeding behaviour. Over the course of the 60-minute assays, control flies interact with each food choice between 20-400 times (Appendix A). While this range seems large, each fly's number of interactions with either food choices are similar, meaning that they do not have a preference. On the other hand, this number can reach the thousands for flies that were strongly attracted to interacting with the light-activating choice (Appendix A). Moreover, flies that demonstrate a preference towards either food choices generally make that choice within the first 20 minutes (Appendix A).

3.2 The neuronal activation of *R70C07-GAL4* suppresses feeding

From the screen, we identified *R70C07-GAL4* to be a driver line of interest, as it showed strong feeding aversion upon neuronal activation (Figure 3-1A). We optogenetically activated this driver again, but replaced the 1% agar in each channel with 1% agar plus 100 mM sucrose to increase the flies' overall attraction to both sides (Figure 3-2B). By increasing the total number of interactions, we can better define the suppressive effects on the light-triggering choice. The comparison between non-retinal-fed and retinal-fed flies that have functional CsChrimson under

the control of *R70C07-GAL4* reveals a significant drop in the number of interactions with the light-triggering choice (Figure3-2D). This was a consequence of retinal-fed flies showing a reduced preference for the light-triggering choice during the 60-minute experiments, while the control flies maintained a minimally positive preference index (Figure 3-2C). Observing this clear deviance from typical feeding behavior, we hypothesized that neurons within the population labelled by *R70C07-GAL4* may be responsible for the inhibition of feeding when they are activated in the natural context.

3.3 *R70C07-GAL4* expression pattern includes leg but not labellar or pharyngeal GRN projections

The strong feeding aversion produced by the activation of R70C07 neurons led us to suspect that this driver may be labelling GRNs as well as central neurons. Immunohistochemistry of the brain of *R70C07-GAL4> CsChrimson* flies revealed 15 strongly labelled cell bodies that are clustered laterally on either side of the SEZ, with arbours that amalgamate into a vertically compacted horseshoe pattern that dips in the center and curves dorsally on the sides (Figure 3-2A). Weaker and sparser projections were also observed in the antennal lobes and superior medial protocerebrum. Importantly, the absence of labellar and pharyngeal taste projections suggests that GRNs from those taste organs are not labelled by this driver (Figure1-2; Figure 3-2A). Conversely, stereotypical leg GRN projections were observed in the SEZ, along with weak leg processes that project along the VNC midline, suggesting that taste neurons in the legs may be labelled by this driver (Stocker, 1994). It is possible that these leg projections contributed to the feeding aversion.

3.4 Split-GAL4s refine the lateral SEZ neuron population

3.4.1 Lateral SEZ neuronal subsets are sufficient to inhibit or promote feeding

To narrow down the exact neurons that may be involved in producing the observed aversive feeding behavior, split-GAL4 lines were created by combining the *R70C07-p65.AD* hemidriver with other DBD hemidrivers (Figure 3-3; Figure 3-4). Subsequently, we performed immunohistochemistry and optogenetic activation assays to characterize the neurons labelled by these split-GAL4s. Interestingly, when presented with the same 1% agar plus 100 mM sucrose choices, retinal-fed flies with *R70C07-p65.AD; R37H08-GAL4.DBD* (*7037*) driving *CsChrimson* (Figure 3-3B-C) showed a decreased preference for the light triggering choice, while *R70C07-p65.AD; R53C05-GAL4.DBD flies* (*7053*; Figure 3-3E-F) strongly preferred the light side. Aside from prominently labelling 6 of the lateral SEZ neurons, *7037* also labels two pairs of neurons that are situated on top of the antennal lobes (Figure 3-3A; Figure 3-5B). On the other hand, *7053* labels 14 lateral SEZ neurons (Figure 3-3D; Figure3-5C). Some staining is also present in the protocerebrum but we are unable to trace these processes back to any cell bodies. Nonetheless, both split-GAL4 combinations successfully eliminated leg projections in the SEZ and most of the VNC projections (Figure 3-3A, D), suggesting that the observed feeding phenotypes are due to mechanisms in the brain as opposed to the periphery. .

3.4.2 Not all neurons of the lateral SEZ population are sufficient to alter feeding behaviours

Not all split-GAL4s had atypical feeding preferences when activated in the STROBE (Figure 3-4). *R70C07-p65.AD; R38E08.DBD* (*7038*), *R70C07-p65.AD; R10E08.DBD* (*7010*) and *R70C07-p65.AD; VT044519.DBD* (*7004*) all successfully isolated subsets of the lateral SEZ neurons (Figure 3-4A, D, G). However, the activation of *7038* and *7010* neuronal subsets did not

significantly alter the PI or the number of interactions on the light-triggering food choice as compared to the non-retinal-fed controls (Figure 3-4B-C, E-F). Close examination of the Z-stacks reveals that *7038* also labels similar protocerebral processes as *7053* (Figure 3-4A; Figure 3-3D). Although we are unsure of whether the lines label the same lateral SEZ neurons, we argue that the protocerebral processes may not be responsible for driving the increase in feeding behaviour in the *7053* line, given that the optogenetic activation of *7038* did not significantly change feeding behaviour. As for *7010*, we see additional faint processes near the antennal lobe region, which we are also unable to trace back to any other cell bodies. Lastly, *7004* did show a statistically significant difference in feeding behaviour between the non-retinal-fed and retinal-fed group (Figure 3-4H, I). However, the very small PI for the experimental group has questionable biological relevance. Altogether, our data suggests that the original lateral SEZ cluster contains subsets that either increase feeding behaviour and decrease feeding behaviour.

3.4.3 Two distinct neuronal groups make up the lateral SEZ population

Intriguingly, through the immunostaining of *7004*, we discovered that the neurons labelled by this split-GAL4 follow a different set of tracts (Figure 3-5D) to form a deeper network within the SEZ than the other split-GAL4s (Figure 3-5B-C). It was originally missed when examining the *R70C07-GAL4* expression because the central arborizations would have appeared to be part of one main network (Figure 3-5A). The *7004* split-GAL4 neurons are more anteriorly located, and project distinctly through the labellar nerve "tunnels," into the posterior SEZ, where the arbours remain mostly ipsilateral. Re-examination of *R70C07-GAL4* expression (Figure 3-5A-B) shows that *7004* labels all of the neurons that have this patterning (Figure3-5G-H). Therefore, we conclude that this subset of neurons is not responsible for the feeding inhibition produced by the optogenetic activation of *R70C07-GAL4.*

3.4.4 Bitter and sweet sensory neurons GRASP with lateral SEZ neurons

Given that the *7037*- and *7053*-labelled neurons are capable of supressing and promoting feeding, we next wondered whether those neurons indeed take part in the aversive and appetitive taste pathways. We used the GRASP technique to check whether the lateral SEZ neurons are in close proximity with sweet and bitter GRNs (Figure 3-6). One half of the split-GFP reporter (*lexAop-spGFP11*) was targeted to either the bitter- or sweet-sensitive GRNs using *Gr66a-LexA* or *Gr5a-LexA* as a driver; and the other half of the split-GFP reporter (*UAS-spGFP1-10*) was targeted to the lateral SEZ neurons with either the *7037* (Figure 3-6A-D), *7053* (Figure 3-6E-H) or *7038* (Figure 3-6I-L) drivers. Unexpectedly, bitter and sweet GRASP signals were detected for all three split-GAL4 lines, suggesting that bitter and sweet GRNs interact with at least one of the neurons labelled in each subset. These results led us to postulate that the lateral SEZ population contains bitter- and sweet-sensitive local neurons that are immediately downstream of GRNs.

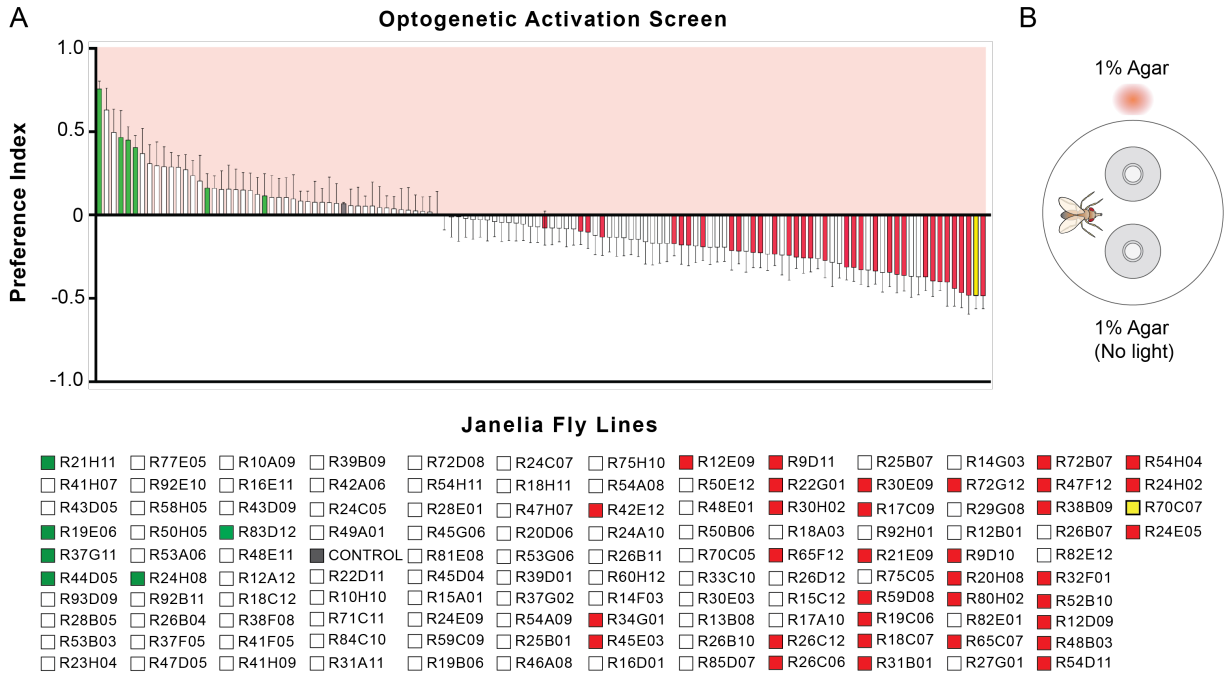

Figure 3-1. Neuronal activation screen using the STROBE.

(**A**) Mean feeding preferences of GAL4 driver lines that were tested in the STROBE; full dataset available in Appendix A. A positive PI (green bar) and a negative PI (red bar) indicate a statistically significant preference for, and preference away from the light-activating channel, respectively, as compared to their genetically identical, non-retinal-fed control (data not shown); non-significant data (white bars) are also displayed (supporting *t*-test results for each genotype also presented in Appendix A). The mean PI (grey) of all the non-retinal-fed control flies for each genotype are displayed as reference only and is not statistically relevant in this context; calculated by averaging the PIs of the controls across all the genotypes tested. *R70C07-GAL4* (yellow bar) was chosen for further characterization due to its strongly aversive behaviour. (**B**) Experimental setup: each STROBE arena contains two channels containing 1% agar, only interactions with the one channel will trigger red light activation (Top). Values represent mean ± SEM. n = 10–37.

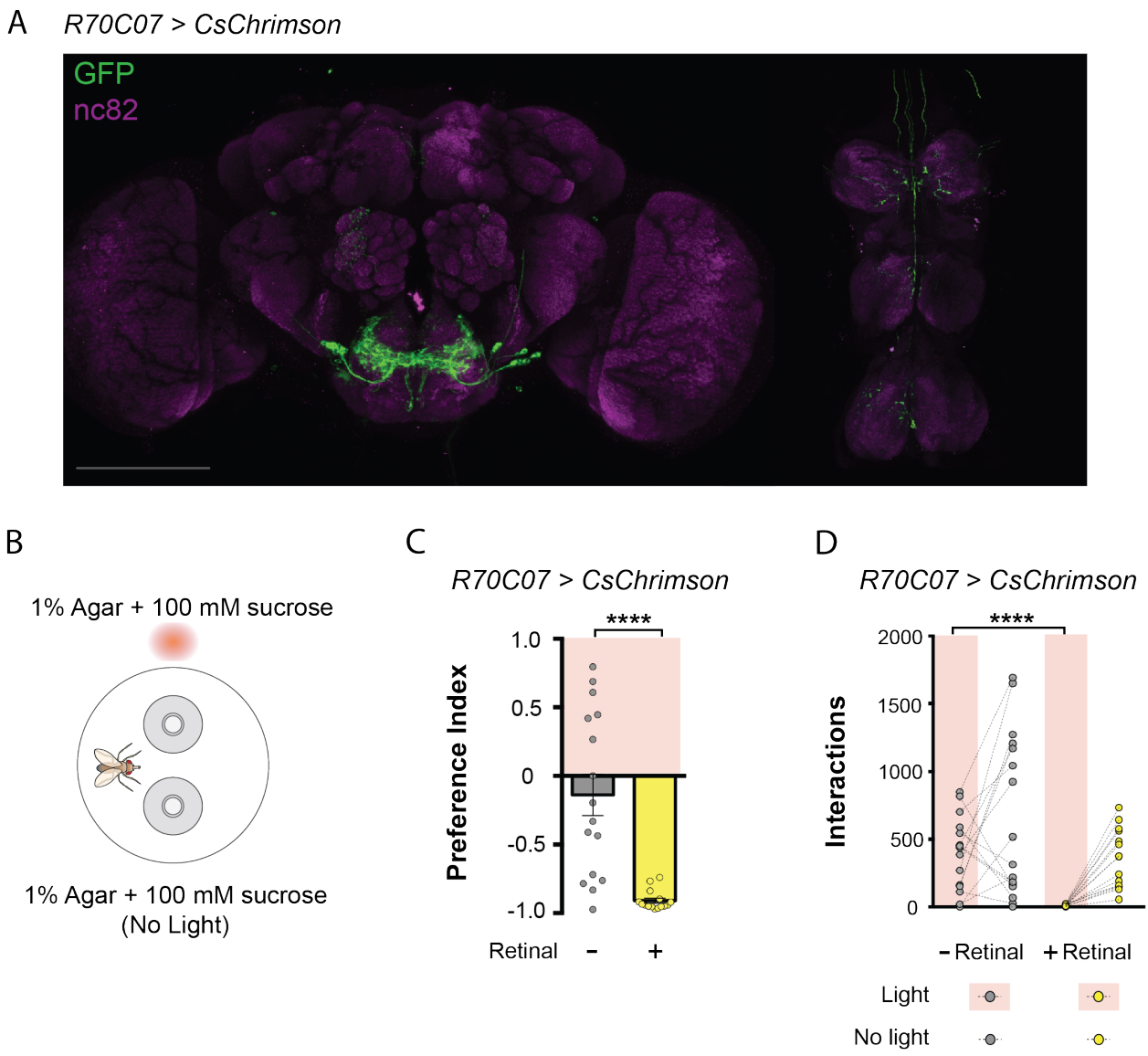

Figure 3-2. Neurons of *R70C07-GAL4* are sufficient in suppressing feeding.

(**A**) Immunofluorescent detection of *UAS-CsChrimson.mVenus* driven by *R70C07-GAL4* in the drosophila brain (Left) and VNC (Right). Antibodies: nc82 used for counterstain (magenta), GFP used for GAL4 expression. (**B**) Experimental setup: both channels of each STROBE arena contain 100 mM sucrose in 1% agar, only interactions with the one channel will trigger red light activation. (**C**) The preference index (PI) is calculated by the (**D**) number of interactions each non-retinal-fed (grey dots) and retinal-fed fly (yellow dots) had with each food choice. Values represent mean ± SEM. n = 15-16. Statistical test: *t*-test. ****p < 0.0001. Images taken at 25x. Scale bar, 100 µm.

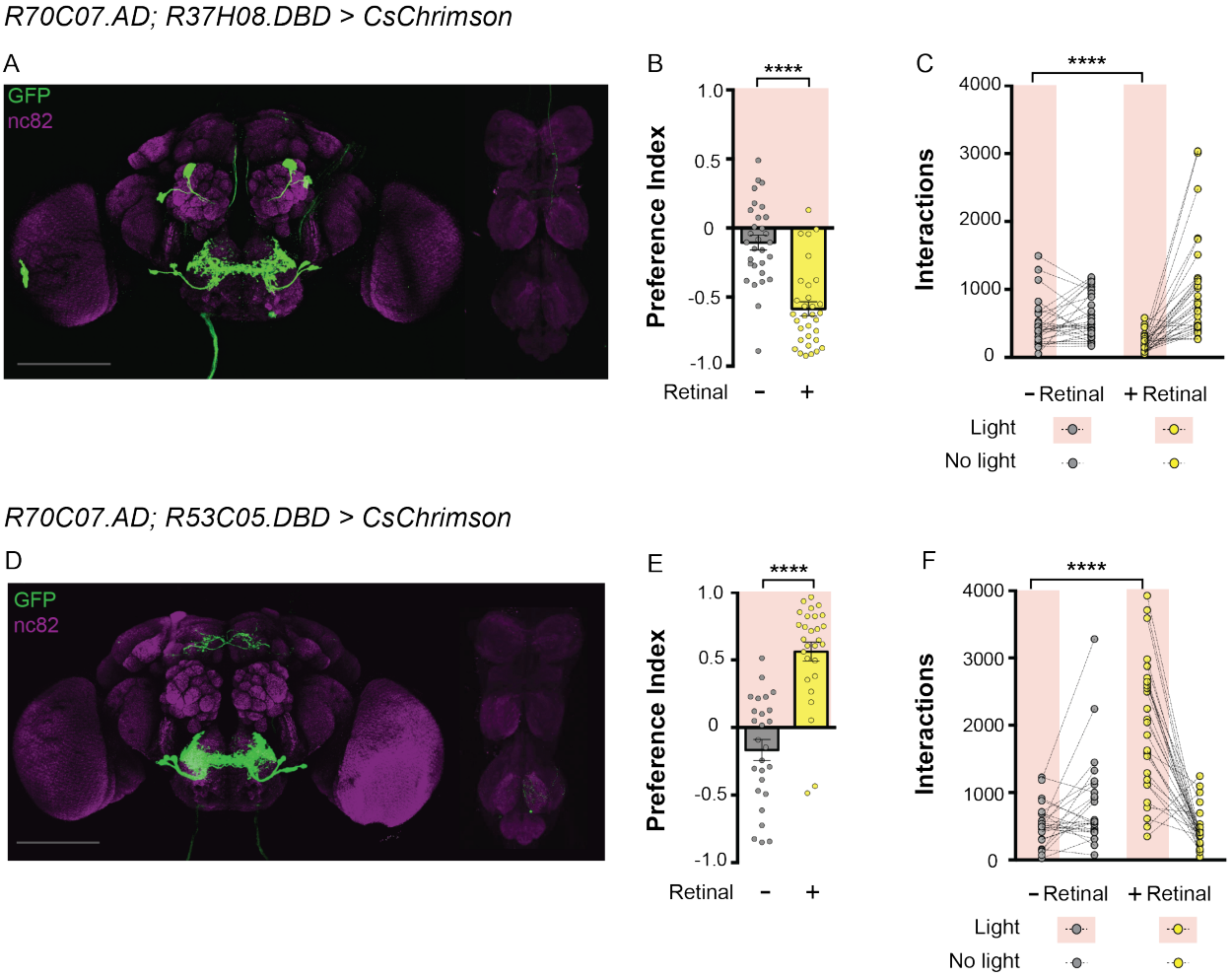

Figure 3-3. Subsets of the lateral SEZ population are sufficient in altering feeding.

Split-GAL4 lines: (**A-C**) *R70C07-p65.AD; R37H08-GAL4.DBD*, (**D-F**) *R70C07-p65.AD; R53C05-GAL4.DBD* were used to drive the expression of *UAS-CsChrimson.mVenus* to detect immunofluorescence in the brain and VNC (**A, D**) and test the effects of activation in the STROBE (**B-C, E-F**). Experimental setup: both channels contain 100 mM sucrose in 1% agar, only interactions with one channel will trigger red light activation. PI (**B, E**) is calculated based on the number of interactions (**C, F**) non-retinal-fed (grey dots) and retinal-fed flies (yellow dots) had with each food choice. Antibodies: nc82 used for counterstain (magenta), GFP used for GAL4 expression. Values represent mean ± SEM. n = 30-32 (**B-C**), n= 26-28 (**E-F**). Statistical test: *t*-test. ****$p < 0.0001$. Images taken at 25x. All scale bars, 100 µm.

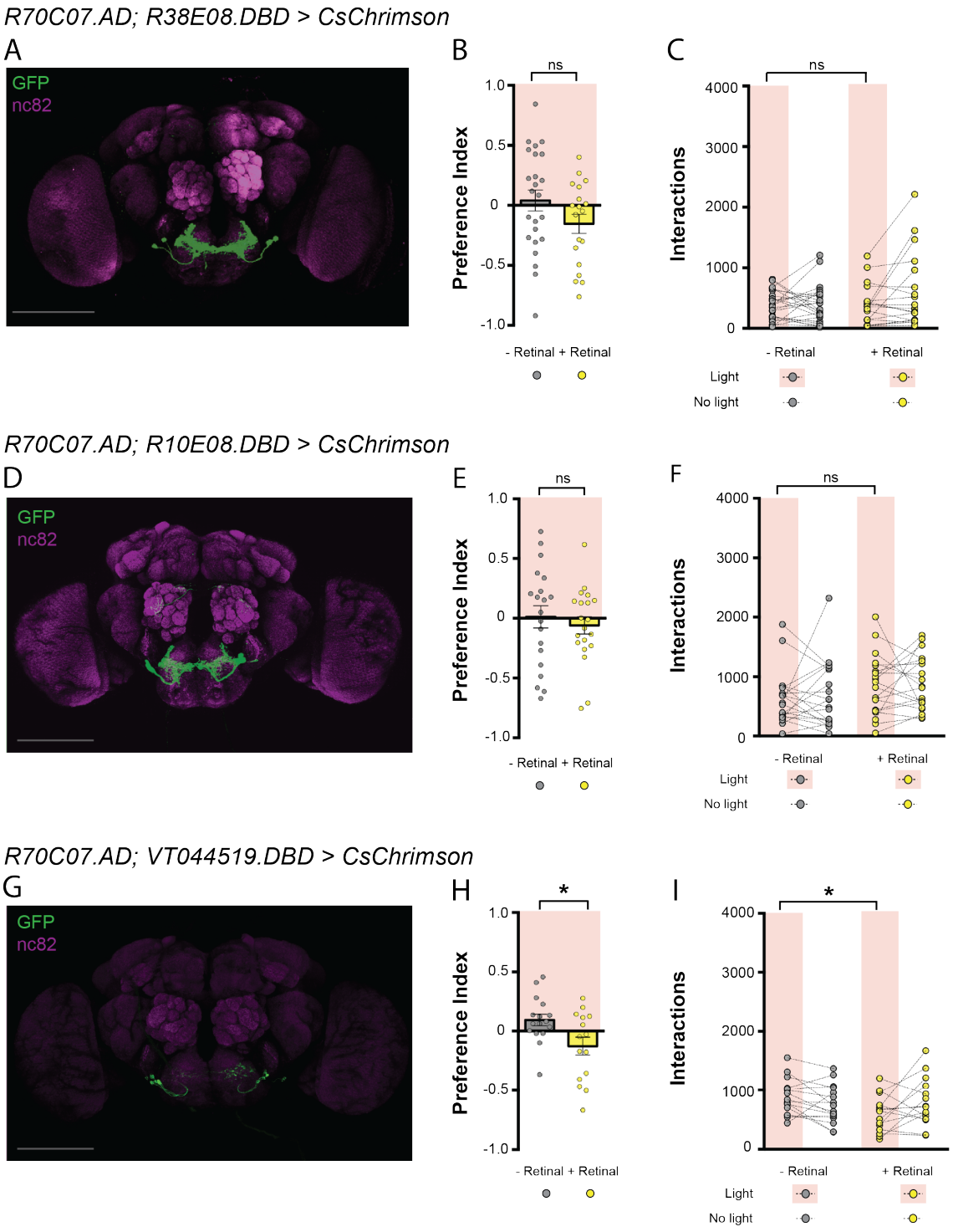

Figure 3-4. Not all lateral SEZ neurons are sufficient in altering feeding.

Split-GAL4 lines: (**A-C**) *R70C07-p65.AD; R38E08.DBD*, (**D-F**) *R70C07-p65.AD; R10E08-GAL4.DBD* and (**G-I**) *R70C07-p65.AD; VT044519.DBD* were used to drive the expression of *UAS-CsChrimson.mVenus* to detect immunofluorescence in the brain (**A, D, G**) and test the effects

of activation in the STROBE (**B-C, E-F, H-I**). Antibodies: nc82 used for counterstain (magenta), GFP used for GAL4 expression. Experimental setup: both channels contain 100 mM sucrose in 1% agar, only interactions with one channel will trigger red light activation. No statistically significant difference in feeding behaviour was observed for the PI (**B, E**) and number of interactions (**C, F**), except for the *7004* line (**H, I**). However, the magnitude of the PI of *7004* flies with functional CsChrimson is too low to be considered biologically relevant. Values represent mean ± SEM. n= 19-24 (**B-C**), n = 20 (**E, F**), and n= 15-16 (**H-I**). Statistical test: *t*-test. Ns, non-significant; *$p < 0.05$. Images taken at 25x. All scale bars, 100 µm.

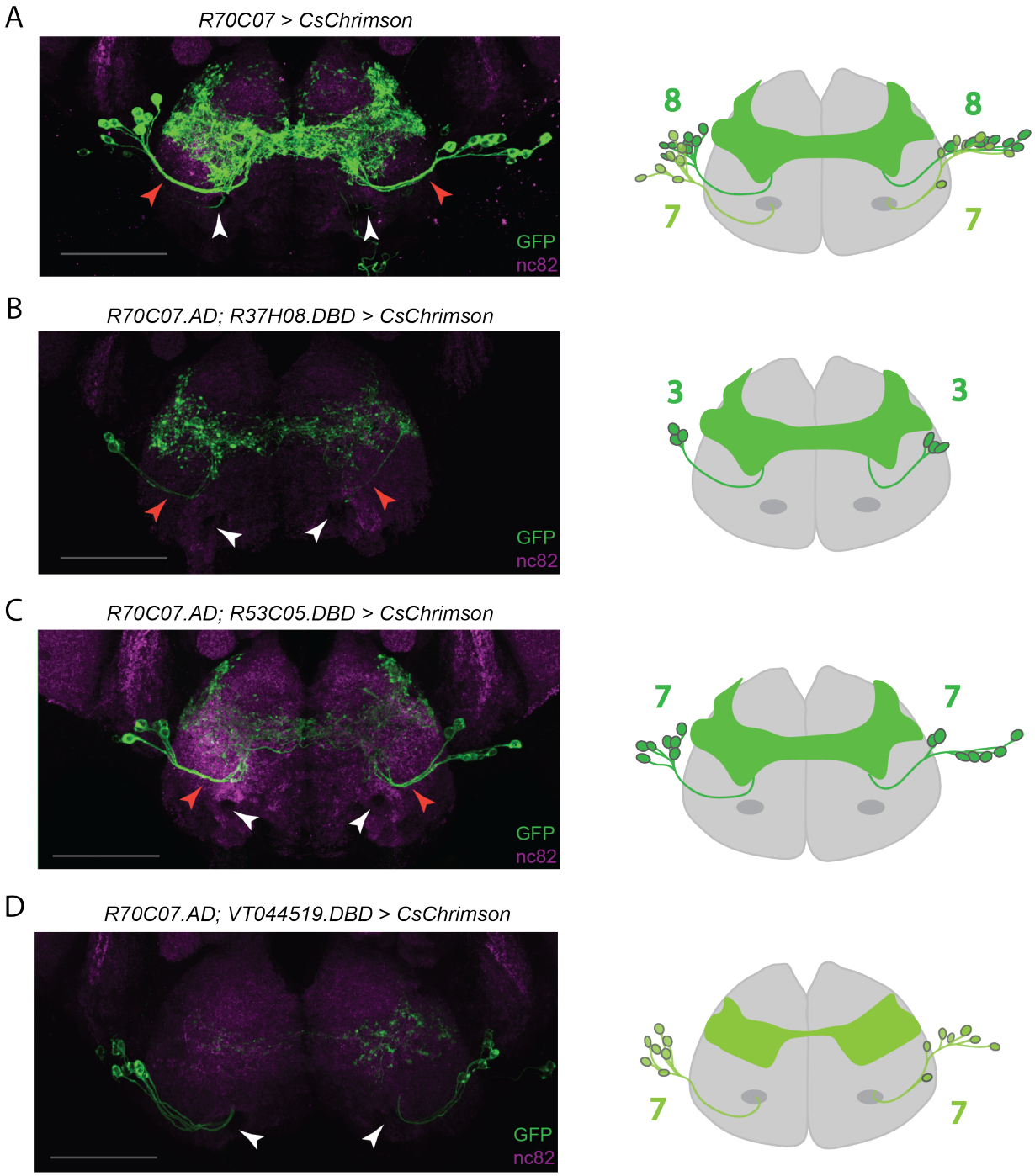

Figure 3-5. Two distinct neuronal groups make up the lateral SEZ population.

Immunofluorescent detection of *UAS-CsChrimson.mVenus* driven by (**A**) *R70C07-GAL4*, (**B**) *R70C07-p65.AD; R37H08-GAL4.DBD* (**C**) *R70C07-p65.AD; R53C05-GAL4.DBD* (**D**) *R70C07-p65.AD; VT044519-GAL4.DBD* in the SEZ with schematics on the right showing the number of neurons labelled by each split-GAL4. *7037* and *7053* labels lateral SEZ neurons that converge onto

similar tracts (red arrow) that arborize into a horseshoe pattern. *7004* labels a distinct group of lateral SEZ neurons that project deeply through the labellar nerve "tunnels" (white arrows) in the ventral SEZ, ultimately arborizing in an ipsilateral fashion. Antibodies: nc82 used for counterstain (magenta), GFP used for GAL4 expression. Images taken at 63x. All scale bars, 50 µm.

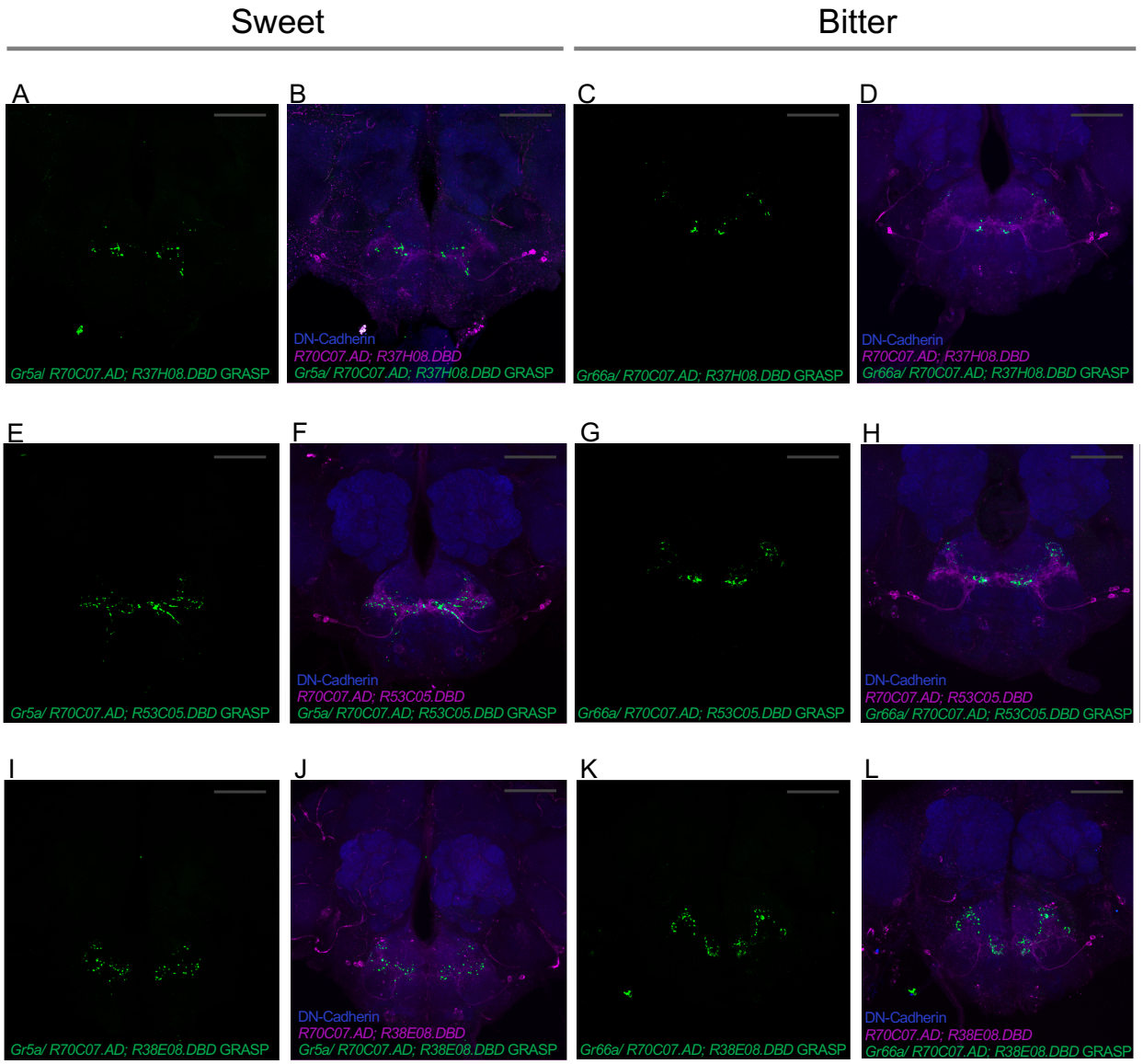

Figure 3-6. The lateral SEZ population contains neurons proximal to sweet and bitter GRNs. Split-GAL4 lines: *R70C07-p65.AD; R37H08-GAL4.DBD* (**A-D**), *R70C07-p65.AD; R53C058-GAL4.DBD* (**E-H**) and *R70C07-p65.AD; R38E08-GAL4.DBD* (**I-L**) were used to drive the expression of *UAS-spGFP1-10*, while *Gr5a-LexA* (**A-B, E-F, I-J**) and *Gr66a-LexA* (**C-D, J-H, K-L**) were used respectively, to drive *lexAop-spGFP11.* Images taken at 63x. Antibodies: DN-Cadherin used for counterstain, DsRed used for GAL4 expression, GFP used for GRASP signal. All scale bars, 50 µm.

Chapter 4: Discussion

4.1 Using the STROBE to identify novel taste neurons

4.1.1 The targeted efficiency for screening purposes

While the goal of this project is to identify novel taste neurons, it also tests the efficiency and robustness of our strategy in achieving this goal. Conventional methods of screening for taste or feeding-related neurons include labour intensive protocols such as PER, CAFE or 2-choice dye feeding assays (Gordon et al., 2009; Kain et al., 2015; Yapici et al., 2016). Both the CAFE and 2-choice dye feeding assays require many animals in order to produce sound data. These assays are used to ask questions regarding neuronal tuning, which require the repetitive and blind testing of tastant panels. While very informative if the experiments are fruitful, it is too much work for screening neurons that may not even be taste- or feeding-related. On the other hand, with our standardized setup up in the STROBE of pitting neuronal activation against the lack of it (in the neutral background of agar), we are only asking the question of whether the neurons of interest can sufficiently increase or decrease feeding. Thus, without the need of testing preferences for specific tastants, we can still reveal primary information about the valence of the neurons. It also reveals collective information about taste and ingestion, whereas PER assays will require the use of separate protocols to acquire both. Thus, for the purposes of initial GAL4 screening, activation experiments in the STROBE are the most ideal due its efficiency and broadly inclusive results.

4.1.2 False positives

Although the robustness of the STROBE in highlighting neuron populations that evoke changes in feeding behaviour is an advantage, screening with the STROBE also has drawbacks.

Nearly one-third of the total number of lines tested in the STROBE produced a significant change in feeding behaviour. This is unlikely due to the visual pre-screening of the GAL4 expression patterns, as lines were mainly chosen for sparseness and novelty, rather than relevancy to the primary taste center. Without targeting our selection to neurons in the SEZ, chances of correctly shortlisting drivers that label taste-related neurons should be low. One potential reasoning for the high hit rate is false positives. Since it is difficult to meaningfully compare the absolute number of feeding events recorded for each channel in a STROBE arena, we transform that data into relative terms. The larger the difference between the number of feeding events on the non-light-triggering and light-triggering choice, the larger the magnitude is for the calculated PI. Similar in principle, the significance of neuronal activation-evoked deviances in feeding behaviour is analyzed based on the comparative PIs of the control and retinal-fed fly groups. Consequently, statistically significant PIs may not just be reflective of authentic differences in behaviour, but also of instances where the controls' PIs trended in the opposite direction as the experimental flies. Evident in our optogenetic activation data (Figure 3-1A; Figure 3-4H-I), some low-magnitude PIs are deemed as statistically significant data, even though they are unlikely to be biologically relevant because the behavioural preference of those flies are effectively neutral. Furthermore, by looking at the average PI of controls (Figure 3-1A), we see that it hovers slightly above 0. This may explain why more fly lines with a negative PI are statistically significant. Another potential explanation for this observation is that inhibited feeding can arise due to other reasons. For example, if the neuronal activation led to an interruption of mobility such as uncontrollable jumping or promotion of sleep, feeding would be adversely affected as well, even though said neuronal pathways are not involved in feeding. Alternatively, it is less likely that the activation of non-taste neuron populations would

be able to orchestrate specific enough actions to consistently create an attraction towards a certain food choice.

Moreover, the factors that may sway control flies to prefer either one of the identically tasting options, are worth further discussion. Although flies are generally believed to be visually insensitive to red light, it appears that they are affected by it to some degree (Helfrich-Förster et al., 2002). For example, red light can be used to entrain circadian rhythm via certain intrinsic rhodopsins (Hanai et al., 2008). This seems less likely to be a confounding factor because entrainment requires long light exposures, whereas the STROBE only creates flashes of light over 1 hour of testing. Additionally, although red light is capable of startling flies, it happens at a higher wavelength than the level at which our STROBE operates at (Klapoetke et al., 2014). Even so, if we suspect that the red light itself is causing behavioural shifts in feeding, we would expect a consistent shift in the direction of preference in the control flies across all tested genotypes. However, this is not what the data shows. The inconsistency points to another possible area of error that is less predictable, where the channels containing agar were contaminated by other tastants left behind from previous experiments. Test arenas were thoroughly cleaned after every use and every PI was calculated by the combined data of at least two separately performed experiments to mitigate this, but it may only have helped dampen the effects. Another caveat is that there may be a base level of retinal that exists in normal fly food, sufficient to enable some amount of photoactivation capabilities in the non-retinal-fed control flies as well. In this situation, we would find that the control flies have preference indices that are always swayed in the direction similar to flies with functional CsChrimson; which was also not observed in our results.

4.2 The dual-modal connectivity of the lateral SEZ neurons

Although the STROBE system is efficient in seeking out a wide range of candidate taste neurons, it may also produce false negatives. For example, the *7038* line did not exhibit an atypical feeding preference upon activation in the STROBE, but still showed positive GRASP signal with sweet and bitter GRNs (Figure 3-4B-C; Figure3-6I-L). Since we do not doubt the authenticity of the GRASP signals, given its punctate appearance in the SEZ and relevant presence around the perimeter of the split-GAL4-labelled processes, we can confirm that the lateral SEZ neurons are in close proximity of GRNs. However, without performing calcium imaging on the lateral SEZ neurons to see if bitter and sweet proboscis stimulations would evoke activity, we are unable to claim the presence of functional connectivity between the two. Nonetheless, other neurons that have been shown to relay or regulate GRN output do systematically GRASP with its respective modality's GRNs (Bohra et al., 2018; Ledue et al., 2016; Miyazaki et al., 2015; Youn et al., 2018), supporting the use of GRASP as a preliminary method for inferring functional connectivity. Thus, if we assume that the lateral SEZ subsets are functionally connected to bitter and sweet GRNs, the next question we ask is why? Is it because (1) these are interneurons that simultaneously communicate with both sweet and bitter GRNs, or (2) the split-GAL4 lines have simply captured combinations of neurons that connect exclusively with either bitter or sweet GRNs?

4.2.1 Lateral SEZ neurons as interneurons that modulate GRNs

The idea of cross-modality communication between GRNs has been proposed before (Chen et al., 2014; Chu et al., 2014; Harris et al., 2015; Jeong et al., 2013; Meunier et al, 2013; Rimal et al., 2019). Meunier and colleagues (2013) discovered that the detection of bitter compounds not only relies on canonical bitter-tuned neurons, but also on the suppression of sugar- and water-responsive cells. This mechanism was later elucidated by Chu and colleagues (2014), attributing

this mixture-inhibition phenotype to GABAergic interneurons that suppress sugar responses upon bitter stimulation. Further confirmation came from a systematic mapping of taste-responsive cells in the brain (Harris et al., 2015). Exposing flies to mixtures of bitter and sweet tastants evoke calcium activity in less neurons than compared to exposing the flies to the tastants separately. To understand whether our neurons may be receiving input from one type of GRN and regulating another, we can use a relatively new genetic tool called targeted-GRASP (t-GRASP), which will give us insight on whether the neurons are pre- or post-synaptically connected to the GRNs (Shearin et al., 2018). If the lateral SEZ neurons are ones similar to the GABAergic interneurons, then we should see pre-synaptically-tethered GRASP signal with bitter GRNs and post-synaptically-tethered GRASP signal with sweet GRNs. Or behaviourally, we can see if red-light activation of CsChrimson in split-GAL4 flies would suppress PER to sucrose. However, if all the lateral SEZ neurons are inhibitory interneurons, we would expect the activation of these neurons to consistently decrease feeding behaviour. Our optogenetic activation data reveals the contrary. Notably, the STROBE-activation setup for testing the split-GAL4 lines involves placing 100 mM sucrose on both channels to increase the general number of interactions, such that inhibitory feeding phenotypes are more defined. Hence, one can argue that the suppressive effects of *7037* neurons on sweet GRNs are sufficient in inhibiting feeding, whereas *7038* neurons' suppression cannot counteract the attractive feeding on the 100 mM sucrose. Regardless, it is particularly the result of the *7053* neuronal activation that undermines this hypothesis that the lateral SEZ neurons are interneurons suppressing appetitive feeding behaviour. While this line has positive GRASP signal with bitter and sweet GRNs like *7037* and *7038*, it shows a dramatic increase in feeding behaviour upon activation, suggesting that the original lateral SEZ population is in fact heterogeneous.

4.2.2 Lateral SEZ neurons as part of bitter- and sweet-exclusive pathways

The observation that positive and negative populations of lateral SEZ neurons may exist also provides a possible explanation to why some split-GAL4 lines did not produce atypical feeding behaviour when optogenetically activated. These lines, such as *7038*, may be labelling a relatively equal number of positively and negatively-valenced neurons, effectively dampening each other's signal. With this hypothesis, it is likely that the *7053* driver predominantly labels neurons associated with the canonically sweet, appetitive pathway, while *7037* predominantly labels neurons associated with the aversive bitter pathway. To confirm this, we can perform *in vivo* calcium imaging with calcium indicator, GCaMP6, in various split-GAL4 neuronal subsets to check if bitter and sweet stimulations would cause a difference in the levels and localization of calcium activity (Chen et al., 2013). Curious to know the directionality of modulation between the GRNs and lateral SEZ neurons, we turned to a recent paper that characterizes a new technique, called trans-Tango which is capable of targeting and labeling post-synaptic cells (Talay et al., 2017). In proving its utility, they used this technique to comprehensively label all the second-order sweet neurons that are downstream of sweet GRNs. Due to the large expanse of secondary processes, they created clonal subsets for the purposes of highlighting the morphology of some of these second-order neurons. Amongst them, one clone closely matches the morphology and locality of the lateral SEZ neurons (Figure 4-1A). Interestingly, the processes appear to be ipsilateral to the cell bodies, suggesting the potential of these lateral SEZ neurons in retaining information about the directionality of incoming taste signals from the periphery. Unfortunately, we are unable to confirm if we have identified the same neurons, but this piece of data contributes to our model that second-order sweet neurons may be encompassed in the lateral SEZ split-GAL4 lines (Figure 4-1B). It would be interesting to know whether the post-synaptic labelling of bitter

GRNs also include the lateral SEZ neurons. This would support the idea that the lateral SEZ population contains neurons from opposing taste pathways. Nonetheless, we also acknowledge the possibility that a combination of modality-integrating interneurons and modality-specific second-order taste neurons exist in the lateral SEZ population.

4.3 Future directions and experiments

Thus far, we have evidence showing that the lateral SEZ neuronal population sufficiently increases and decreases feeding. We speculate that two different populations of neurons are driving these opposing behaviours, with the aversive lateral SEZ subsets being responsive to unpalatable substances, and the appetitive subsets being responsive to attractive tastants (Figure 4-1). By silencing the split-GAL4 lateral SEZ subsets, we can perform 2-choice dye feeding assays to identify whether these neurons are necessary for the regular attraction of palatable substances or the avoidance of non-palatable substances. A good starting point would be to first test if the *7053* neurons are necessary for the preference towards consuming sucrose and if the *7037* neurons are necessary for bitter-avoidance. Meanwhile, we can strengthen our model by creating additional driver lines that can separately label the bitter and sweet GRN-associating lateral SEZ subsets. Nevertheless, our current data re-ignites the long-standing discussion of whether opposing taste pathways, like bitter and sweet, remain segregated as the labelled lines theory suggests, or do the pathways intersect early on in the circuitry.

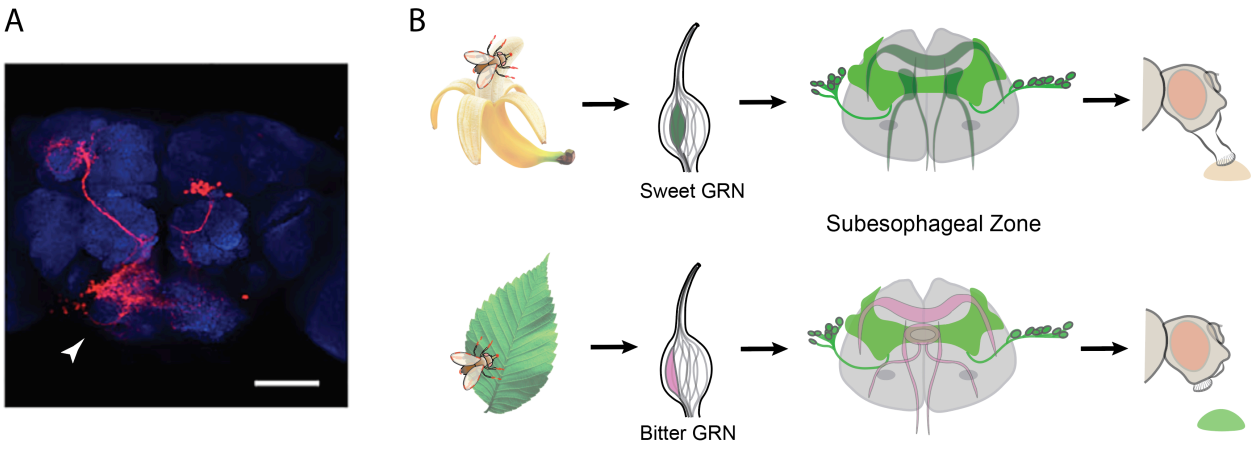

Figure 4-1. Model: Lateral SEZ neurons receive GRN input to inform feeding decisions. (**A**) Immunofluorescent staining of the clonal analysis of second-order neurons of *Gr64f*-positive GRNs in the brain. (Replicated from Talay et al., 2017; Scale bar, 50 µm). Post-synaptic *Gr64f* neurons (white arrow) are morphologically similar to the lateral SEZ neurons. (**B**) Our model suggests that the lateral SEZ neurons (green) are post-synaptic to sweet (dark green) and bitter (pink) GRNs. Upon encountering sweet or bitter foods, differential GRN inputs onto the lateral SEZ population causes either the promotion (top) or inhibition (bottom) of feeding.

Chapter 5: Conclusion

This study was set out in pursuit of identifying novel taste neurons. Our results show that novel subsets of candidate neurons located bilaterally in the SEZ are sufficient in promoting and inhibiting feeding. Intriguingly, the subsets seem to GRASP with both sweet and bitter GRNs, regardless of the feeding phenotype produced by optogenetic activation. Of the second-order taste neurons that have been identified, most exclusively relay either sweet or bitter signals. (Bohra et al., 2018; Kain et al., 2015; Kim et al., 2017; Yapici et al., 2016). Therefore, we postulate that this morphologically-grouped population of lateral SEZ neurons is made up of neurons that connect exclusively with either bitter or sweet neurons to inform on feeding decisions. Fundamentally, the optogenetic activation assay results probed us to consider how the simultaneous activation of local neurons that are members of opposing taste pathways could lead to differential feeding responses.

This is an important aspect of taste detection in nature because food sources are often mixtures of different tastes that would activate different taste pathways. How a fly, or any animal process these complex mixtures to promote the correct feeding behaviour strongly determines survivorship. If it is the case where differently-tuned GRNs have differently-weighted influence on making feeding decisions, then compromises in this infrastructure would greatly affect an animal's nutritional homeostasis. In humans, this has been proposed as one of the many reasons why the incidence of obesity is increasing (Rolls, 2012). Our body has evolved over many generations to rely on the dynamic interaction between various environmental chemosensory input and satiety signals to know when to initiate eating and when to stop. However, in the industrialized world we have now, where the palatability and availability of foods have increased substantially, our body's ability to convey satiety signals has not kept up with the same trajectory (Rolls, 2012).

The outcome is being overstimulated by food, and ultimately overeating. Thus, understanding how sensory input informs consumption behaviours, and how modality-sensitive this mechanism is, may shed light on ways to alleviate obesity risk factors and create foods that will not disrupt this system.

References

Adler, E., Hoon, M. A., Mueller, K. L., Chandrashekar, J., Ryba, N. J. P., & Zuker, C. S. (2000). A Novel Family of Mammalian Taste Receptors, *100*, 693–702.

Azevedo, F. A. C., Carvalho, L. R. B., Grinberg, L. T., Farfel, J. M., Ferretti, R. E. L., Leite, R. E. P., … Herculano-Houzel, S. (2009). Equal Numbers of Neuronal and Nonneuronal Cells Make the Human Brain an Isometrically Scaled-Up Primate Brain, *541*(June 2008), 532–541. https://doi.org/10.1002/cne.21974

Baines, R. A., Uhler, J. P., Thompson, A., Sweeney, S. T., & Bate, M. (2001). Altered electrical properties in Drosophila neurons developing without synaptic transmission. *Journal of Neuroscience*, *21*(5), 1523–1531. https://doi.org/10.1523/jneurosci.21-05-01523.2001

Bohra, A. A., Kallman, B. R., Reichert, H., Vijayraghavan, K., Bohra, A. A., Kallman, B. R., … Vijayraghavan, K. (2018). Identification of a Single Pair of Interneurons for Bitter Taste Processing in the Drosophila Brain. *Current Biology*, *28*(6), 847-858.e3. https://doi.org/10.1016/j.cub.2018.01.084

Brand, A. H., & Perrimon, N. (1993). Targeted gene expression as a means of altering cell fates and generating dominant phenotypes. *Development*, *118*, 401–415. https://doi.org/10.1101/lm.1331809

Busch, S., Selcho, M., Ito, K., & Tanimoto, H. (2009). A map of octopaminergic neurons in the Drosophila brain. *Journal of Comparative Neurology*, *513*(6), 643–667. https://doi.org/10.1002/cne.21966

Cameron, P., Hiroi, M., Ngai, J., & Scott, K. (2010). The molecular basis for water taste in Drosophila. *Nature*, *465*(May), 91–96. https://doi.org/10.1038/nature09011

Chabaud, M. A., Devaud, J. M., Pham-Delègue, M. H., Preat, T., & Kaiser, L. (2006). Olfactory conditioning of proboscis activity in Drosophila melanogaster. *Journal of Comparative Physiology A: Neuroethology, Sensory, Neural, and Behavioral Physiology*, *192*(12), 1335–1348. https://doi.org/10.1007/s00359-006-0160-3

Chandrashekar, J., Kuhn, C., Oka, Y., Yarmolinsky, D. A., Hummler, E., Ryba, N. J. P., & Zuker, C. S. (2010). The cells and peripheral representation of sodium taste in mice. *Nature*, *464*(March). https://doi.org/10.1038/nature08783

Chen, T. W., Wardill, T. J., Sun, Y., Pulver, S. R., Renninger, S. L., Baohan, A., … Kim, D. S. (2013). Ultrasensitive fluorescent proteins for imaging neuronal activity. *Nature*, *499*(7458), 295–300. https://doi.org/10.1038/nature12354

Chen, Y. D., Ahmad, S., Amin, K., & Dahanukar, A. (2019). A subset of brain neurons controls regurgitation in adult Drosophila melanogaster. *Journal of Experimental Biology*, (September). https://doi.org/10.1242/jeb.210724

Chen, Z., Wang, Q., & Wang, Z. (2010). The Amiloride-Sensitive Epithelial Na+ Channel PPK28 Is Essential for Drosophila Gustatory Water Reception. *The Journal of Neuroscience*, *30*(18), 6247 LP – 6252. Retrieved from http://www.jneurosci.org/content/30/18/6247.abstract

Chu, B., Chui, V., Mann, K., & Gordon, M. D. (2014). Presynaptic gain control drives sweet and bitter taste integration in Drosophila. *Current Biology*, *24*(17), 1978–1984. https://doi.org/10.1016/j.cub.2014.07.020

Clyne, P. J., Warr, C. G., & Carlson, J. R. (2000). Candidate Taste Receptors in Drosophila, *287*(March), 1830–1835.

Dahanukar, A., Foster, K., Naters, W. M. V. D. G. Van, & Carlson, J. R. (2001). A Gr receptor is

required for response to the sugar trehalose in taste neurons of Drosophila. *Nature Neuroscience*, *4*(12), 1182–1186. https://doi.org/10.1038/nn765

Dahanukar, A., Lei, Y., Kwon, J. Y., & Carlson, J. R. (2007). Two Gr Genes Underlie Sugar Reception in Drosophila. *Neuron*, *56*, 503–516. https://doi.org/10.1016/j.neuron.2007.10.024

Dethier, V. G. (1976). *The Hungry Fly*. Cambridge, MA: Harvard University Press.

Duffy, J. B. (2002). GAL4 system in Drosophila: A fly geneticist's Swiss army knife. *Genesis*, *34*(1–2), 1–15. https://doi.org/10.1002/gene.10150

Dunipace, L., Meister, S., Mcnealy, C., & Amrein, H. (2001). Spatially restricted expression of candidate taste receptors in the Drosophila gustatory system. *Current Biology*, *11*, 822–835.

Feinberg, E. H., Vanhoven, M. K., Bendesky, A., Wang, G., Fetter, R. D., Shen, K., & Bargmann, C. I. (2008). GFP Reconstitution Across Synaptic Partners (GRASP) Defines Cell Contacts and Synapses in Living Nervous Systems, 353–363. https://doi.org/10.1016/j.neuron.2007.11.030

Fischer, J. A., Giniger, E., Maniatis, T., & Ptashne, M. (1988). GAL4 activates transcription in Drosophila. *Letters to Nature*, *332*, 853–856.

Flood, T. F., Iguchi, S., Gorczyca, M., White, B., Ito, K., & Yoshihara, M. (2013). A single pair of interneurons commands the Drosophila feeding motor program. *Nature*, *498*(7456), 83–87. https://doi.org/10.1038/nature12208

French, A. S., Sellier, M., Agha, M. A., Guigue, A., Chabaud, X., Reeb, X. P. D., … Tetxlc, G. C. (2015). Dual Mechanism for Bitter Avoidance in Drosophila. *Journal of Neuroscience*, *35*(9), 3990–4004. https://doi.org/10.1523/JNEUROSCI.1312-14.2015

Fujii, S., Yavuz, A., Song, X., Amrein, H., Fujii, S., Yavuz, A., & Slone, J. (2015). A Drosophila

Sugar Receptors in Sweet Taste Perception, Olfaction, and Internal Nutrient Sensing. *Current Biology*, *25*(5), 621–627. https://doi.org/10.1016/j.cub.2014.12.058

Gendre, N., Lüer, K., Friche, S., Grillenzoni, N., Ramaekers, A., Technau, G. M., & Stocker, R. F. (2004). Integration of complex larval chemosensory organs into the adult nervous system of Drosophila. https://doi.org/10.1242/dev.00879

Glendinning, J. I. (2007). How Do Predators Cope With Chemically Defended Foods ? *Biological Bulletin*, *213*(3), 252–266.

Gordon, M. D., & Scott, K. (2009). Motor Control in a Drosophila Taste Circuit. *Neuron*, *61*(3), 373–384. https://doi.org/10.1016/j.neuron.2008.12.033

Hanai, S., Hamasaka, Y., & Ishida, N. (2008). Circadian entrainment to red light in Drosophila: Requirement of Rhodopsin 1 and Rhodopsin 6. *NeuroReport*, *19*(14), 1441–1444. https://doi.org/10.1097/WNR.0b013e32830e4961

Harris, D. T., Kallman, B. R., Mullaney, B. C., Scott, K., Harris, D. T., Kallman, B. R., … Scott, K. (2015). Representations of Taste Modality in the Drosophila. *Neuron*, *86*(6), 1449–1460. https://doi.org/10.1016/j.neuron.2015.05.026

Helfrich-Förster, C., Edwards, T., Yasuyama, K., Wisotzki, B., Schneuwly, S., Stanewsky, R., … Hofbauer, A. (2002). The extraretinal eyelet of Drosophila: Development, ultrastructure, and putative circadian function. *Journal of Neuroscience*, *22*(21), 9255–9266. https://doi.org/10.1523/jneurosci.22-21-09255.2002

Hiroi, M., Meunier, N., & Tanimura, T. (2004). Responding to Sweet-Salty and Bitter Taste in Drosophila. *Journal of Neurobiology*, *61*(3), 333–342. https://doi.org/10.1002/neu.20063

Inagaki, H. K., Ben-Tabou De-Leon, S., Wong, A. M., Jagadish, S., Ishimoto, H., Barnea, G., … Anderson, D. J. (2012). Visualizing neuromodulation in vivo: TANGO-mapping of

dopamine signaling reveals appetite control of sugar sensing. *Cell*, *148*(3), 583–595. https://doi.org/10.1016/j.cell.2011.12.022

Inagaki, H. K., Panse, K. M., & Anderson, D. J. (2014). Independent, reciprocal neuromodulatory control of sweet and bitter taste sensitivity during starvation in Drosophila. *Neuron*, *84*(4), 806–820. https://doi.org/10.1016/j.neuron.2014.09.032

Ito, K., Shinomiya, K., Ito, M., Armstrong, J. D., Boyan, G., Hartenstein, V., … Vosshall, L. B. (2014). A systematic nomenclature for the insect brain. *Neuron*, *81*(4), 755–765. https://doi.org/10.1016/j.neuron.2013.12.017

Itskov, P. M., Moreira, J.-M., Vinnik, E., Lopes, G., Safarik, S., Dickinson, M. H., & Ribeiro, C. (2014). Automated monitoring and quantitative analysis of feeding behaviour in Drosophila. *Nature Communications*, *5*, 4560. https://doi.org/10.1038/ncomms5560

Ja, W. W., Carvalho, G. B., Mak, E. M., De La Rosa, N. N., Fang, A. Y., Liong, J. C., … Benzer, S. (2007). Prandiology of Drosophila and the CAFE assay. *Proceedings of the National Academy of Sciences of the United States of America*, *104*(20), 8253–8256. https://doi.org/10.1073/pnas.0702726104

Jeong, Y. T., Shim, J., Oh, S. R., Yoon, H. I., Kim, C. H., Moon, S. J., & Montell, C. (2013). An odorant-binding protein required for suppression of sweet taste by bitter chemicals. *Neuron*, *79*(4), 725–737. https://doi.org/10.1016/j.neuron.2013.06.025

Jiao, Y., Moon, S. J., & Montell, C. (2007). A Drosophila gustatory receptor required for the responses to sucrose , glucose , and maltose identified by mRNA tagging. *PNAS*, *104*(35), 14110–14115.

Jiao, Y., Moon, S. J., Wang, X., Ren, Q., & Montell, C. (2008). Gr64f Is Required in Combination with Other Gustatory Receptors for Sugar Detection in Drosophila. *Current*

Biology, *18*(22), 1797–1801. https://doi.org/10.1016/j.cub.2008.10.009

Kain, P., & Dahanukar, A. (2015). Secondary Taste Neurons that Convey Sweet Taste and Starvation in the Drosophila Brain. *Neuron*, *85*(4), 819–832. https://doi.org/10.1016/j.neuron.2015.01.005

Kim, H., Kirkhart, C., Scott, K., States, U., Wills, H., & States, U. (2017). Long-range projection neurons in the taste circuit of Drosophila, 1–24. https://doi.org/10.7554/eLife.23386

Klapoetke, N. C., Murata, Y., Kim, S. S., Pulver, S. R., Birdsey-Benson, A., Cho, Y. K., … Boyden, E. S. (2014). Independent optical excitation of distinct neural populations. *Nature Methods*, *11*(3), 338–346. https://doi.org/10.1038/nmeth.2836

Krashes, M. J., DasGupta, S., Vreede, A., White, B., Armstrong, J. D., & Waddell, S. (2009). A Neural Circuit Mechanism Integrating Motivational State with Memory Expression in Drosophila. *Cell*, *139*(2), 416–427. https://doi.org/10.1016/j.cell.2009.08.035

Kwon, J. Y., Dahanukar, A., Weiss, Li. A., & Carlson, J. R. (2014). A map of taste neuron projections in the Drosophila CNS. *Journal of Biosciences*, *39*(September), 565–574. https://doi.org/10.1007/s12038-014-9448-6

Lai, S. L., & Lee, T. (2006). Genetic mosaic with dual binary transcriptional systems in Drosophila. *Nature Neuroscience*, *9*(5), 703–709. https://doi.org/10.1038/nn1681

Ledue, E. E., Mann, K., Koch, E., Chu, B., Dakin, R., Gordon, M. D., … Gordon, M. D. (2016). Starvation-Induced Depotentiation of Bitter Taste Drosophila. *Current Biology*, *26*(21), 2854–2861. https://doi.org/10.1016/j.cub.2016.08.028

Lee, M. J., Sung, H. Y., Jo, H., Kim, H., Choi, M. S., & Kwon, J. Y. (2017). Ionotropic Receptor 76b Is Required for Gustatory Aversion to Excessive Na + in Drosophila. *Molecules and Cells*, *40*(10), 787–795.

Lee, Y., Kim, S. H., & Montell, C. (2010). Avoiding DEET through Insect Gustatory Receptors. *Neuron*, *67*(4), 555–561. https://doi.org/10.1016/j.neuron.2010.07.006

Lee, Y., Moon, S. J., & Montell, C. (2009). Multiple gustatory receptors required for the caffeine response in Drosophila. *Proceedings of the National Academy of Sciences of the United States of America*, *106*(11), 4495–4500. https://doi.org/10.1073/pnas.0811744106

Ling, F., Dahanukar, A., Weiss, L. A., Kwon, J. Y., & Carlson, J. R. (2014). The Molecular and Cellular Basis of Taste Coding in the Legs of Drosophila, *34*(21), 7148–7164. https://doi.org/10.1523/JNEUROSCI.0649-14.2014

Liu, T., Starostina, E., Vijayan, V., & Pikielny, C. W. (2012). Two Drosophila DEG / ENaC Channel Subunits Have Distinct Functions in Gustatory Neurons That Activate Male Courtship. *Journal of Neuroscience*, *32*(34), 11879–11889. https://doi.org/10.1523/JNEUROSCI.1376-12.2012

Lohr, D., Venkov, P., & Zlatanova, J. (1995). Transcriptional regulation in the yeast GAL gene family: A complex genetic network. *FASEB J,* 9(9): 777-87. https://doi.org/10.1096/fasebj.9.97601342

Lu, B., Lamora, A., Sun, Y., Welsh, M. J., & Ben-shahar, Y. (2012). ppk23-Dependent Chemosensory Functions Contribute to Courtship Behavior in Drosophila melanogaster. *PLOS Genetics*, *8*(3), 1–13. https://doi.org/10.1371/journal.pgen.1002587

Luan, H., Peabody, N. C., Vinson, C. R. R., & White, B. H. (2006). Refined Spatial Manipulation of Neuronal Function by Combinatorial Restriction of Transgene Expression. *Neuron*, *52*(3), 425–436. https://doi.org/10.1016/j.neuron.2006.08.028

Manzo, A., Silies, M., Gohl, D. M., & Scott, K. (2012). Motor neurons controlling fluid ingestion in Drosophila, *109*(16), 6307–6312. https://doi.org/10.1073/pnas.1120305109

Marella, S., Fischler, W., Kong, P., Asgarian, S., Rueckert, E., & Scott, K. (2006). Imaging taste responses in the fly brain reveals a functional map of taste category and behavior. *Neuron*, *49*(2), 285–295. https://doi.org/10.1016/j.neuron.2005.11.037

Marella, S., Mann, K., & Scott, K. (2012). Dopaminergic Modulation of Sucrose Acceptance Behavior in Drosophila. *Neuron*, *73*(5), 941–950. https://doi.org/10.1016/j.neuron.2011.12.032

May, C. E., Vaziri, A., Lin, Y. Q., Grushko, O., Khabiri, M., Wang, Q. P., … Dus, M. (2019). High Dietary Sugar Reshapes Sweet Taste to Promote Feeding Behavior in Drosophila melanogaster. *Cell Reports*, *27*(6), 1675-1685.e7. https://doi.org/10.1016/j.celrep.2019.04.027

McGuire, S. E., Mao, Z., & Davis, R. L. (2004). Spatiotemporal gene expression targeting with the TARGET and gene-switch systems in Drosophila. *Science's STKE : Signal Transduction Knowledge Environment*, *2004*(220), 1–11. https://doi.org/10.1126/stke.2202004pl6

Meunier, N., Rospars, J., & Tanimura, T. (2003). Peripheral Coding of Bitter Taste in Drosophila. https://doi.org/10.1002/neu.10235

Miyazaki, T., Lin, T. Y., Ito, K., Lee, C. H., & Stopfer, M. (2015). A gustatory second-order neuron that connects sucrose-sensitive primary neurons and a distinct region of the gnathal ganglion in the Drosophila brain. *Journal of Neurogenetics*, *29*(2–3), 144–155. https://doi.org/10.3109/01677063.2015.1054993

Mohammad, F., Stewart, J., Ott, S., Chlebikova, K., Chua, J. Y., Koh, T.-W., … Claridge-Chang, A. (2016). Potent optogenetic inhibition of behavior with anion channelrhodopsins. *BioRxiv*, *14*(3), 1–24. https://doi.org/http://dx.doi.org/10.1101/082255

Moon, S. J., Köttgen, M., Jiao, Y., Xu, H., & Montell, C. (2006). A Taste Receptor Required for the Caffeine Response In Vivo. *Current Biology*, *16*, 1812–1817. https://doi.org/10.1016/j.cub.2006.07.024

Musso, P., Junca, P., Jelen, M., Feldman-kiss, D., Zhang, H., Chan, R. C. W., & Gordon, M. D. (2019). Closed-loop optogenetic activation of peripheral or central neurons modulates feeding in freely moving Drosophila, 1–23.

Oka, Y., Butnaru, M., Buchholtz, L. Von, Ryba, N. J. P., & Zuker, C. S. (2013). High salt recruits aversive taste pathways. *Nature*, *494*(7438), 472–475. https://doi.org/10.1038/nature11905

Pfieffer, B. D., Jenett, A., Hammonds, A. S., Ngo, T.-T. B., Misra, S., Murphy, C., … Rubin, G. M. (2008). Tools for neuroanatomy and neurogenetics in Drosophila. *PNAS*, *105*(28), 9715–9720. https://doi.org/10.5694/j.1326-5377.1975.tb111372.x

Rajashekhar, K. P., & Singh, R. N. (1994). Organization of motor neurons innervating the proboscis musculature in Drosophila melanogaster meigen (diptera : Drosophilidae). *International Journal of Insect Morphology and Embryology*, *23*(3), 225–242. Retrieved from http://www.sciencedirect.com.ezp-prod1.hul.harvard.edu/science/article/pii/0020732294900205

Robertson, H. M., Warr, C. G., & Carlson, J. R. (2003). Molecular evolution of the insect chemoreceptor gene superfamily in Drosophila melanogaster, *100*, 14537–14542.

Rolls, E. T. (2012). Taste, olfactory and food texture reward processing in the brain and the control of appetite. *Proceedings of the Nutrition Society*, *71*(4), 488–501. https://doi.org/10.1017/S0029665112000821

Schwarz, O., Bohra, A. A., Liu, X., & Reichert, H. (2017). Motor control of Drosophila feeding

behavior, 1–32. https://doi.org/10.7554/eLife.19892

Scott, K., Brady, R., Cravchik, A., Morozov, P., Rzhetsky, A., Zuker, C., … York, N. (2001). A Chemosensory Gene Family Encoding Candidate Gustatory and Olfactory Receptors in Drosophila, *104*, 661–673.

Shearin, H. K., Quinn, C. D., Mackin, R. D., Macdonald, I. S., & Stowers, R. S. (2018). t-GRASP, a targeted GRASP for assessing neuronal connectivity. *Journal of Neuroscience Methods*, *306*(January), 94–102. https://doi.org/10.1016/j.jneumeth.2018.05.014

Simpson, J. H. (2009). *Mapping and Manipulating Neural Circuits in the Fly Brain. Genetic Dissection of Neural Circuits and Behavior* (1st ed., Vol. 65). Elsevier Inc. https://doi.org/10.1016/S0065-2660(09)65003-3

Singh, R. N. (1997). Neurobiology of the Gustatory Systems of Drosophila and Some Terrestrial Insects. *Microscopy Research and Technique*, *39*, 547–563.

Slone, J., Daniels, J., Amrein, H., & Carolina, N. (2007). Sugar Receptors in Drosophila. *Current Biology*, *17*, 1809–1816. https://doi.org/10.1016/j.cub.2007.09.027

Srivastava, D. P., Yu, E. J., Kennedy, K., Chatwin, H., Reale, V., Hamon, M., … Evans, P. D. (2005). Rapid, nongenomic responses to ecdysteroids and catecholamines mediated by a novel Drosophila G-protein-coupled receptor. *Journal of Neuroscience*, *25*(26), 6145–6155. https://doi.org/10.1523/JNEUROSCI.1005-05.2005

Stafford, J. W., Lynd, K. M., Jung, A. Y., & Gordon, M. D. (2012). Integration of Taste and Calorie Sensing in Drosophila. *The Journal of Neuroscience*, *32*(42), 14767–14774. https://doi.org/10.1523/JNEUROSCI.1887-12.2012

Starostina, E., Liu, T., Vijayan, V., Zheng, Z., Siwicki, K. K., & Pikielny, C. W. (2012). A Drosophila DEG / ENaC Subunit Functions Specifically in Gustatory Neurons Required for

Male Courtship Behavior. *Journal of Neuroscience*, *32*(13), 4665–4674. https://doi.org/10.1523/JNEUROSCI.6178-11.2012

Steck, K., Walker, S. J., Itskov, P. M., Baltazar, C., Moreira, J. M., & Ribeiro, C. (2018). Internal amino acid state modulates yeast taste neurons to support protein homeostasis in Drosophila. *ELife*, *7*, 1–29. https://doi.org/10.7554/eLife.31625

Stocker, R. F. (1994). The organization of the chemosensory system in Drosophila melanogaster: a rewiew. *Cell and Tissue Research*, *275*(1), 3–26. https://doi.org/10.1007/BF00305372

Talay, M., Richman, E. B., Snell, N. J., Hartmann, G. G., Fisher, J. D., Sorkaç, A., … Barnea, G. (2017). Transsynaptic Mapping of Second-Order Taste Neurons in Flies by trans-Tango. *Neuron*, *96*(4), 783-795.e4. https://doi.org/10.1016/j.neuron.2017.10.011

Thistle, R., Cameron, P., Ghorayshi, A., Dennison, L., & Scott, K. (2012). Contact Chemoreceptors Mediate Male-Male Repulsion and Male-Female Attraction during Drosophila Courtship. *Cell*, *149*(5), 1140–1151. https://doi.org/10.1016/j.cell.2012.03.045

Thorne, N., Chromey, C., Bray, S., Amrein, H., Building, C., & Carolina, N. (2004). Taste Perception and Coding in Drosophila, *14*, 1065–1079. https://doi.org/10.1016/j

Toda, H., Zhao, X., & Dickson, B. J. (2012). The Drosophila Female Aphrodisiac Pheromone Activates ppk23 + Sensory Neurons to Elicit Male Courtship Behavior. *Cell Reports*, *1*(6), 599–607. https://doi.org/10.1016/j.celrep.2012.05.007

Vosshall, L. B., & Stocker, R. F. (2007). Molecular Architecture of Smell and Taste in Drosophila. https://doi.org/10.1146/annurev.neuro.30.051606.094306

Wang, Z., Singhvi, A., Kong, P., & Scott, K. (2004). Taste Representations in the Drosophila Brain, *117*, 981–991.

Weiss, L. A., Dahanukar, A., Kwon, J. Y., Banerjee, D., & Carlson, J. R. (2011). Bitter Taste in

Drosophila. *Neuron*, *69*(2), 258–272. https://doi.org/10.1016/j.neuron.2011.01.001

Wong, R., Piper, M. D. W., Wertheim, B., & Partridge, L. (2009). Quantification of food intake in Drosophila. *PLoS ONE*, *4*(6). https://doi.org/10.1371/journal.pone.0006063

Wu, Q., Zhao, Z., & Shen, P. (2005). Regulation of aversion to noxious food by Drosophila neuropeptide Y- and insulin-like systems. *Nature Neuroscience*, *8*(10), 1350–1355. https://doi.org/10.1038/nn1540

Yapici, N., Cohn, R., Schusterreiter, C., Ruta, V., & Vosshall, L. B. (2016). A Taste Circuit that Regulates Ingestion by Integrating Food and Hunger Signals. *Cell*, *165*(3), 715–729. https://doi.org/10.1016/j.cell.2016.02.061

Youn, H., Kirkhart, C., Chia, J., & Scott, K. (2018). A subset of octopaminergic neurons that promotes feeding initiation in drosophila melanogaster. *PLoS ONE*, *13*(6), 1–16. https://doi.org/10.1371/journal.pone.0198362

Zhang, Y. V, Ni, J., & Montell, C. (2013). The Molecular Basis for Attractive Salt-Taste Coding in Drosophila. *Science*, *340*(June), 1334–1339.

Appendices

Appendix A

Legend

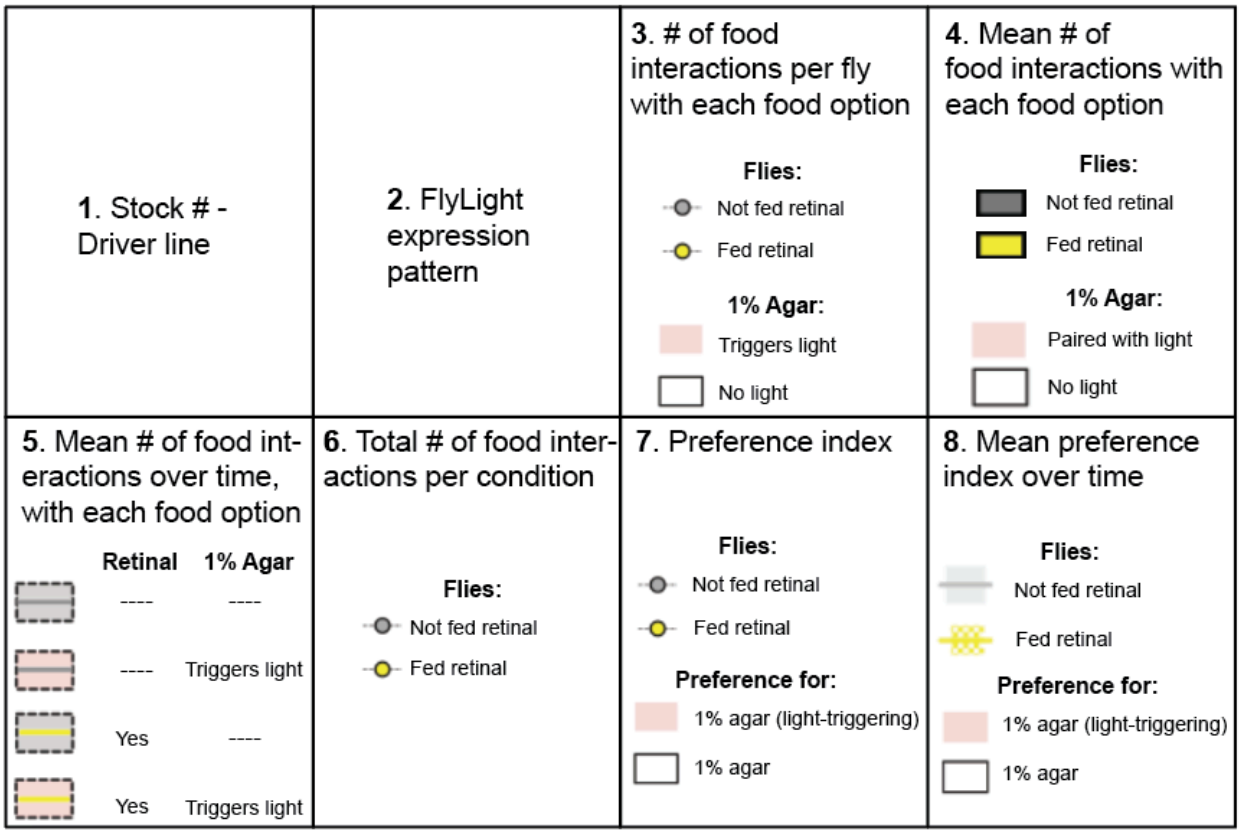

1.

40730 -

w[1118];P{y[+t7.7] w[+mC]=GMR9D10 -GAL4}attP2

2.

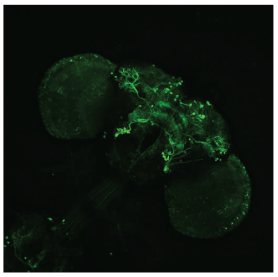

3.

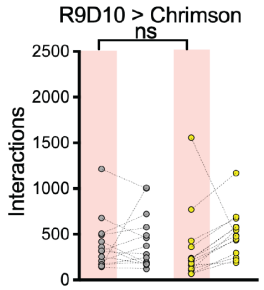

4.

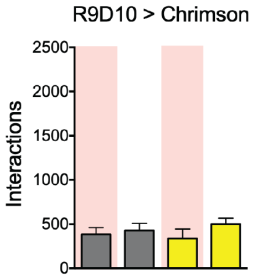

5.

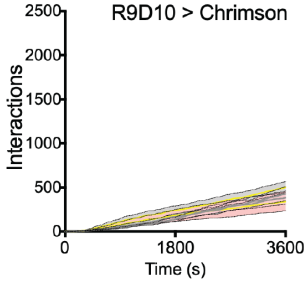

6.

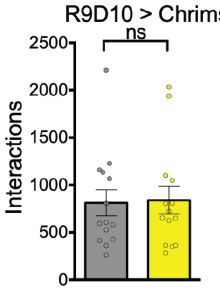

7.

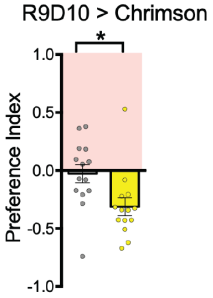

8.

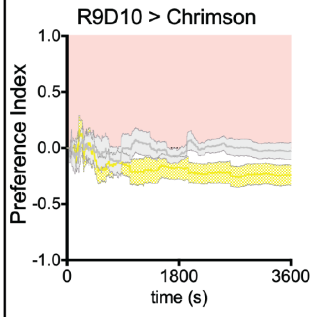

1.

40731 -

w[1118]; P{y[+t7.7] w[+mC]=GMR9D11 -GAL4}attP2

2.

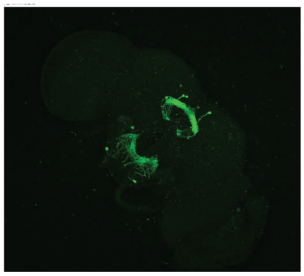

3.

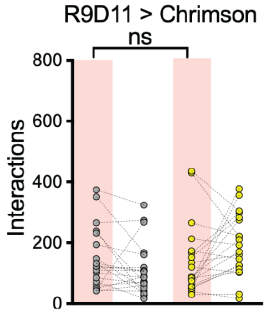

4.

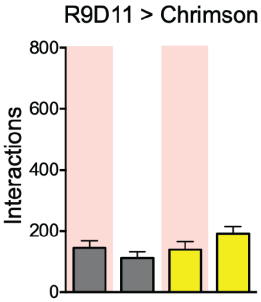

5.

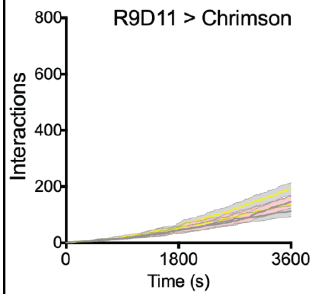

6.

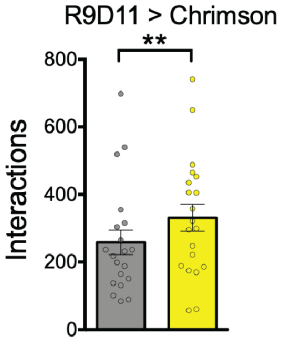

7.

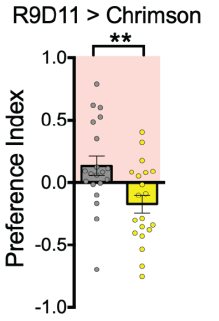

8.

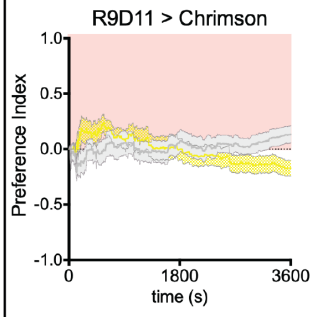

1.

48238 -

w[1118]; P{y[+t7.7] w[+mC]=GMR10A09 -GAL4}attP2

2.

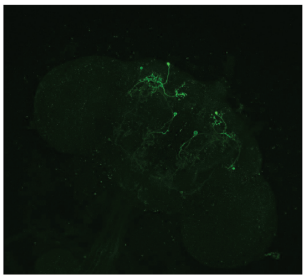

3.

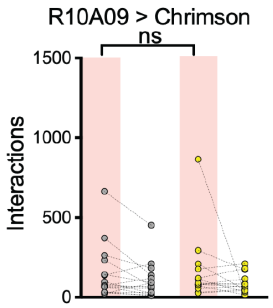

4.

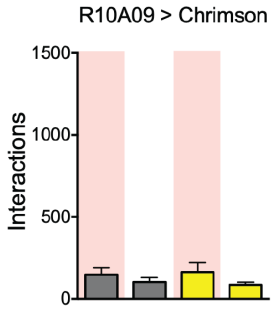

5.

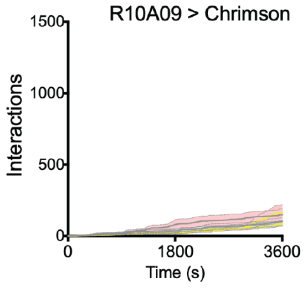

6.

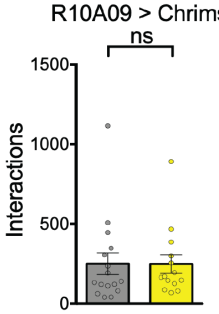

7.

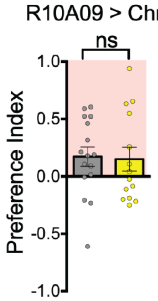

8.

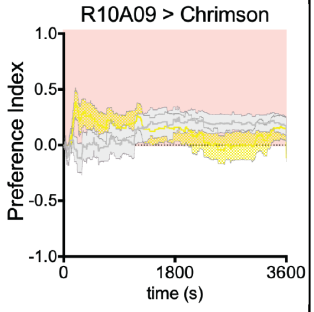

1.

48445 -

w[1118]; P{y[+t7.7] w[+mC]=GMR10H10 -GAL4}attP2

2.

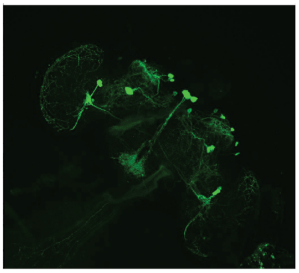

3.

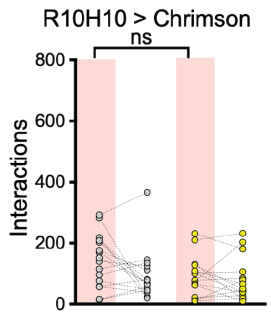

4.

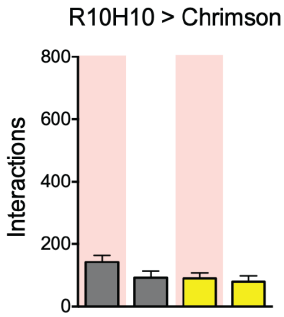

5.

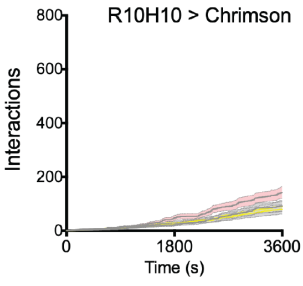

6.

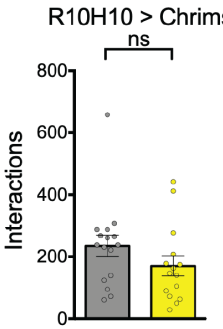

7.

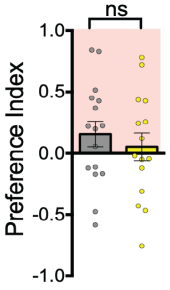

8.

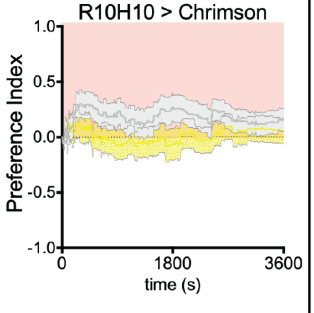

1.

48486 -

w[1118]; P{y[+t7.7] w[+mC]=GMR12A12 -GAL4}attP2

2.

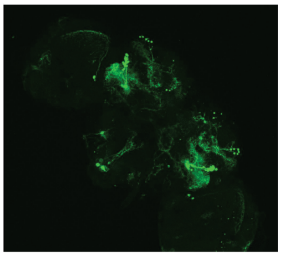

3.

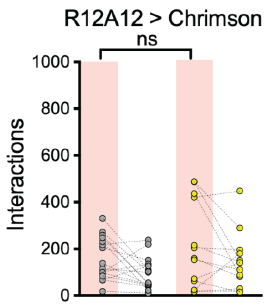

4.

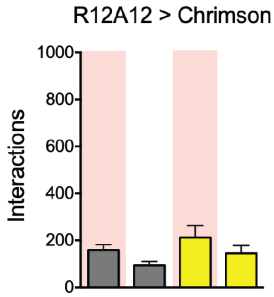

5.

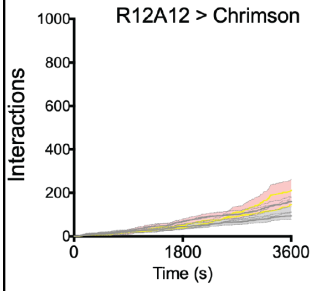

6.

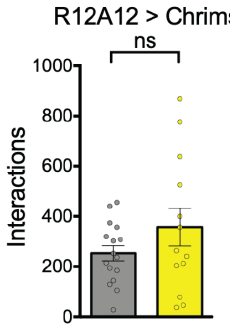

7.

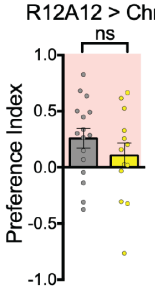

8.

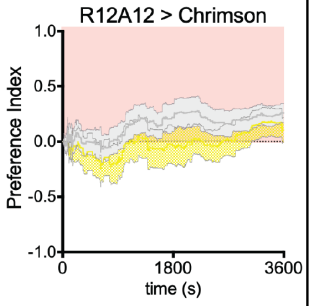

1.

48487 -

w[1118]; P{y[+t7.7] w[+mC]=GMR12B01 -GAL4}attP2

2.

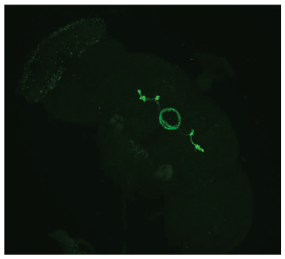

3.

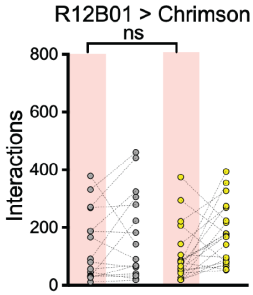

4.

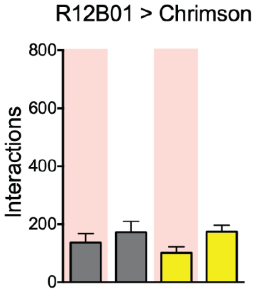

5.

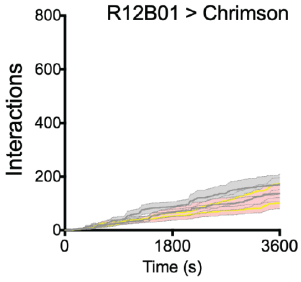

6.

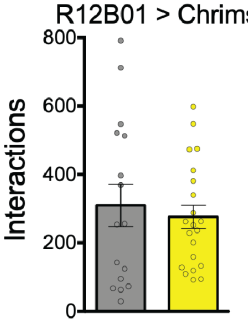

7.

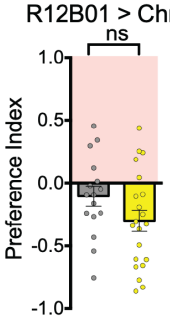

8.

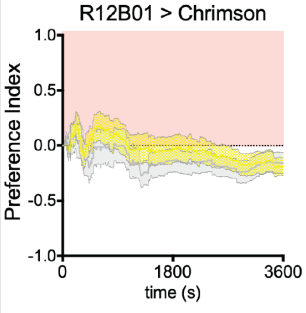

1.

48503 -

w[1118]; P{y[+t7.7] w[+mC]=GMR12D09 -GAL4}attP2

2.

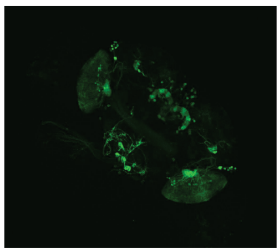

3.

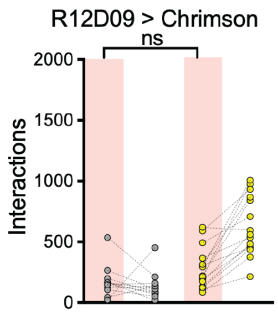

4.

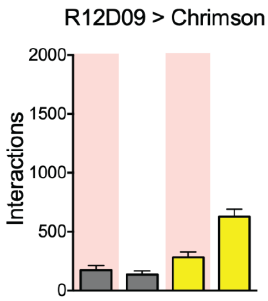

5.

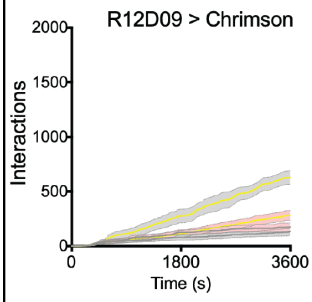

6.

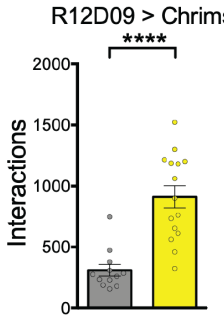

7.

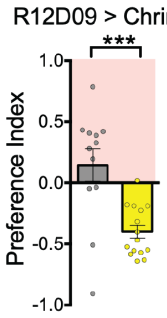

8.

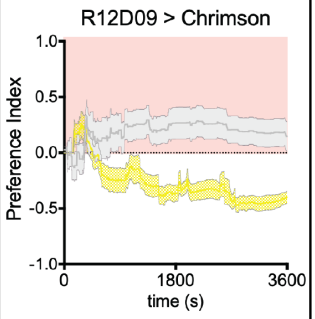

1.

48510 -

w[1118]; P{y[+t7.7] w[+mC]=GMR12E09 -GAL4}attP2

2.

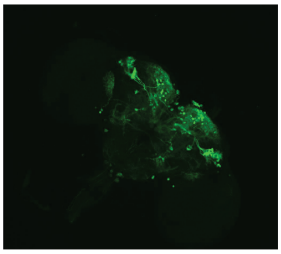

3.

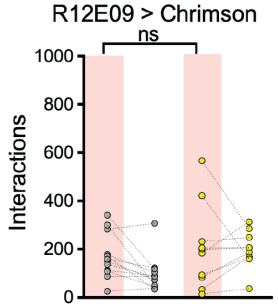

4.

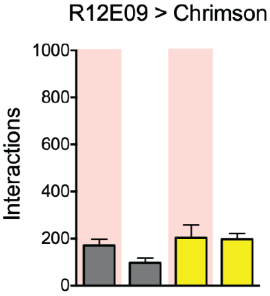

5.

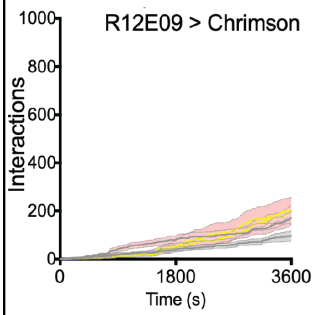

6.

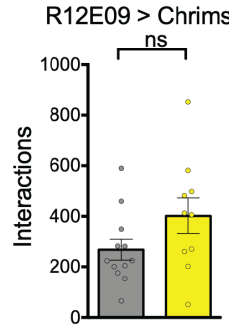

7.

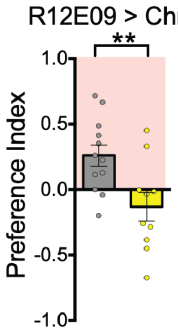

8.

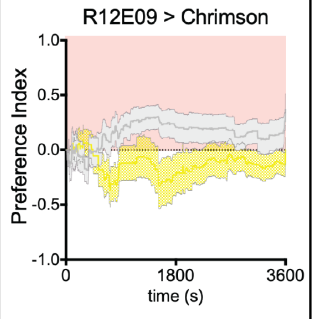

1.

48546 -

w[1118]; P{y[+t7.7] w[+mC]=GMR13B08 -GAL4}attP2

2.

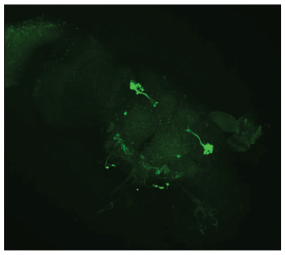

3.

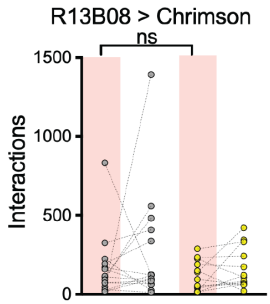

4.

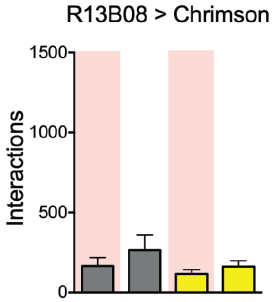

5.

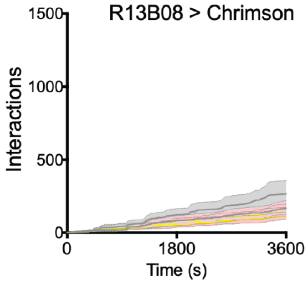

6.

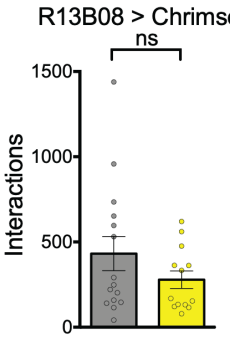

7.

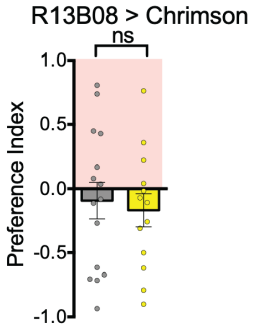

8.

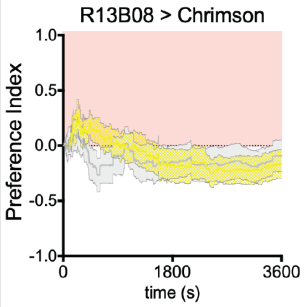

1.

48648 -

w[1118]; P{y[+t7.7] w[+mC]=GMR14F03 -GAL4}attP2

2.

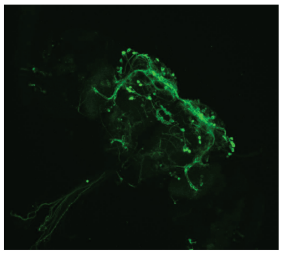

3.

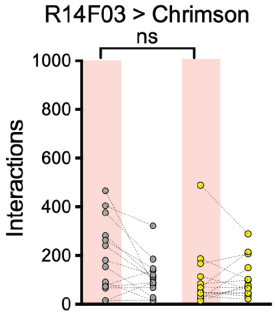

4.

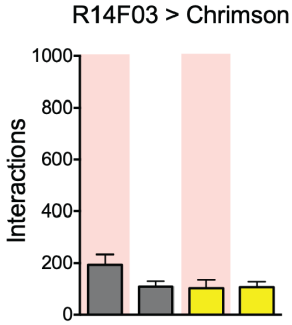

5.

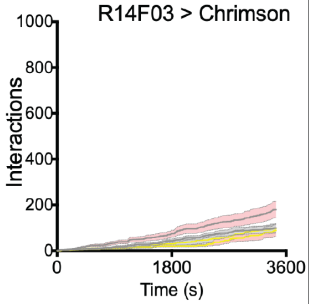

6.

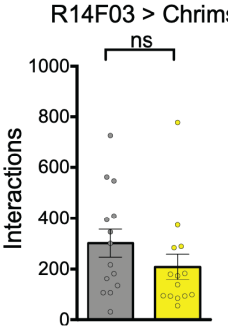

7.

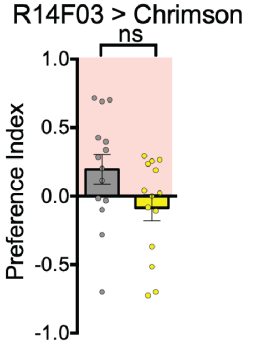

8.

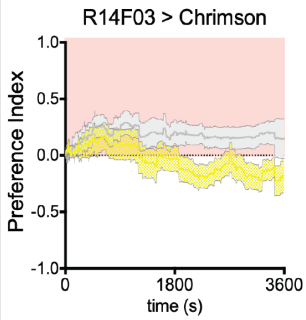

1.

48657 -

w[1118]; P{y[+t7.7] w[+mC]=GMR14G03 -GAL4}attP2

2.

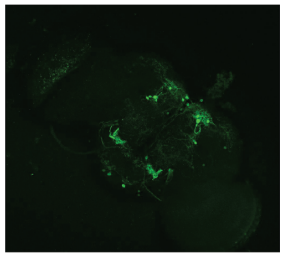

3.

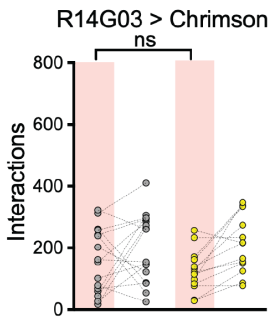

4.

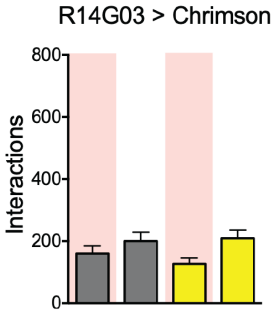

5.

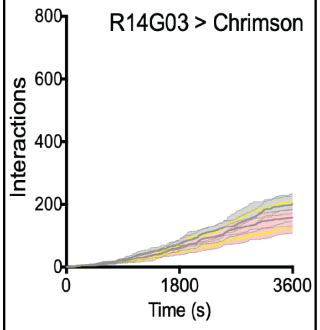

6.

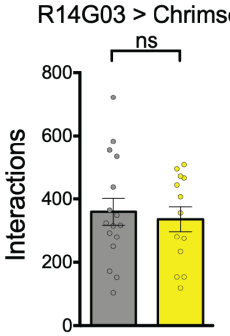

7.

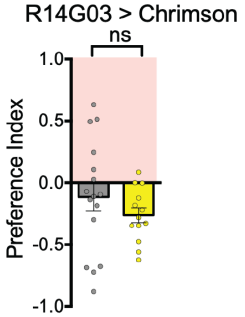

8.

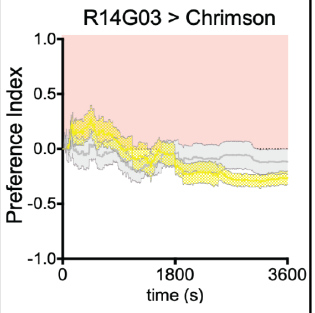

1.

48670 -

w[1118]; P{y[+t7.7] w[+mC]=GMR15A01 -GAL4}attP2

2.

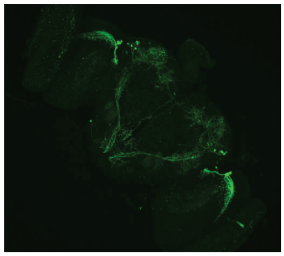

3.

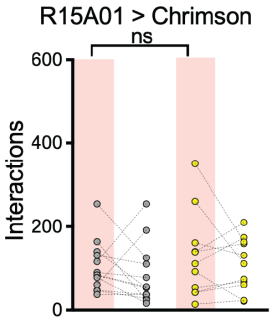

4.

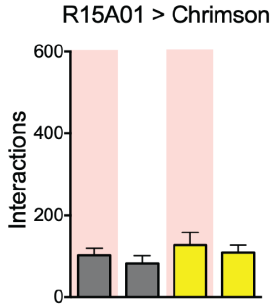

5.

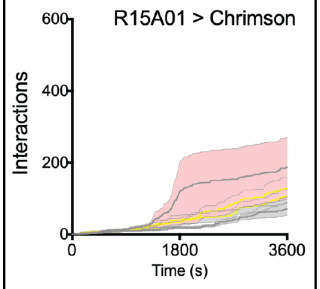

6.

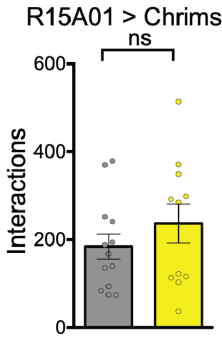

7.

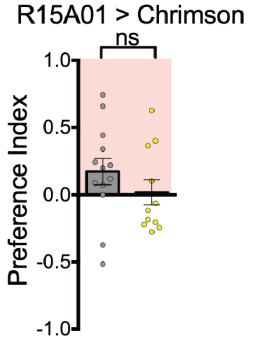

8.

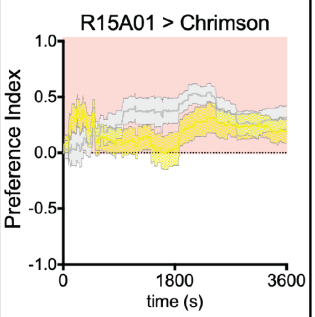

1.

49264 -

w[1118]; P{y[+t7.7] w[+mC]=GMR15C12 -GAL4}attP2

2.

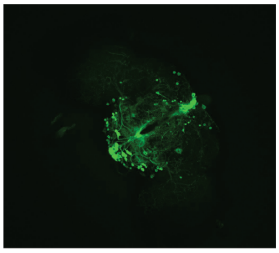

3.

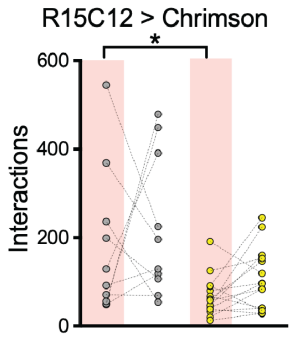

4.

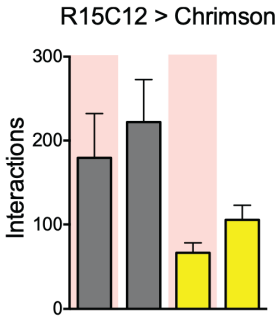

5.

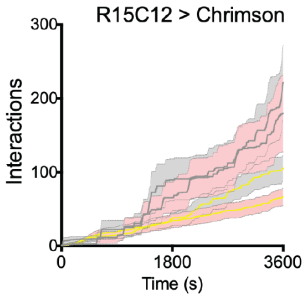

6.

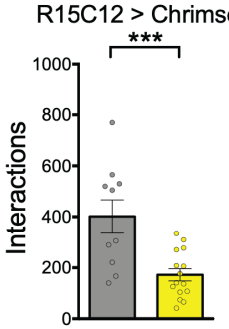

7.

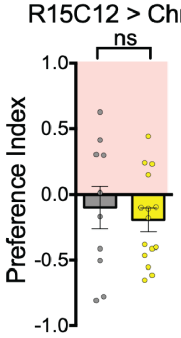

8.

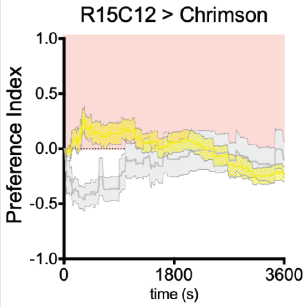

1.

48722 -

w[1118]; P{y[+t7.7] w[+mC]=GMR16D01 -GAL4}attP2

2.

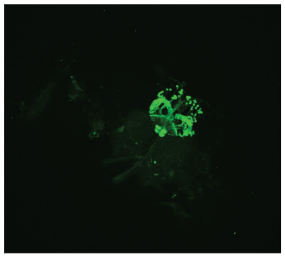

3.

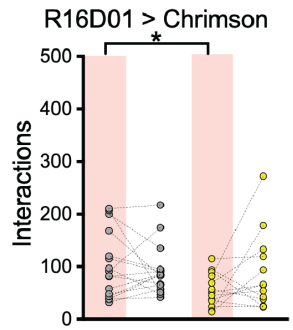

4.

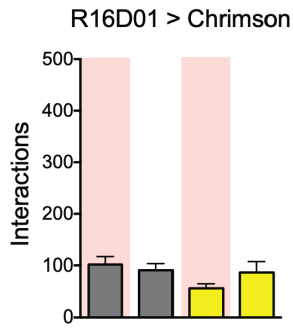

5.

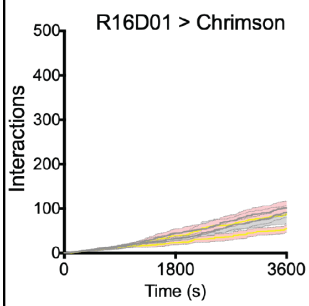

6.

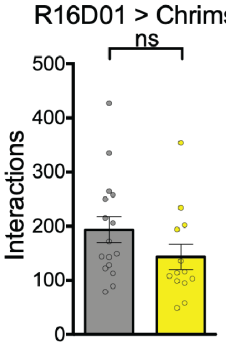

7.

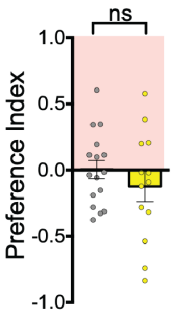

8.

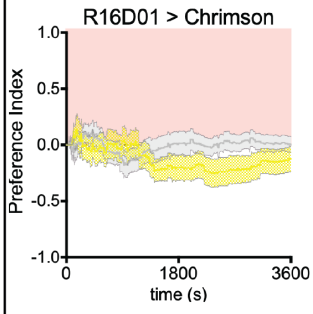

1.

48729 -

w[1118]; P{y[+t7.7] w[+mC]=GMR16E11 -GAL4}attP2

2.

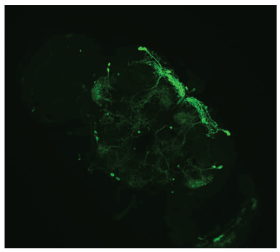

3.

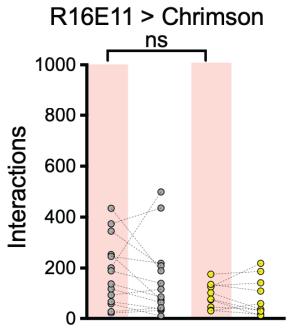

4.

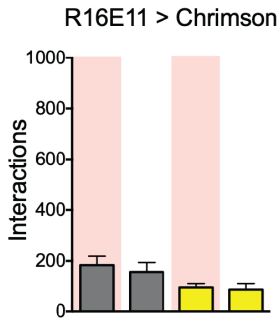

5.

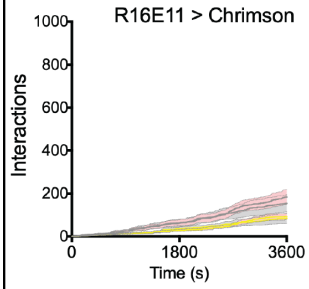

6.

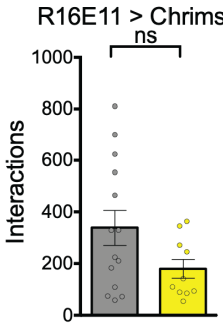

7.

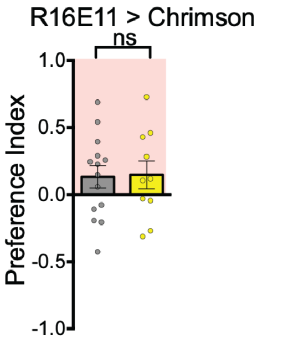

8.

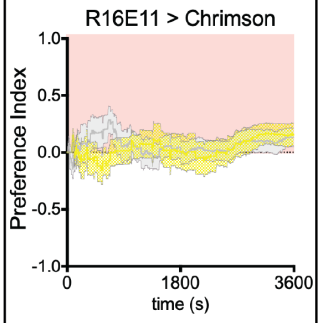

1.

48751 -

w[1118]; P{y[+t7.7] w[+mC]=GMR17A10 -GAL4}attP2

2.

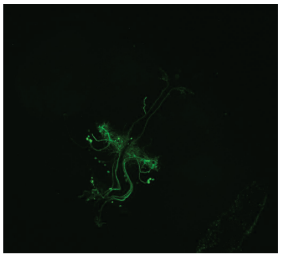

3.

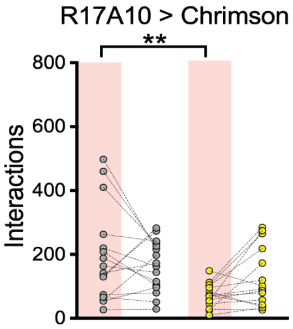

4.

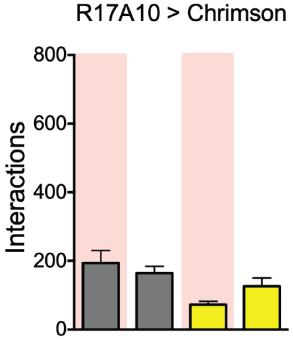

5.

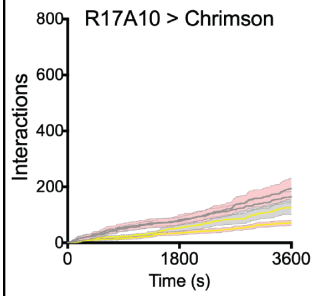

6.

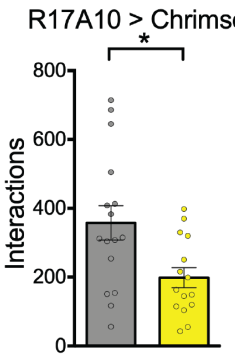

7.

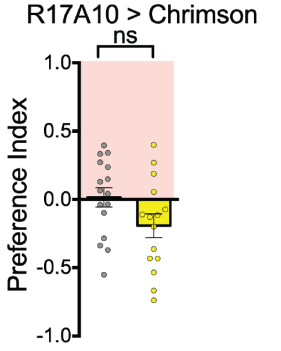

8.

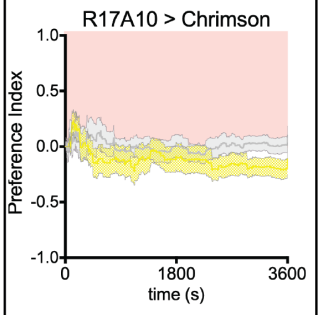

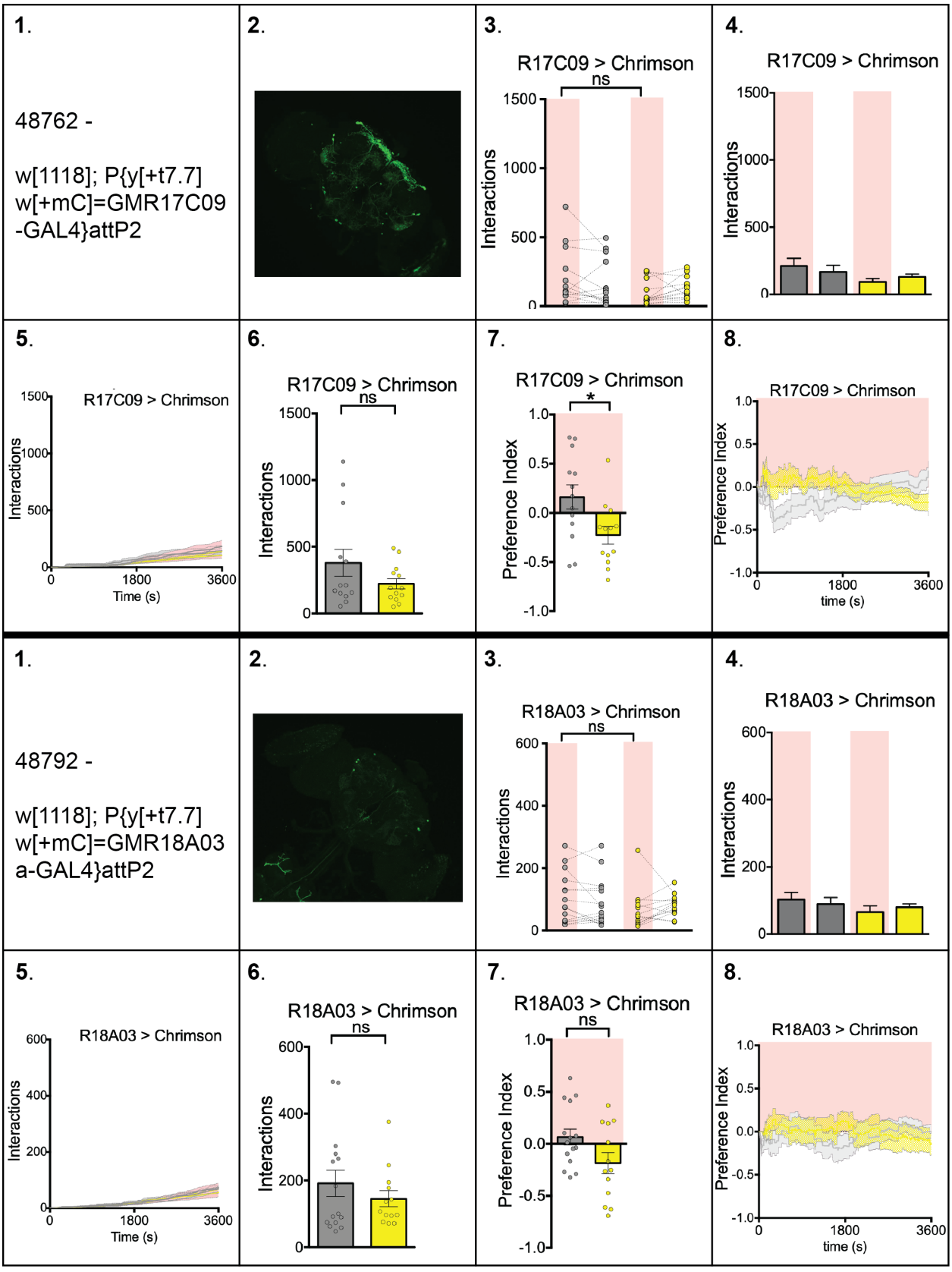
1.
48762 -
w[1118]; P{y[+t7.7] w[+mC]=GMR17C09 -GAL4}attP2
2.
3.
R17C09 > Chrimson
ns
Interactions
4.
R17C09 > Chrimson
Interactions
5.
R17C09 > Chrimson
Interactions
Time (s)
6.
R17C09 > Chrimson
ns
Interactions
7.
R17C09 > Chrimson
*
Preference Index
8.
R17C09 > Chrimson
Preference Index
time (s)
1.
48792 -
w[1118]; P{y[+t7.7] w[+mC]=GMR18A03 a-GAL4}attP2
2.
3.
R18A03 > Chrimson
ns
Interactions
4.
R18A03 > Chrimson
Interactions
5.
R18A03 > Chrimson
Interactions
Time (s)
6.
R18A03 > Chrimson
ns
Interactions
7.
R18A03 > Chrimson
ns
Preference Index
8.
R18A03 > Chrimson
Preference Index
time (s)

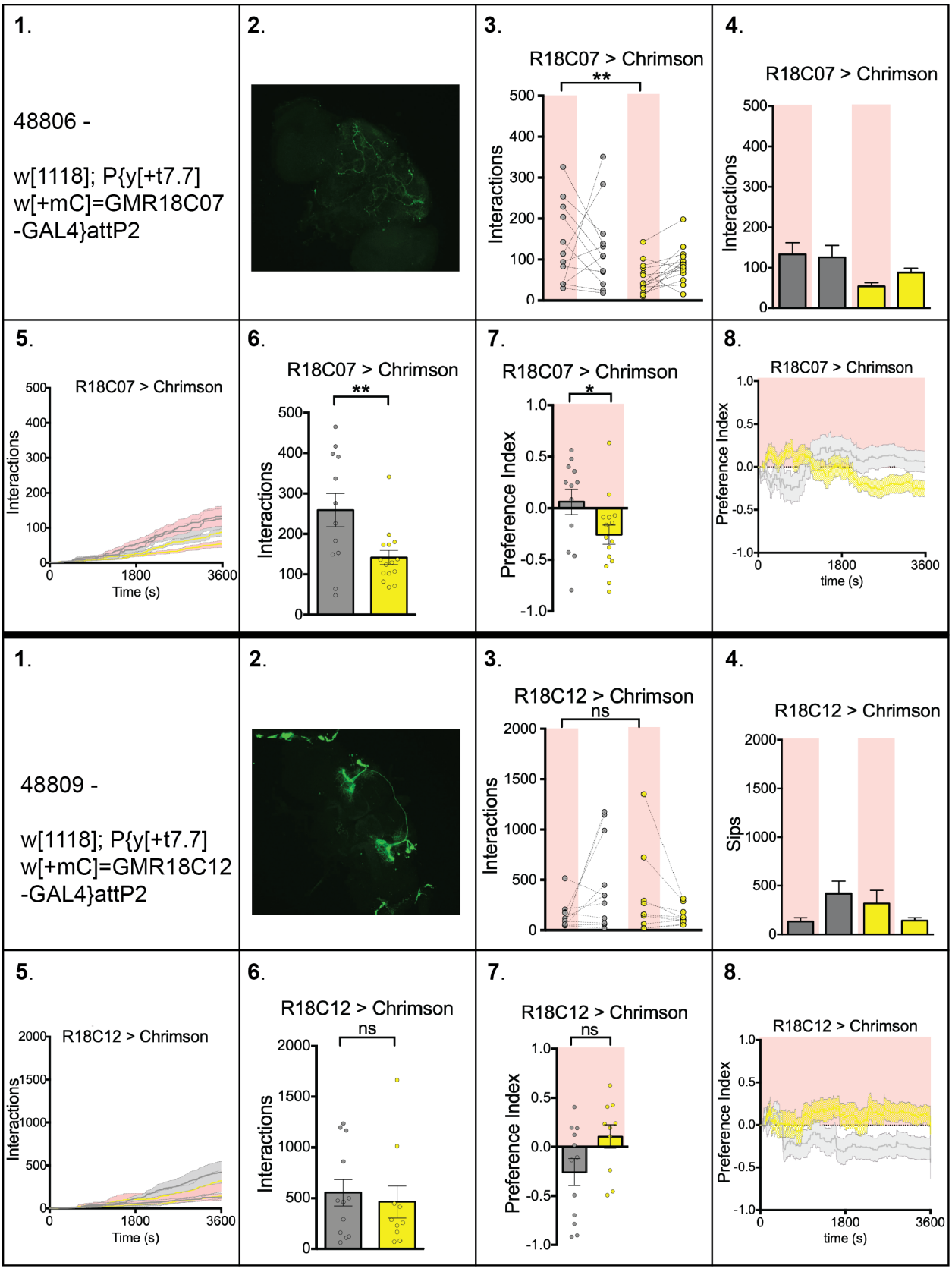
1.
48806 -
w[1118]; P{y[+t7.7]
w[+mC]=GMR18C07
-GAL4}attP2
2.
3.
R18C07 > Chrimson
**
Interactions
4.
R18C07 > Chrimson
Interactions
5.
R18C07 > Chrimson
Interactions
Time (s)
6.
R18C07 > Chrimson
**
Interactions
7.
R18C07 > Chrimson
*
Preference Index
8.
R18C07 > Chrimson
Preference Index
time (s)
1.
48809 -
w[1118]; P{y[+t7.7]
w[+mC]=GMR18C12
-GAL4}attP2
2.
3.
R18C12 > Chrimson
ns
Interactions
4.
R18C12 > Chrimson
Sips
5.
R18C12 > Chrimson
Interactions
Time (s)
6.
R18C12 > Chrimson
ns
Interactions
7.
R18C12 > Chrimson
ns
Preference Index
8.
R18C12 > Chrimson
Preference Index
time (s)

1.

48832 -

w[1118]; P{y[+t7.7] w[+mC]=GMR18H11 -GAL4}attP2

2.

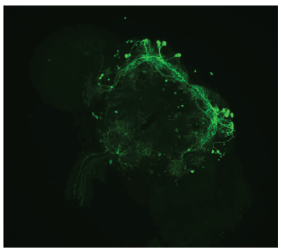

3.

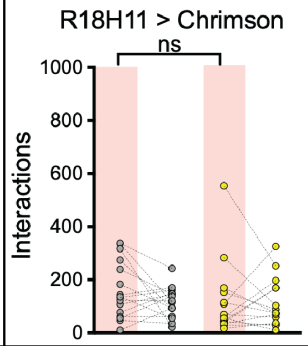

4.

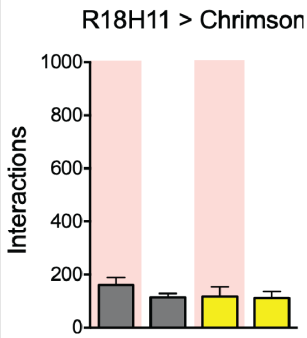

5.

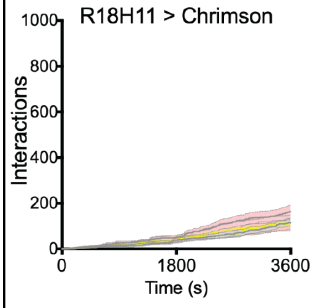

6.

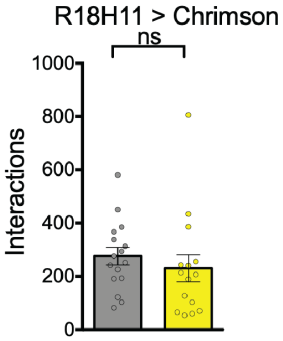

7.

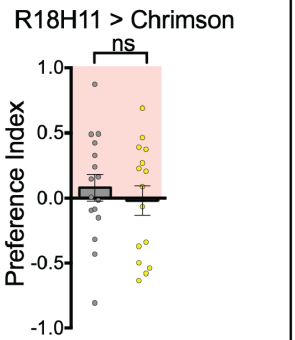

8.

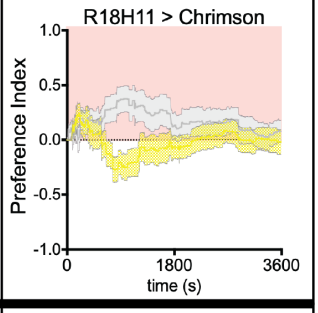

1.

48609 -

w[1118]; P{y[+t7.7] w[+mC]=GMR19B06 -GAL4}attP2

2.

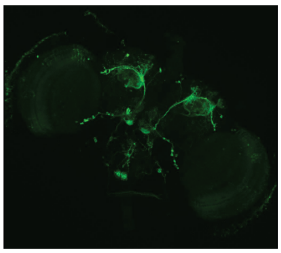

3.

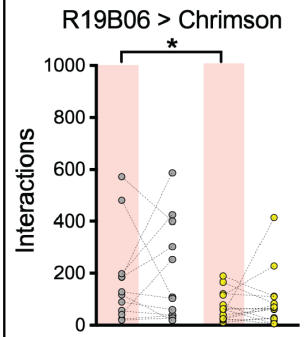

4.

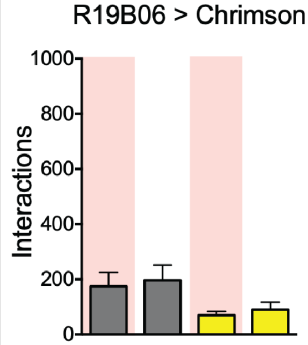

5.

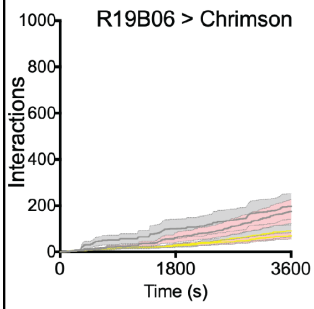

6.

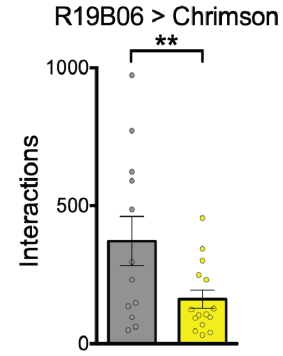

7.

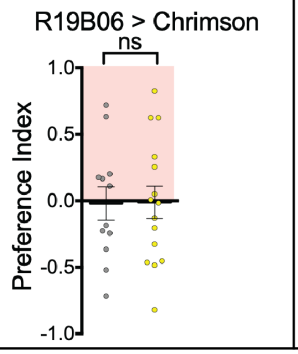

8.

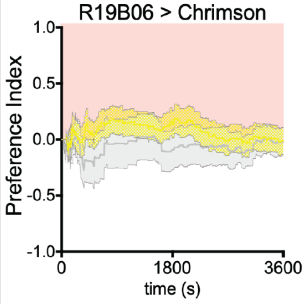

1.

48843 -

w[1118]; P{y[+t7.7] w[+mC]=GMR19C06 -GAL4}attP2

2.

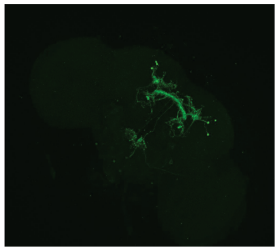

3.

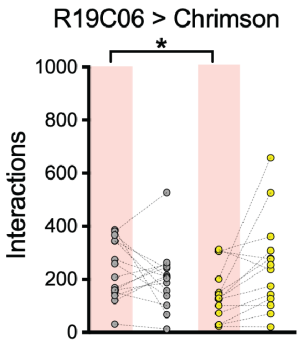

4.

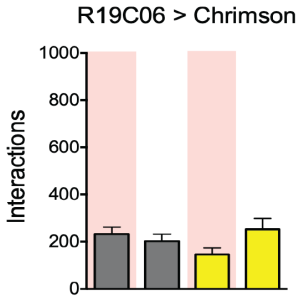

5.

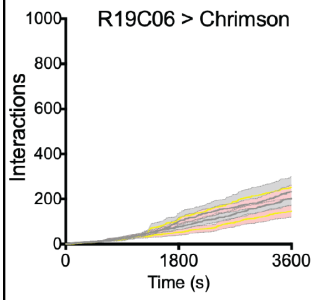

6.

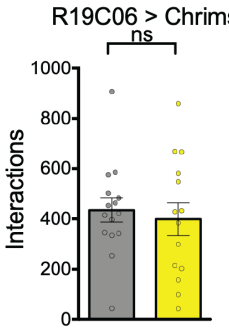

7.

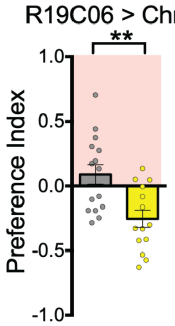

8.

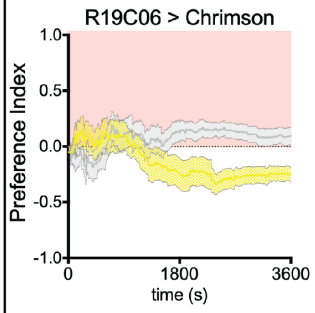

1.

48850 -

w[1118]; P{y[+t7.7] w[+mC]=GMR19E06 -GAL4}attP2

2.

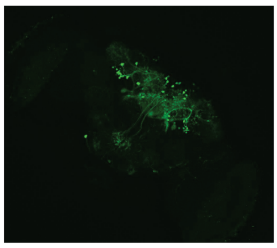

3.

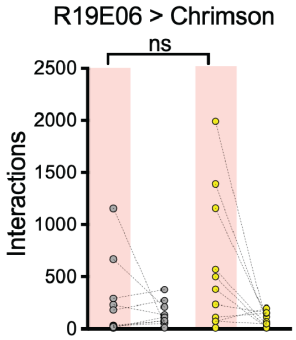

4.

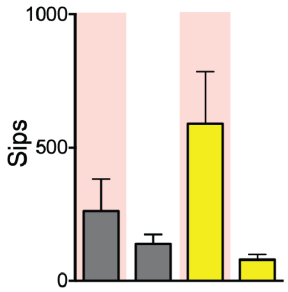

5.

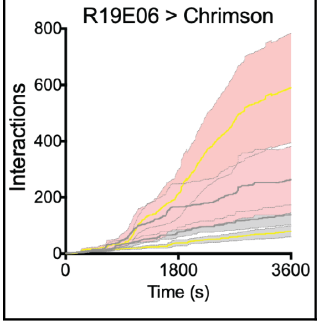

6.

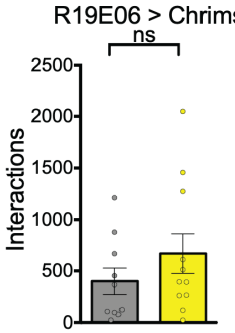

7.

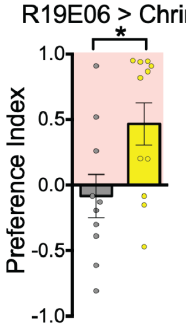

8.

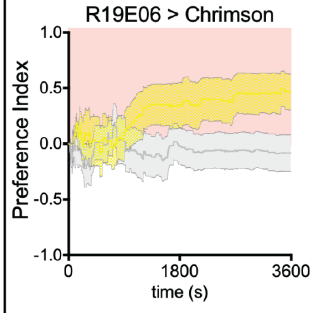

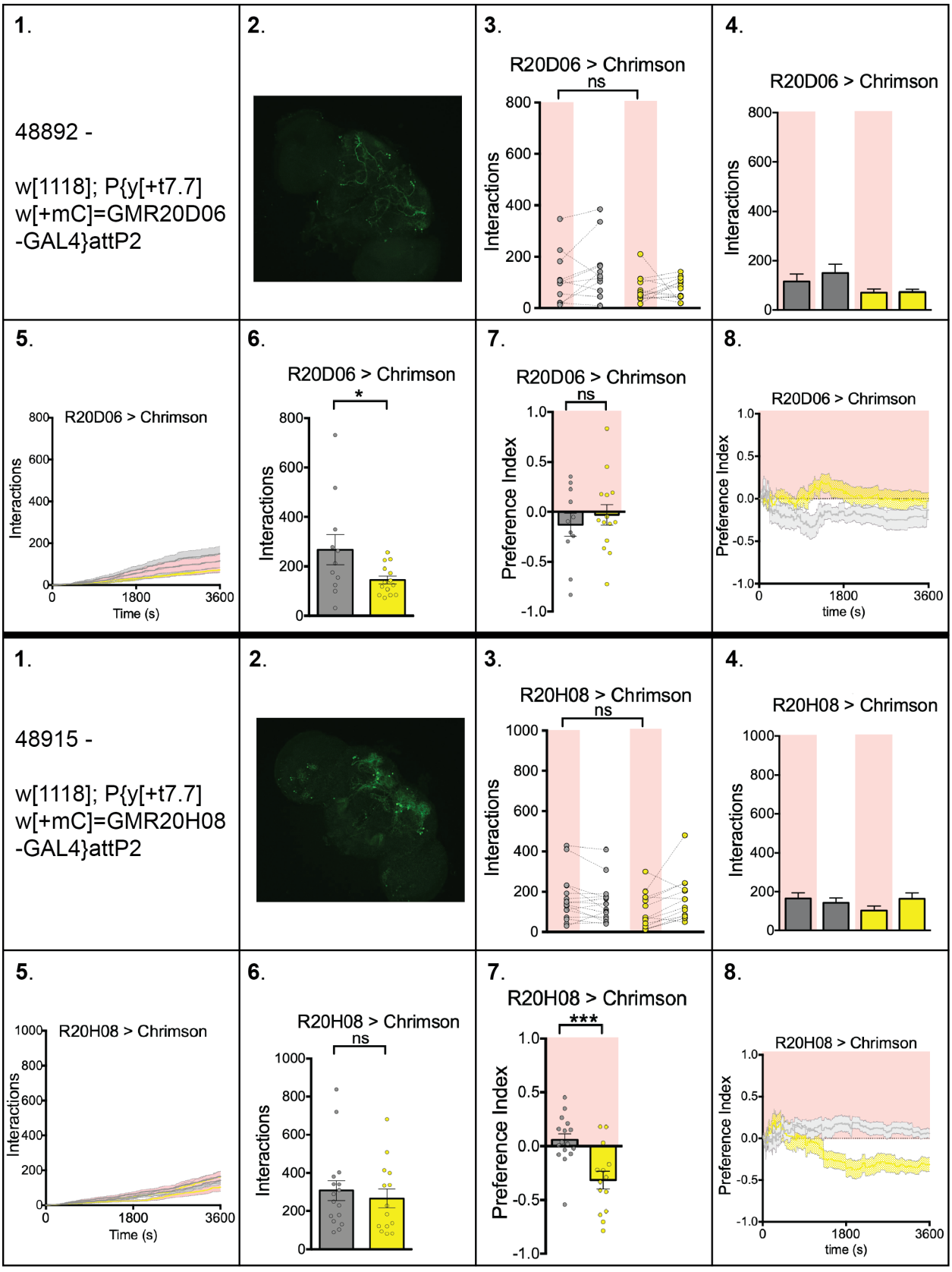
1.
48892 -
w[1118]; P{y[+t7.7] w[+mC]=GMR20D06 -GAL4}attP2
2.
3.
R20D06 > Chrimson
ns
Interactions
4.
R20D06 > Chrimson
Interactions
5.
R20D06 > Chrimson
Interactions
Time (s)
6.
R20D06 > Chrimson
*
Interactions
7.
R20D06 > Chrimson
ns
Preference Index
8.
R20D06 > Chrimson
Preference Index
time (s)
1.
48915 -
w[1118]; P{y[+t7.7] w[+mC]=GMR20H08 -GAL4}attP2
2.
3.
R20H08 > Chrimson
ns
Interactions
4.
R20H08 > Chrimson
Interactions
5.
R20H08 > Chrimson
Interactions
Time (s)
6.
R20H08 > Chrimson
ns
Interactions
7.
R20H08 > Chrimson
***
Preference Index
8.
R20H08 > Chrimson
Preference Index
time (s)

1.

48948 -

w[1118]; P{y[+t7.7] w[+mC]=GMR21E09 -GAL4}attP2

2.

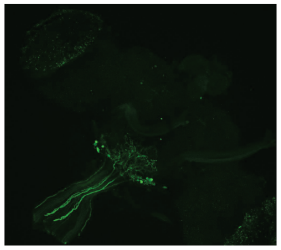

3.

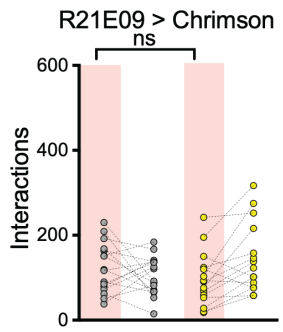

4.

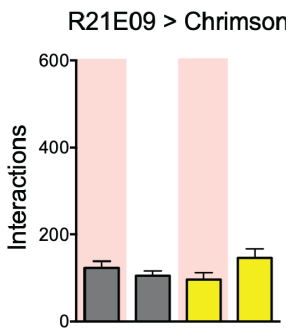

5.

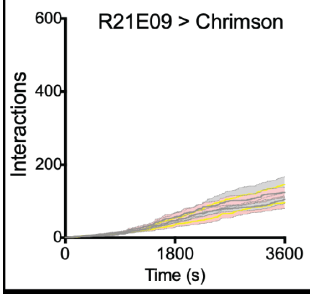

6.

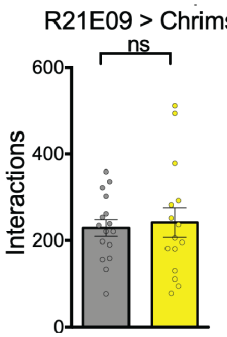

7.

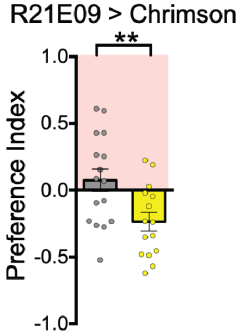

8.

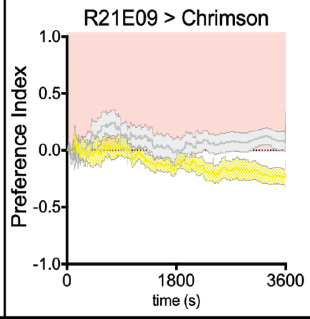

1.

48960 -

w[1118]; P{y[+t7.7] w[+mC]=GMR21H11 -GAL4}attP2

2.

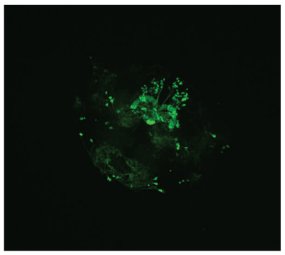

3.

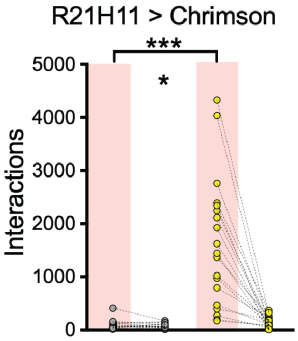

4.

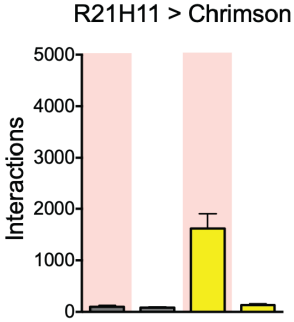

5.

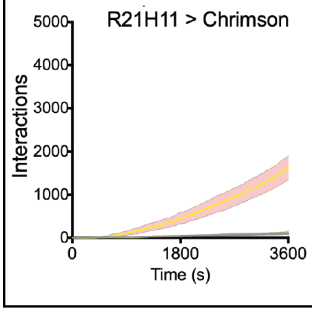

6.

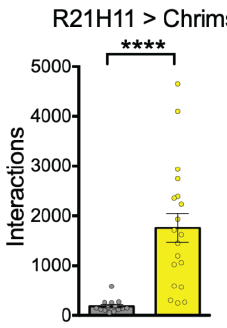

7.

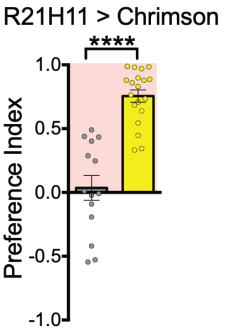

8.

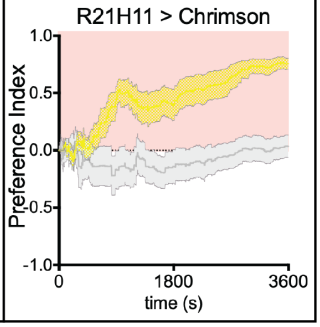

1.

48982 -

w[1118]; P{y[+t7.7] w[+mC]=GMR22D11 -GAL4}attP2

2.

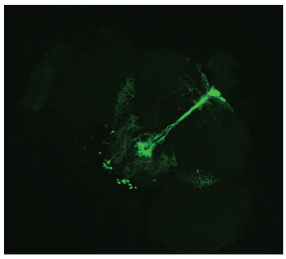

3.

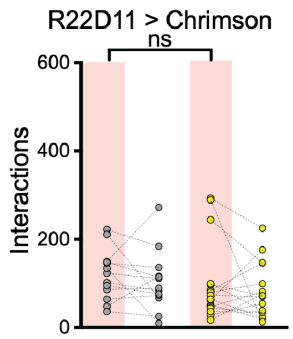

4.

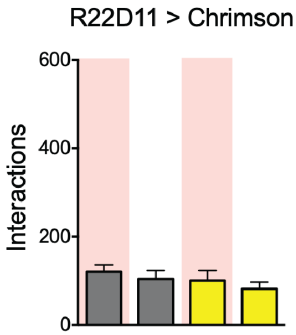

5.

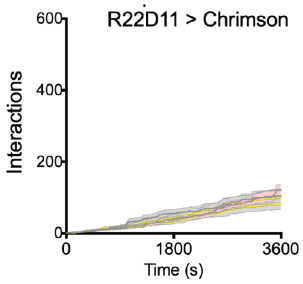

6.

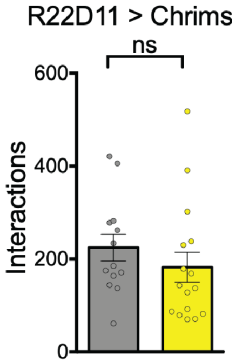

7.

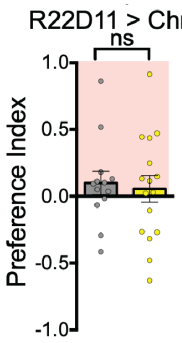

8.

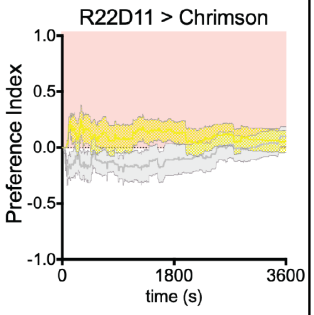

1.

48996 -

w[1118]; P{y[+t7.7] w[+mC]=GMR22G01 -GAL4}attP2

2.

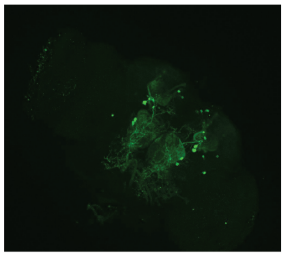

3.

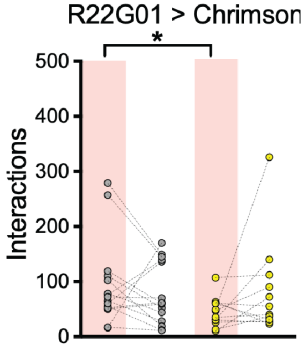

4.

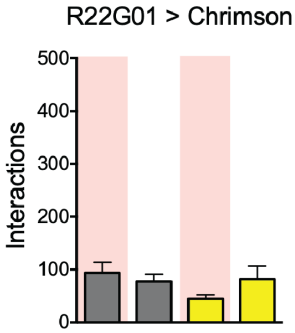

5.

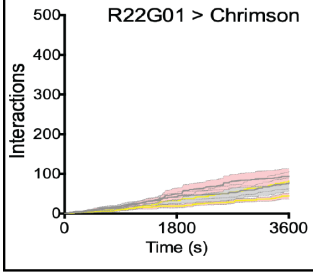

6.

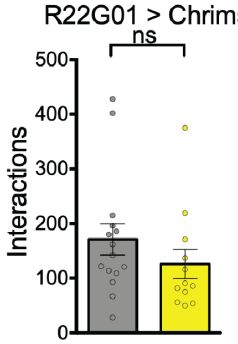

7.

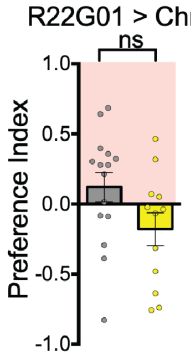

8.

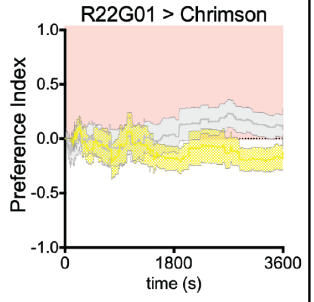

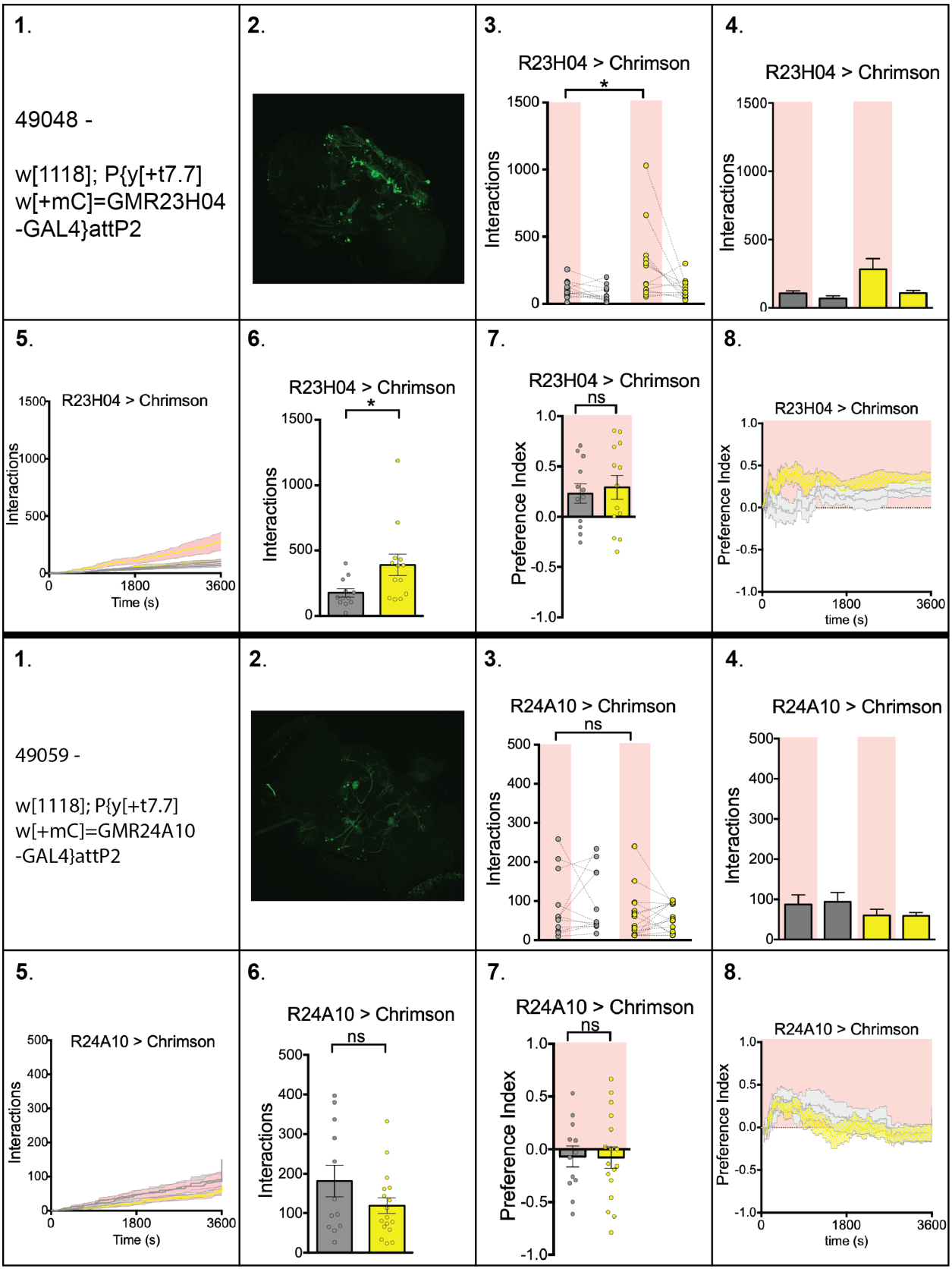
1.
49048 -
w[1118]; P{y[+t7.7]
w[+mC]=GMR23H04
-GAL4}attP2
2.
3.
R23H04 > Chrimson
*
Interactions
1500
1000
500
0
4.
R23H04 > Chrimson
Interactions
5.
R23H04 > Chrimson
Interactions
Time (s)
0
1800
3600
6.
R23H04 > Chrimson
*
Interactions
7.
R23H04 > Chrimson
ns
Preference Index
1.0
0.5
0.0
-0.5
-1.0
8.
R23H04 > Chrimson
Preference Index
time (s)
1.
49059 -
w[1118]; P{y[+t7.7]
w[+mC]=GMR24A10
-GAL4}attP2
2.
3.
R24A10 > Chrimson
ns
Interactions
500
400
300
200
100
0
4.
R24A10 > Chrimson
Interactions
5.
R24A10 > Chrimson
Interactions
Time (s)
0
1800
3600
6.
R24A10 > Chrimson
ns
Interactions
7.
R24A10 > Chrimson
ns
Preference Index
1.0
0.5
0.0
-0.5
-1.0
8.
R24A10 > Chrimson
Preference Index
time (s)

1. 49313 - w[1118]; P{y[+t7.7] w[+mC]=GMR24C05 -GAL4}attP2	**2.** 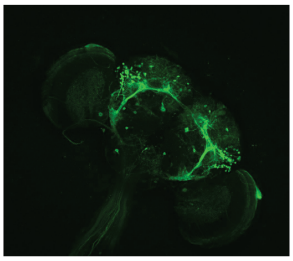	**3.** 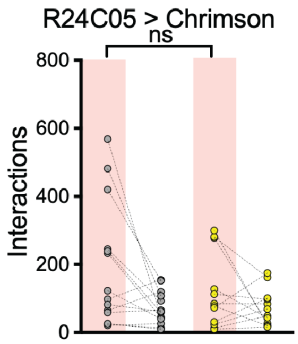	**4.** 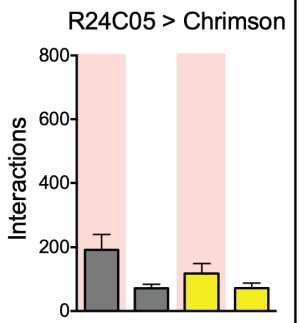
5. 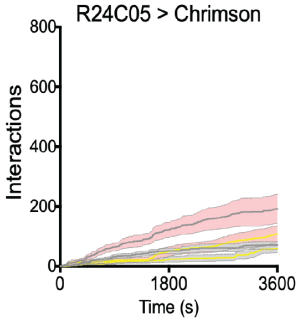	**6.** 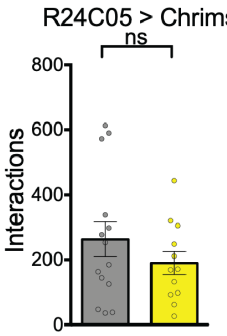	**7.** 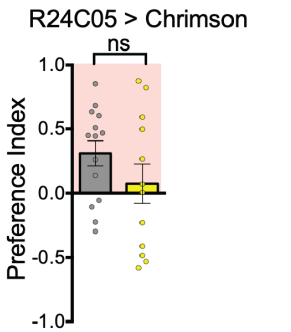	**8.** 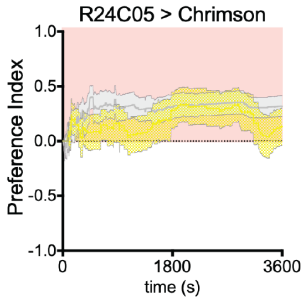
1. 49074 - w[1118]; P{y[+t7.7] w[+mC]=GMR24C07 -GAL4}attP2	**2.** 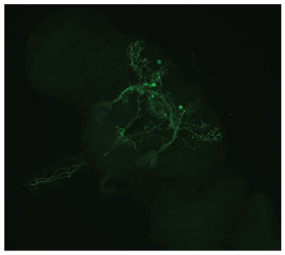	**3.** 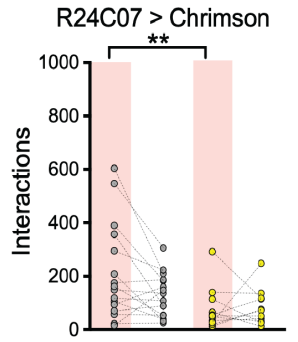	**4.** 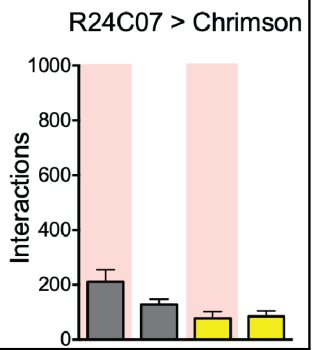
5. 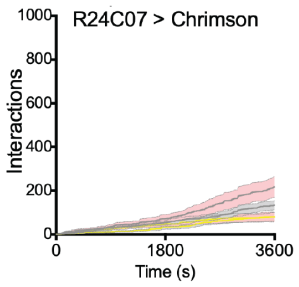	**6.** 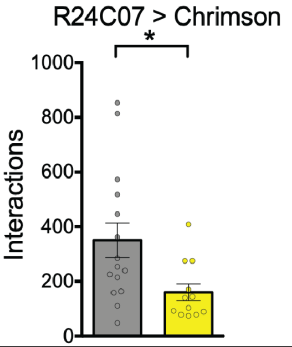	**7.** 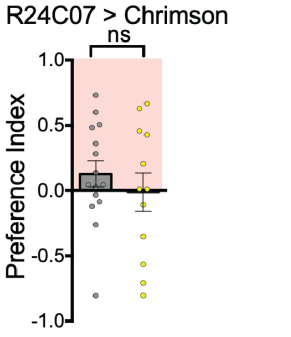	**8.** 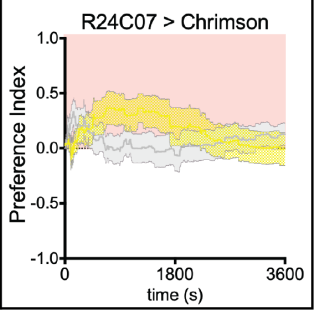

1.

49081 -

w[1118]; P{y[+t7.7] w[+mC]=GMR24E05 -GAL4}attP2

2.

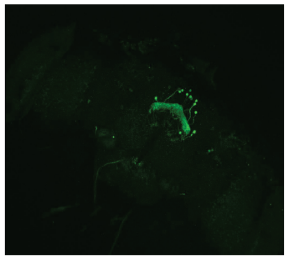

3.

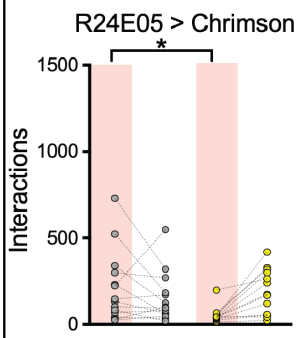

4.

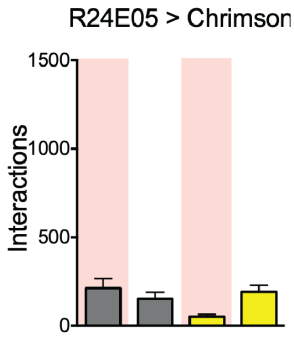

5.

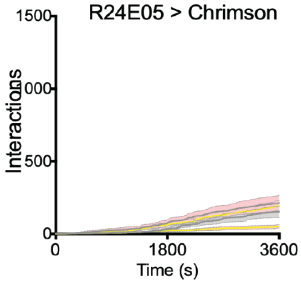

6.

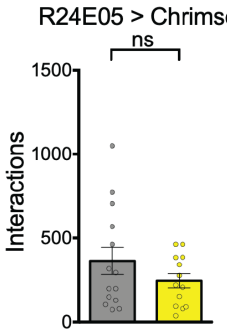

7.

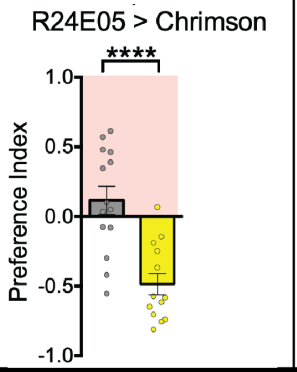

8.

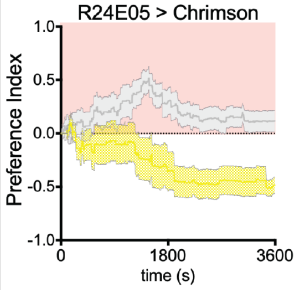

1.

49083 -

w[1118]; P{y[+t7.7] w[+mC]=GMR24E09 -GAL4}attP2

2.

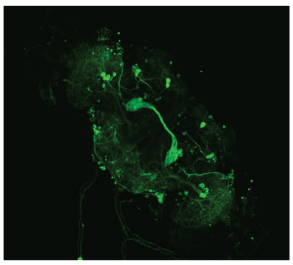

3.

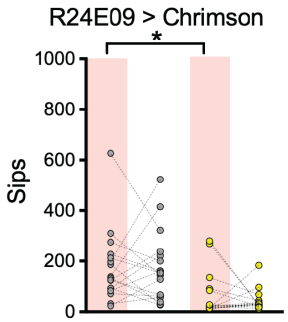

4.

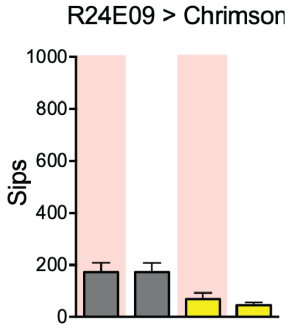

5.

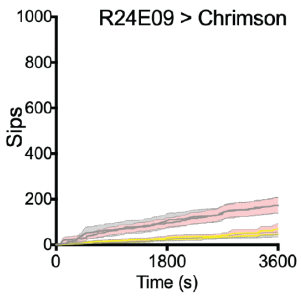

6.

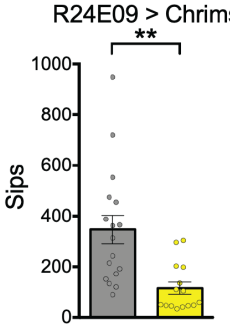

7.

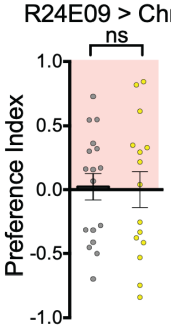

8.

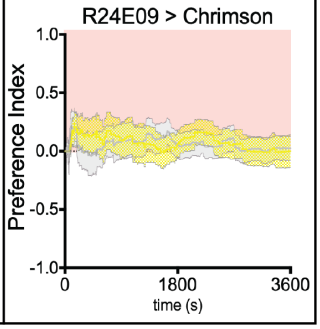

1.

49097 -

w[1118]; P{y[+t7.7] w[+mC]=GMR24H02 -GAL4}attP2

2.

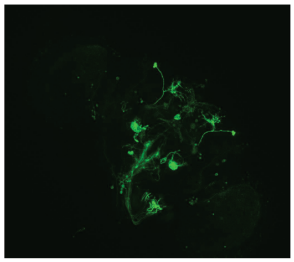

3.

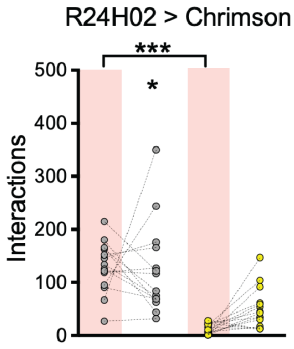

4.

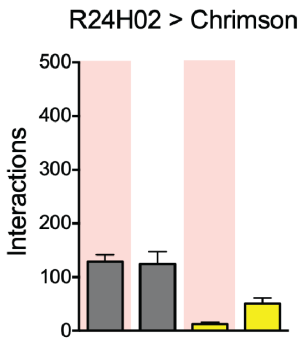

5.

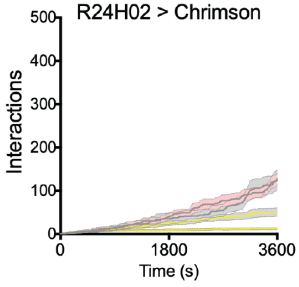

6.

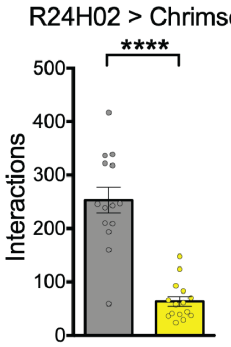

7.

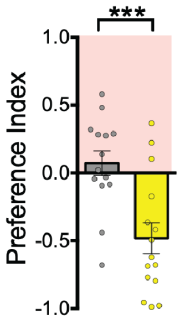

8.

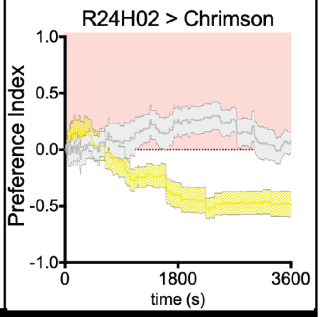

1.

49100 -

w[1118]; P{y[+t7.7] w[+mC]=GMR24H08 -GAL4}attP2

2.

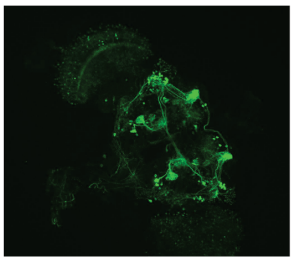

3.

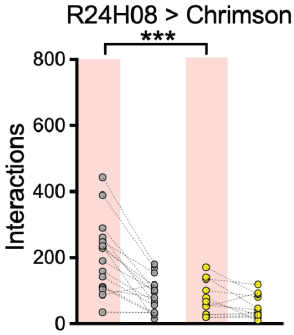

4.

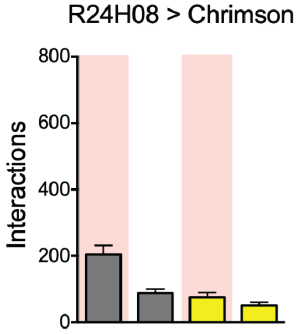

5.

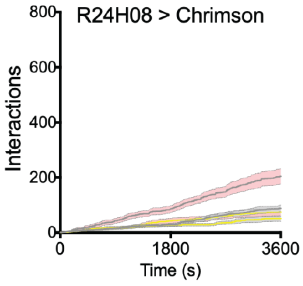

6.

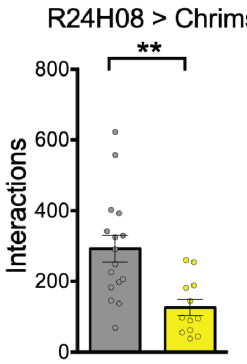

7.

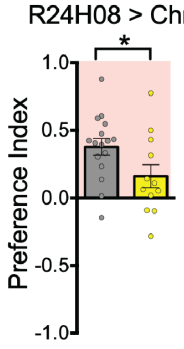

8.

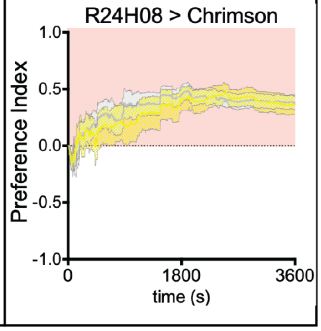

1.

49108 -

w[1118]; P{y[+t7.7] w[+mC]=GMR25B01 -GAL4}attP2

2.

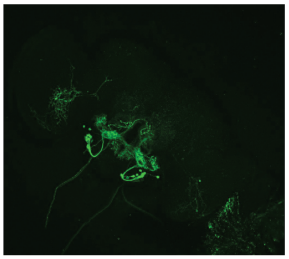

3.

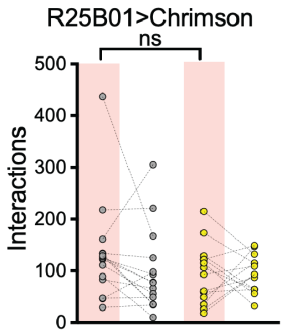

4.

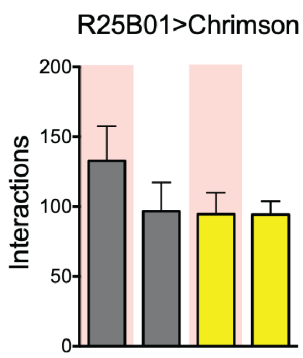

5.

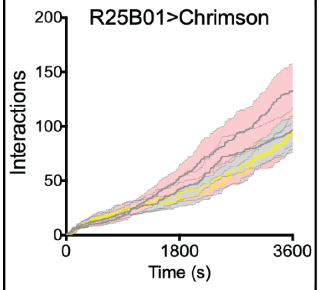

6.

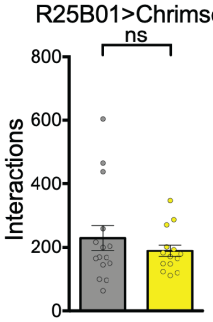

7.

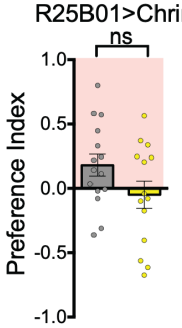

8.

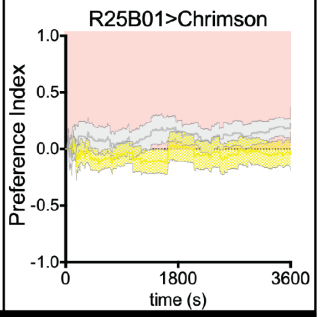

1.

49112 -

w[1118]; P{y[+t7.7] w[+mC]=GMR25B07 -GAL4}attP2

2.

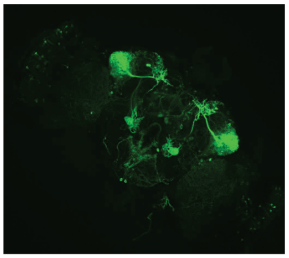

3.

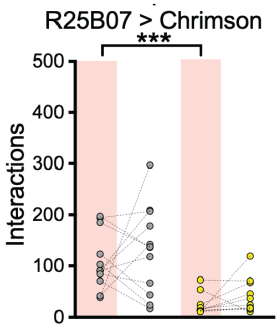

4.

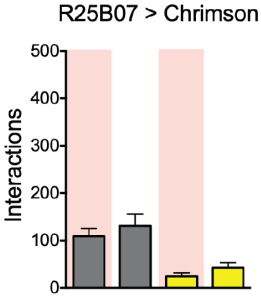

5.

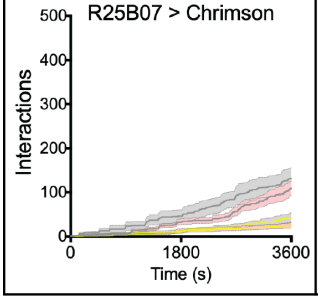

6.

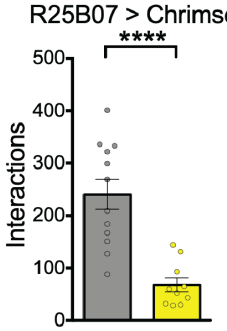

7.

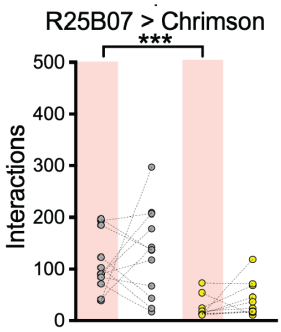

8.

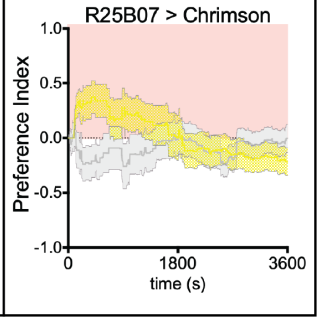

1.

49158 -

w[1118]; P{y[+t7.7] w[+mC]=GMR26B04 -GAL4}attP2

2.

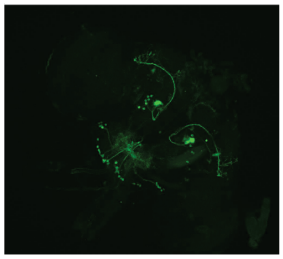

3.

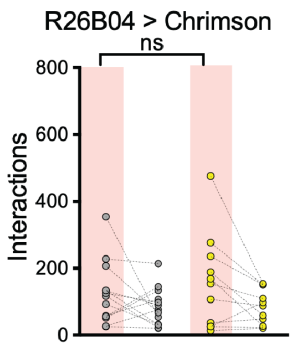

4.

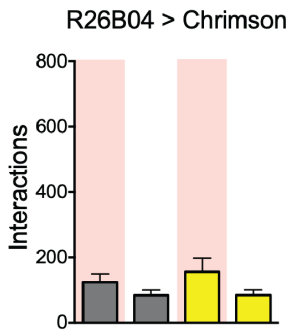

5.

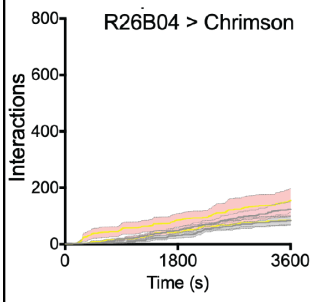

6.

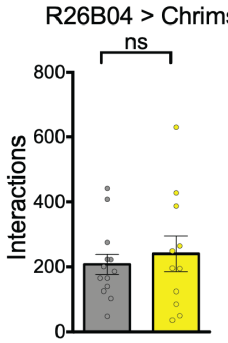

7.

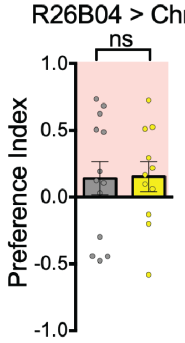

8.

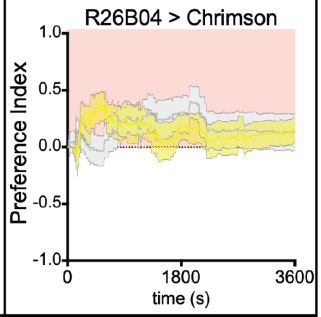

1.

49160 -

w[1118]; P{y[+t7.7] w[+mC]=GMR26B07 -GAL4}attP2

2.

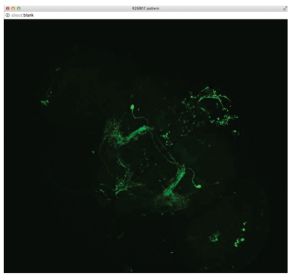

3.

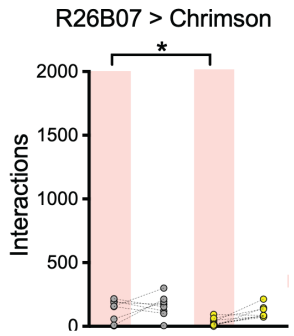

4.

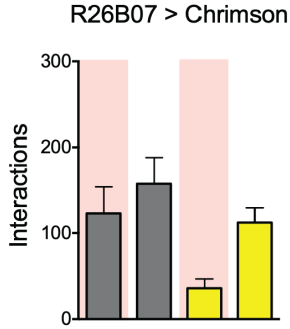

5.

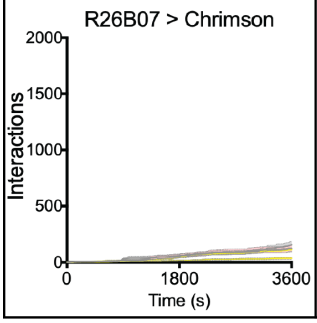

6.

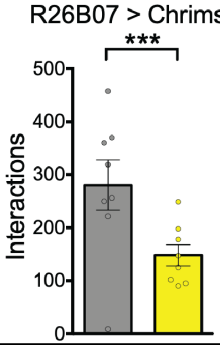

7.

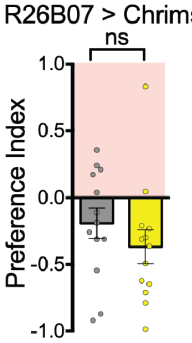

8.

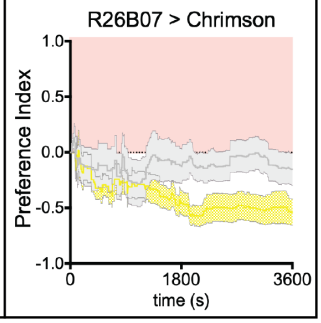

1.

49163 -

w[1118]; P{y[+t7.7] w[+mC]=GMR26B10 -GAL4}attP2

2.

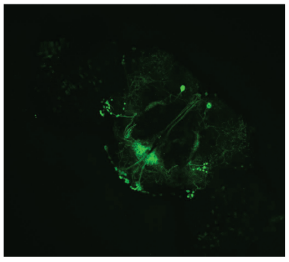

3.

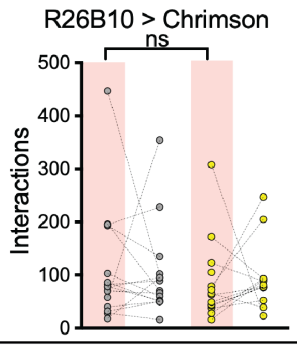

4.

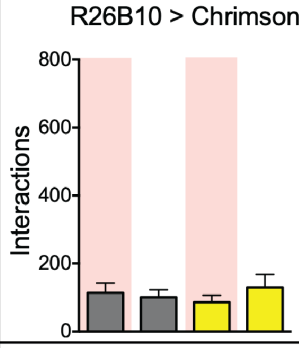

5.

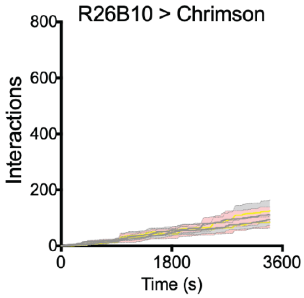

6.

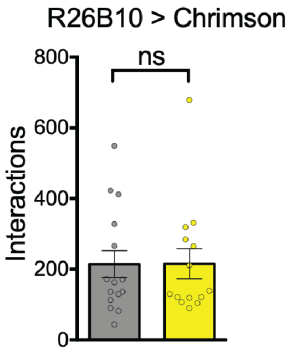

7.

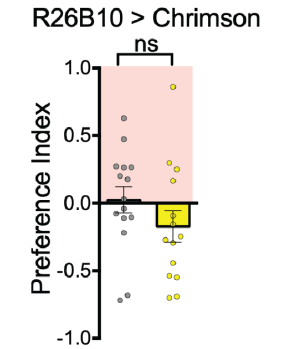

8.

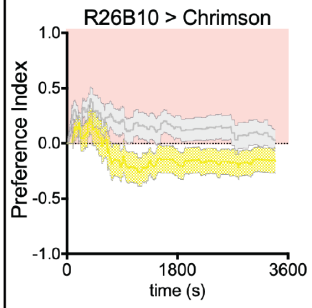

1.

49164 -

w[1118]; P{y[+t7.7] w[+mC]=GMR26B11 -GAL4}attP2

2.

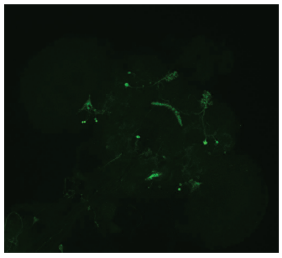

3.

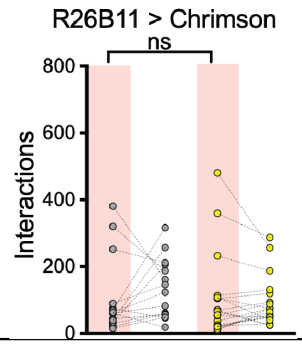

4.

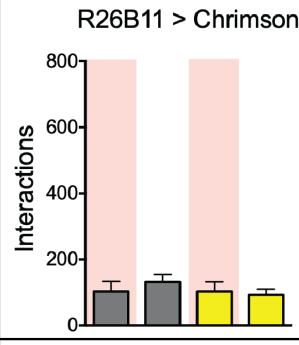

5.

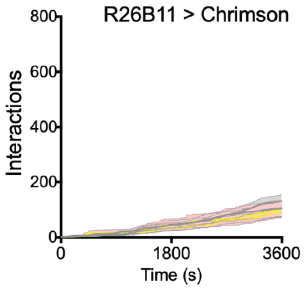

6.

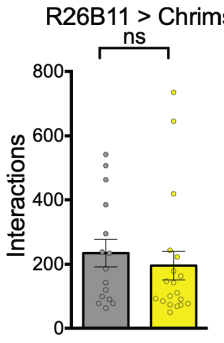

7.

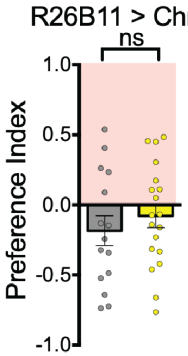

8.

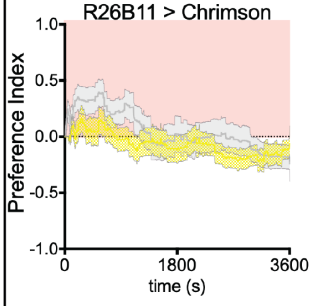

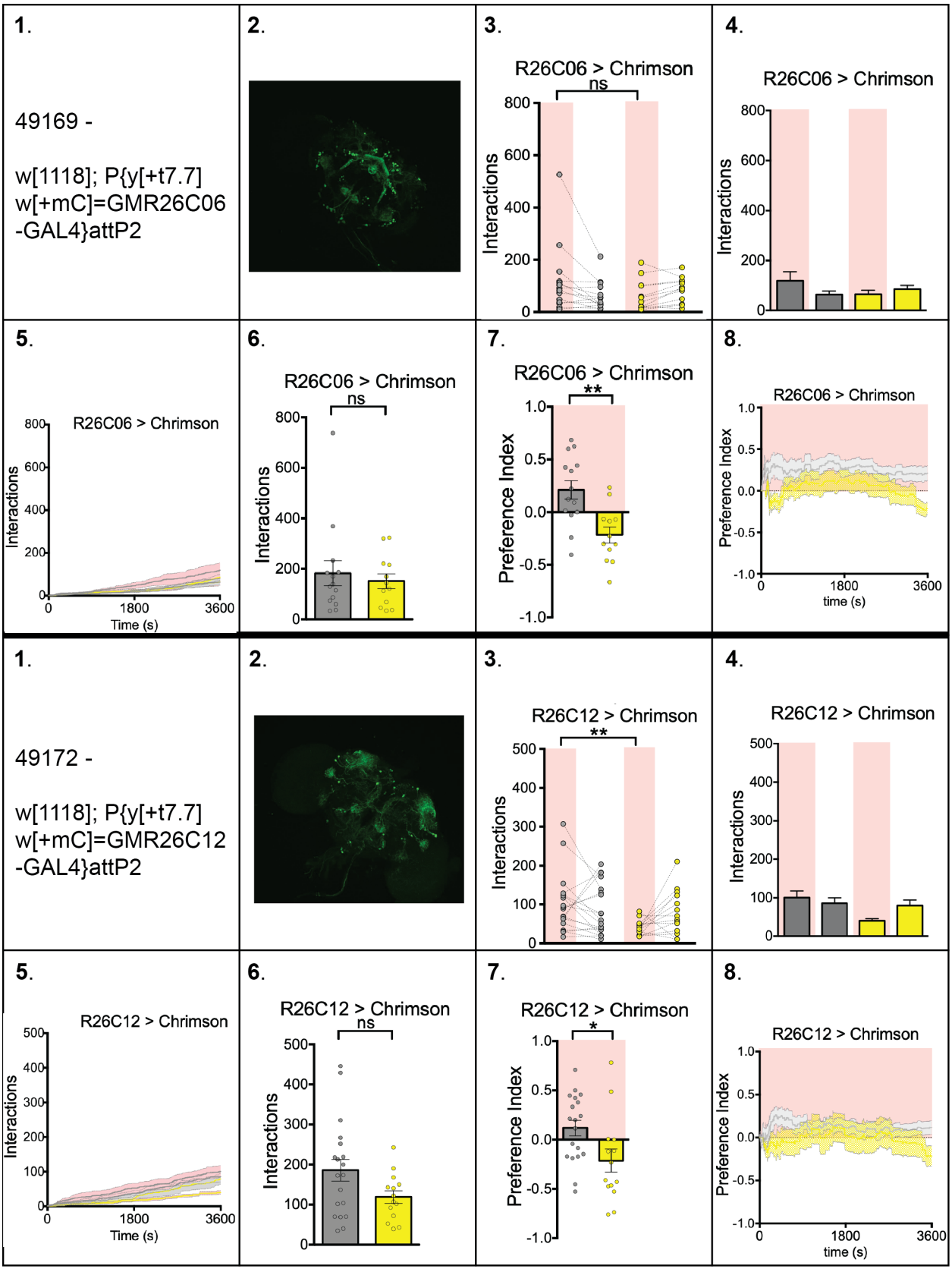
1.
49169 -
w[1118]; P{y[+t7.7] w[+mC]=GMR26C06 -GAL4}attP2
2.
3.
R26C06 > Chrimson
ns
Interactions
4.
R26C06 > Chrimson
Interactions
5.
R26C06 > Chrimson
Interactions
Time (s)
6.
R26C06 > Chrimson
ns
Interactions
7.
R26C06 > Chrimson
**
Preference Index
8.
R26C06 > Chrimson
Preference Index
time (s)
1.
49172 -
w[1118]; P{y[+t7.7] w[+mC]=GMR26C12 -GAL4}attP2
2.
3.
R26C12 > Chrimson
**
Interactions
4.
R26C12 > Chrimson
Interactions
5.
R26C12 > Chrimson
Interactions
Time (s)
6.
R26C12 > Chrimson
ns
Interactions
7.
R26C12 > Chrimson
*
Preference Index
8.
R26C12 > Chrimson
Preference Index
time (s)

1.

49324 -

w[1118]; P{y[+t7.7] w[+mC]=GMR26D12 -GAL4}attP2

2.

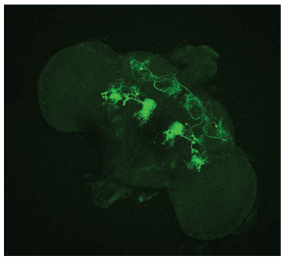

3.

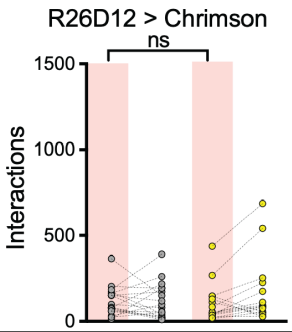

4.

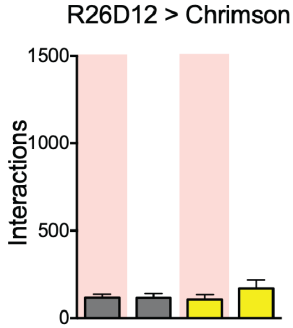

5.

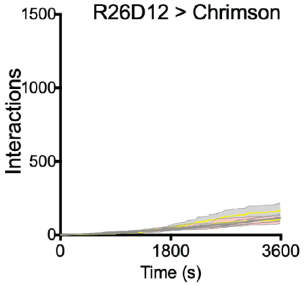

6.

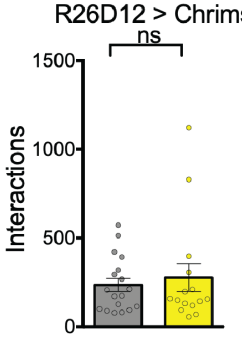

7.

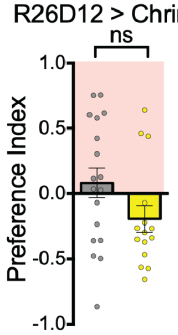

8.

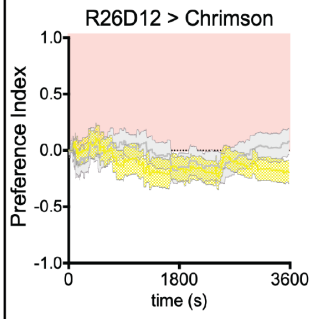

1.

49233 -

w[1118]; P{y[+t7.7] w[+mC]=GMR27G01 -GAL4}attP2

2.

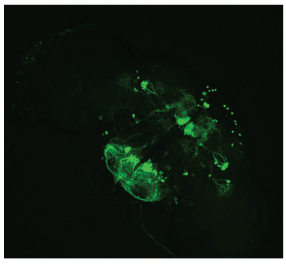

3.

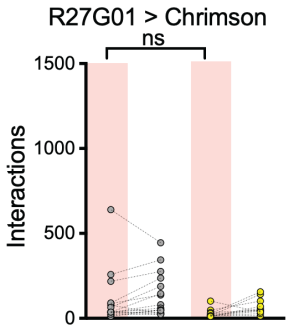

4.

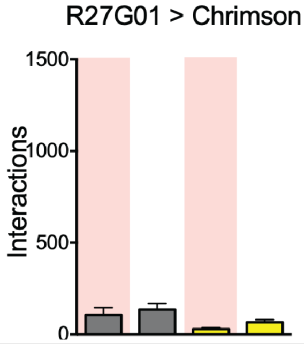

5.

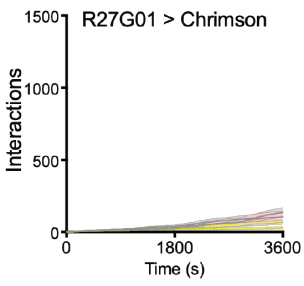

6.

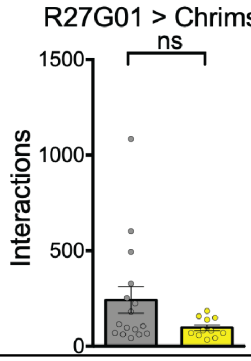

7.

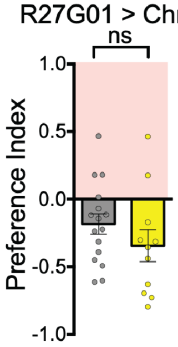

8.

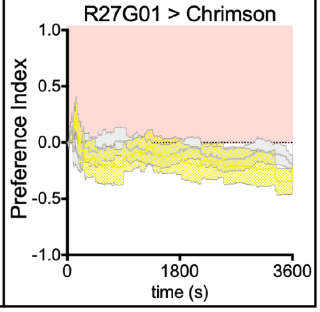

1.

49447 -

w[1118]; P{y[+t7.7] w[+mC]=GMR28B05 -GAL4}attP2

2.

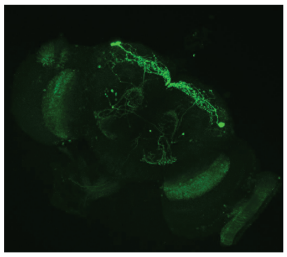

3.

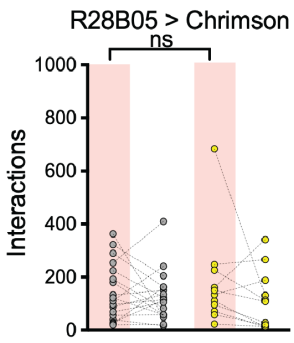

4.

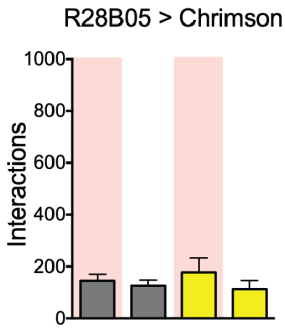

5.

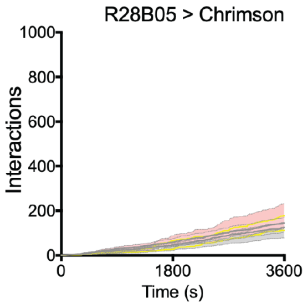

6.

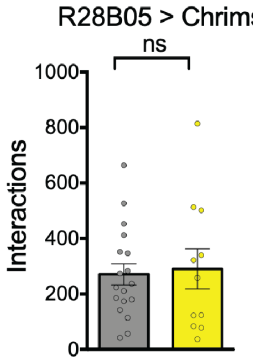

7.

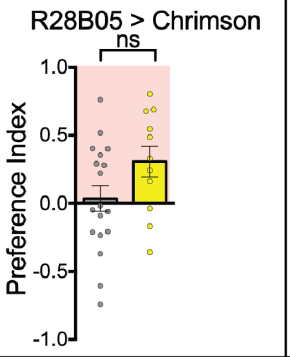

8.

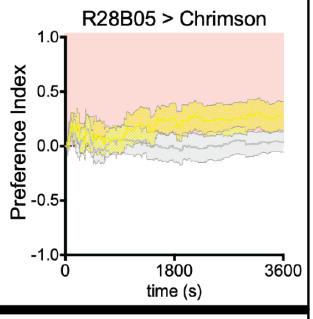

1.

49457 -

w[1118]; P{y[+t7.7] w[+mC]=GMR28E01 -GAL4}attP2

2.

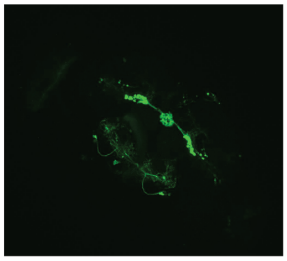

3.

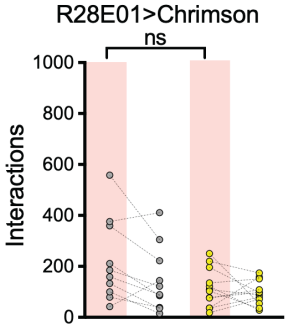

4.

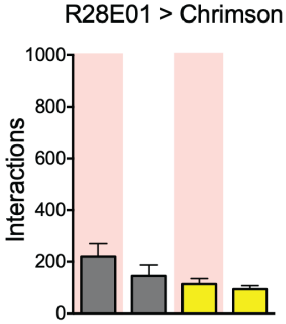

5.

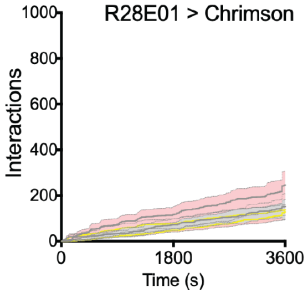

6.

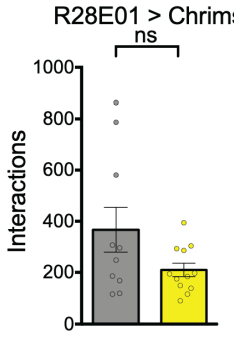

7.

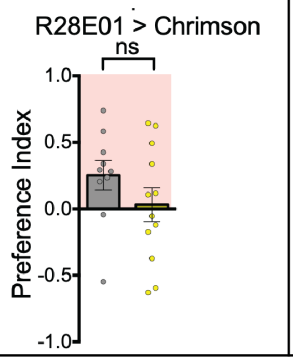

8.

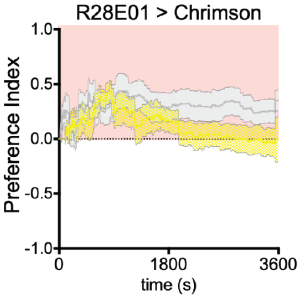

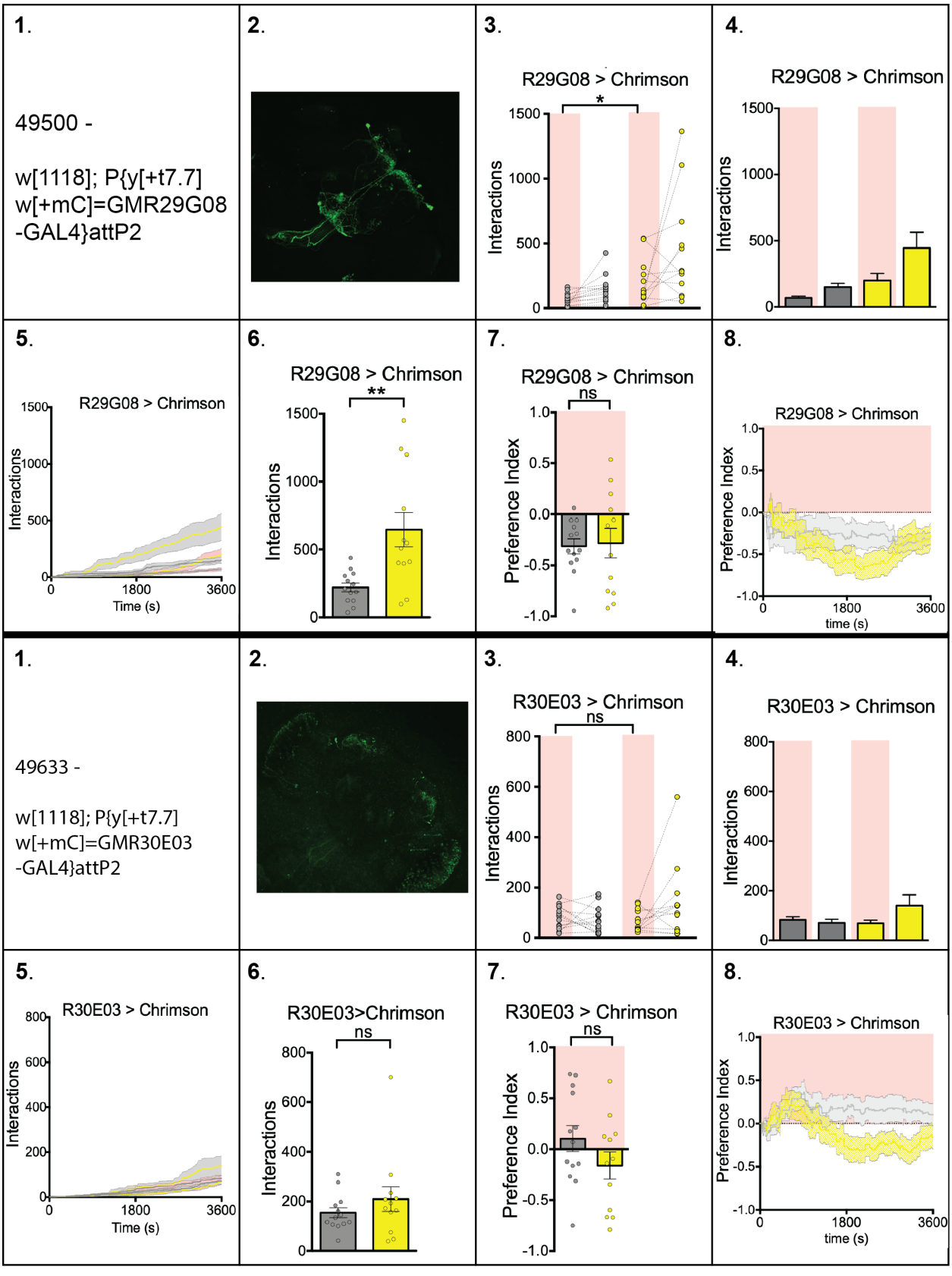
1.
49500 -
w[1118]; P{y[+t7.7]
w[+mC]=GMR29G08
-GAL4}attP2
2.
3.
R29G08 > Chrimson
*
Interactions
1500
1000
500
0
4.
R29G08 > Chrimson
Interactions
1500
1000
500
0
5.
R29G08 > Chrimson
Interactions
1500
1000
500
0
0
1800
3600
Time (s)
6.
R29G08 > Chrimson
**
Interactions
1500
1000
500
0
7.
R29G08 > Chrimson
ns
Preference Index
1.0
0.5
0.0
-0.5
-1.0
8.
R29G08 > Chrimson
Preference Index
1.0
0.5
0.0
-0.5
-1.0
0
1800
3600
time (s)
1.
49633 -
w[1118]; P{y[+t7.7]
w[+mC]=GMR30E03
-GAL4}attP2
2.
3.
R30E03 > Chrimson
ns
Interactions
800
600
400
200
0
4.
R30E03 > Chrimson
Interactions
800
600
400
200
0
5.
R30E03 > Chrimson
Interactions
800
600
400
200
0
0
1800
3600
Time (s)
6.
R30E03>Chrimson
ns
Interactions
800
600
400
200
0
7.
R30E03 > Chrimson
ns
Preference Index
1.0
0.5
0.0
-0.5
-1.0
8.
R30E03 > Chrimson
Preference Index
1.0
0.5
0.0
-0.5
-1.0
0
1800
3600
time (s)

1.

49637 -

w[1118]; P{y[+t7.7] w[+mC]=GMR30E09 -GAL4}attP2

2.

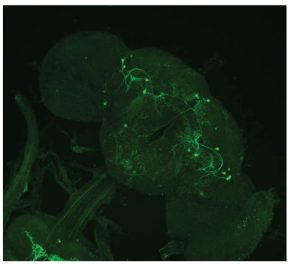

3.

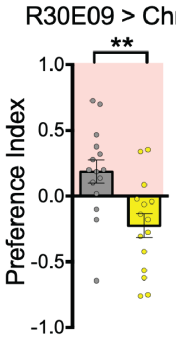

4.

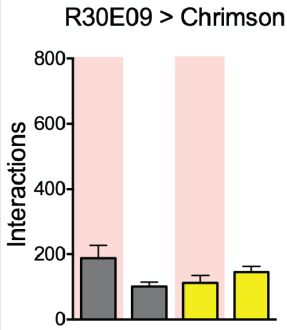

5.

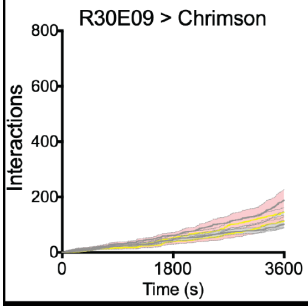

6.

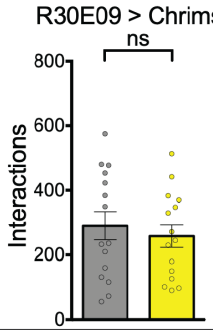

7.

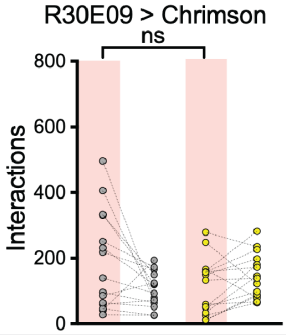

8.

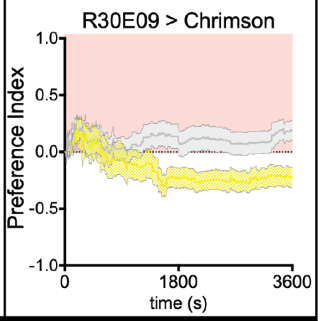

1.

49649 -

w[1118]; P{y[+t7.7] w[+mC]=GMR30H02 -GAL4}attP2

2.

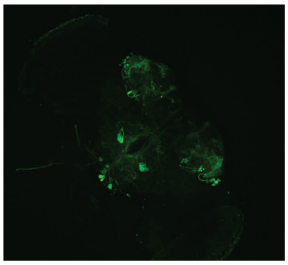

3.

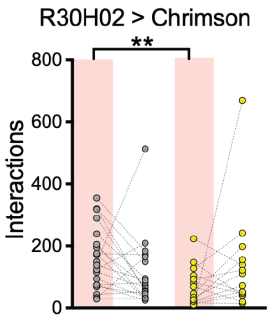

4.

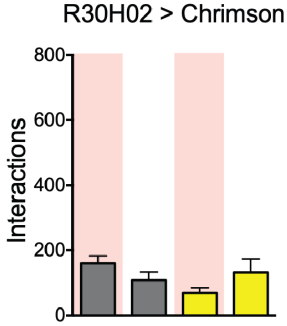

5.

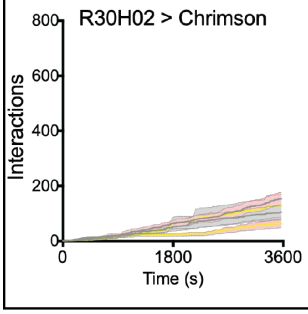

6.

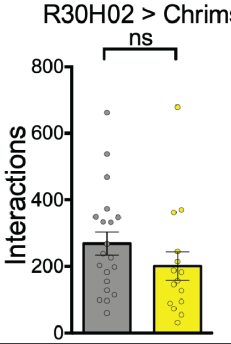

7.

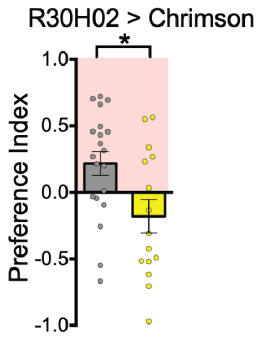

8.

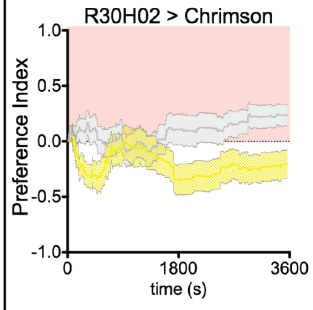

1.

49660 -

w[1118]; P{y[+t7.7] w[+mC]=GMR31A11 -GAL4}attP2

2.

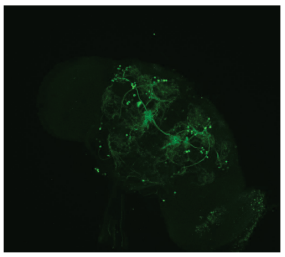

3.

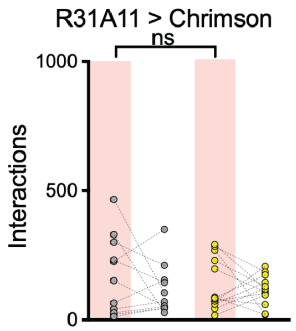

4.

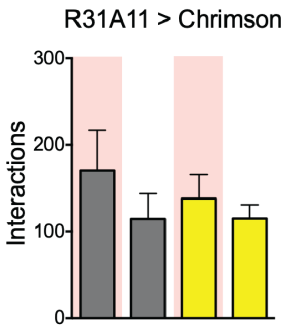

5.

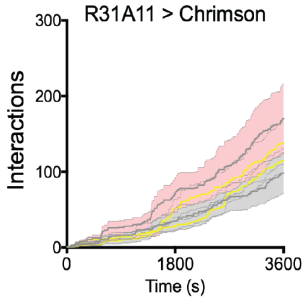

6.

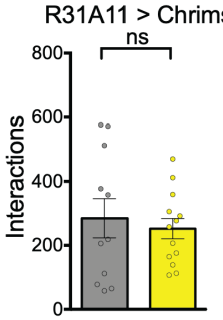

7.

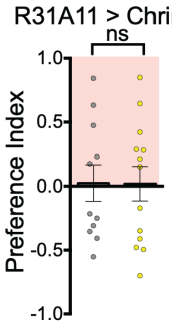

8.

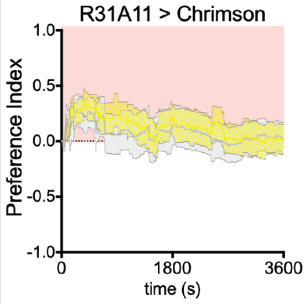

1.

49662 -

w[1118]; P{y[+t7.7] w[+mC]=GMR31B01 -GAL4}attP2

2.

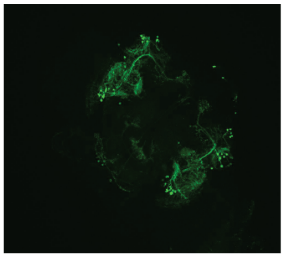

3.

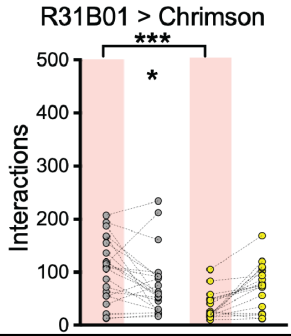

4.

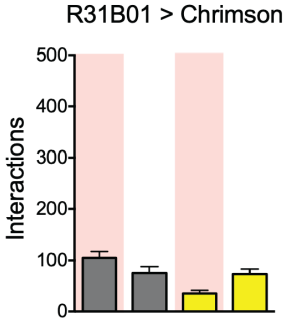

5.

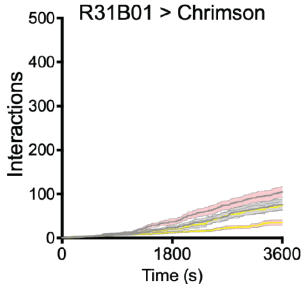

6.

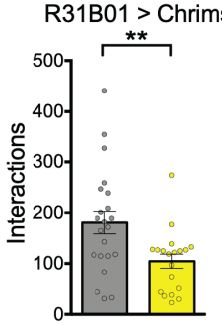

7.

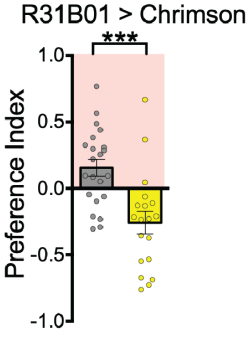

8.

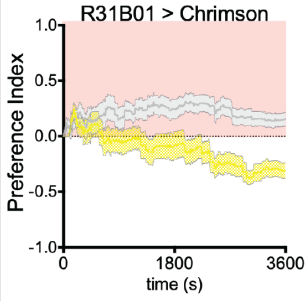

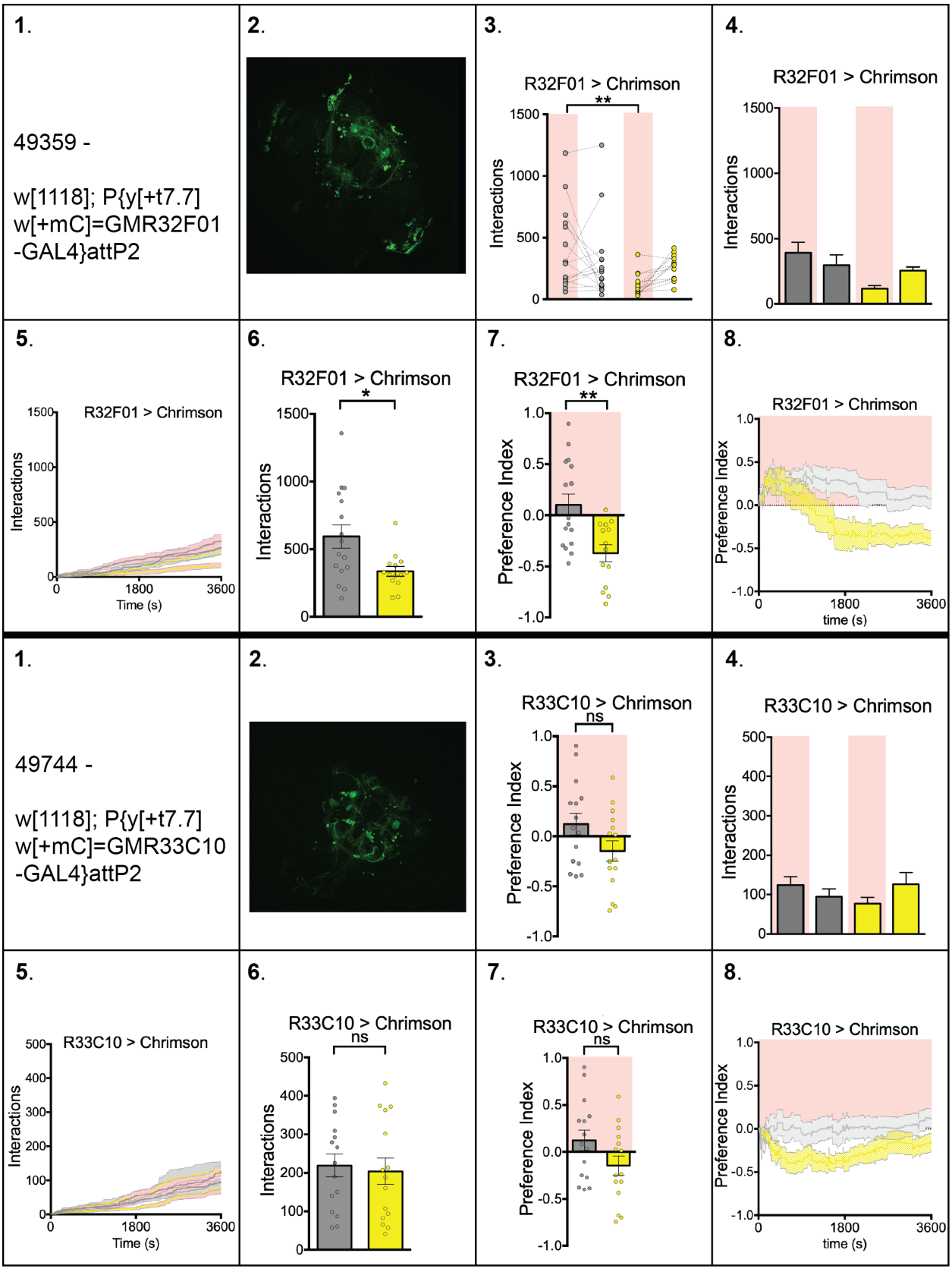
1.
49359 -
w[1118]; P{y[+t7.7]
w[+mC]=GMR32F01
-GAL4}attP2
2.
3.
R32F01 > Chrimson
**
Interactions
1500
1000
500
0
4.
R32F01 > Chrimson
Interactions
1500
1000
500
0
5.
R32F01 > Chrimson
Interactions
1500
1000
500
0
0
1800
3600
Time (s)
6.
R32F01 > Chrimson
*
Interactions
1500
1000
500
0
7.
R32F01 > Chrimson
**
Preference Index
1.0
0.5
0.0
-0.5
-1.0
8.
R32F01 > Chrimson
Preference Index
1.0
0.5
0.0
-0.5
-1.0
0
1800
3600
time (s)
1.
49744 -
w[1118]; P{y[+t7.7]
w[+mC]=GMR33C10
-GAL4}attP2
2.
3.
R33C10 > Chrimson
ns
Preference Index
1.0
0.5
0.0
-0.5
-1.0
4.
R33C10 > Chrimson
Interactions
500
400
300
200
100
0
5.
R33C10 > Chrimson
Interactions
500
400
300
200
100
0
0
1800
3600
Time (s)
6.
R33C10 > Chrimson
ns
Interactions
500
400
300
200
100
0
7.
R33C10 > Chrimson
ns
Preference Index
1.0
0.5
0.0
-0.5
-1.0
8.
R33C10 > Chrimson
Preference Index
1.0
0.5
0.0
-0.5
-1.0
0
1800
3600
time (s)

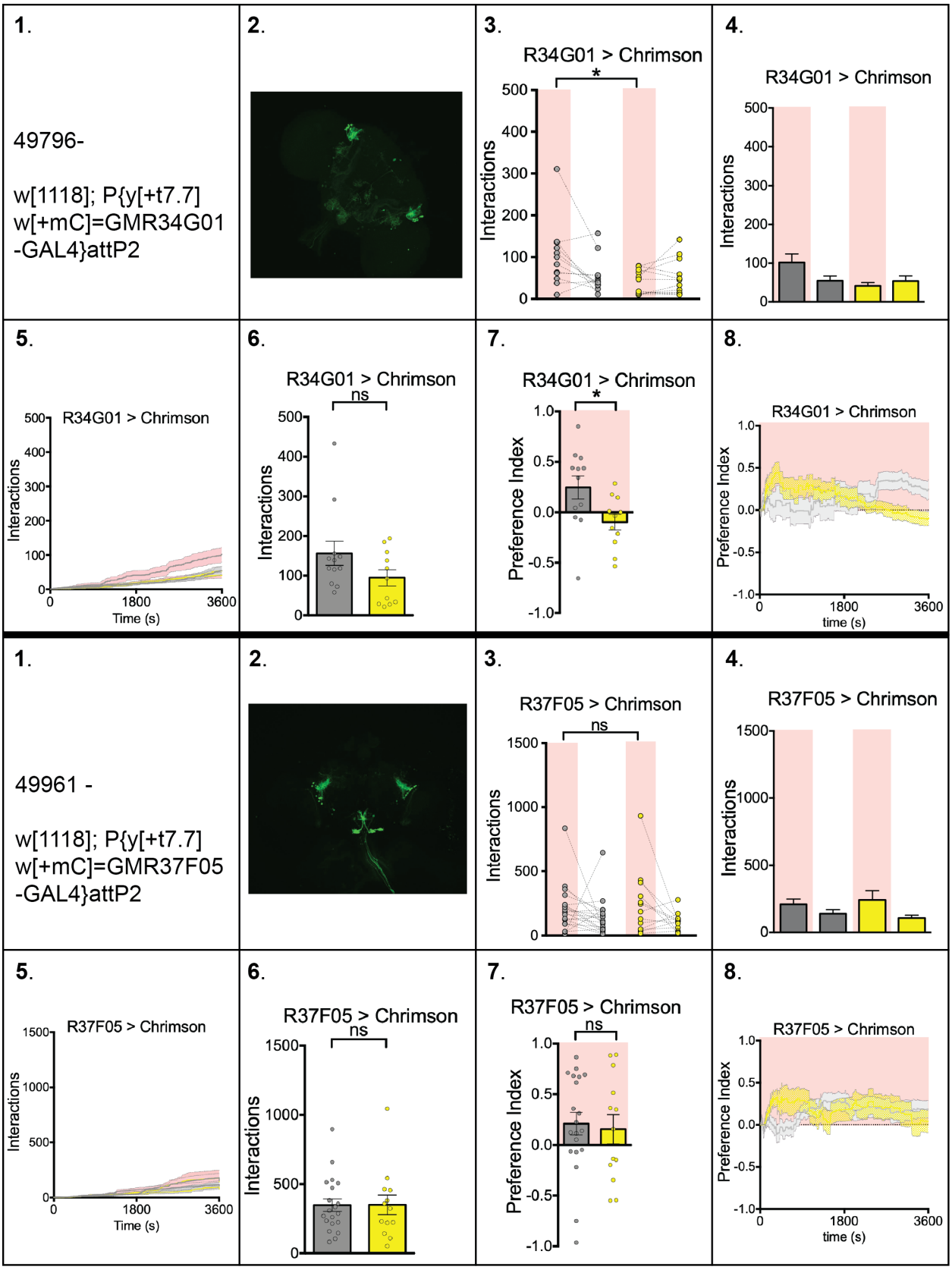
1.
49796-
w[1118]; P{y[+t7.7]
w[+mC]=GMR34G01
-GAL4}attP2
2.
3.
R34G01 > Chrimson
*
Interactions
4.
R34G01 > Chrimson
Interactions
5.
R34G01 > Chrimson
Interactions
Time (s)
6.
R34G01 > Chrimson
ns
Interactions
7.
R34G01 > Chrimson
*
Preference Index
8.
R34G01 > Chrimson
Preference Index
time (s)
1.
49961 -
w[1118]; P{y[+t7.7]
w[+mC]=GMR37F05
-GAL4}attP2
2.
3.
R37F05 > Chrimson
ns
Interactions
4.
R37F05 > Chrimson
Interactions
5.
R37F05 > Chrimson
Interactions
Time (s)
6.
R37F05 > Chrimson
ns
Interactions
7.
R37F05 > Chrimson
ns
Preference Index
8.
R37F05 > Chrimson
Preference Index
time (s)

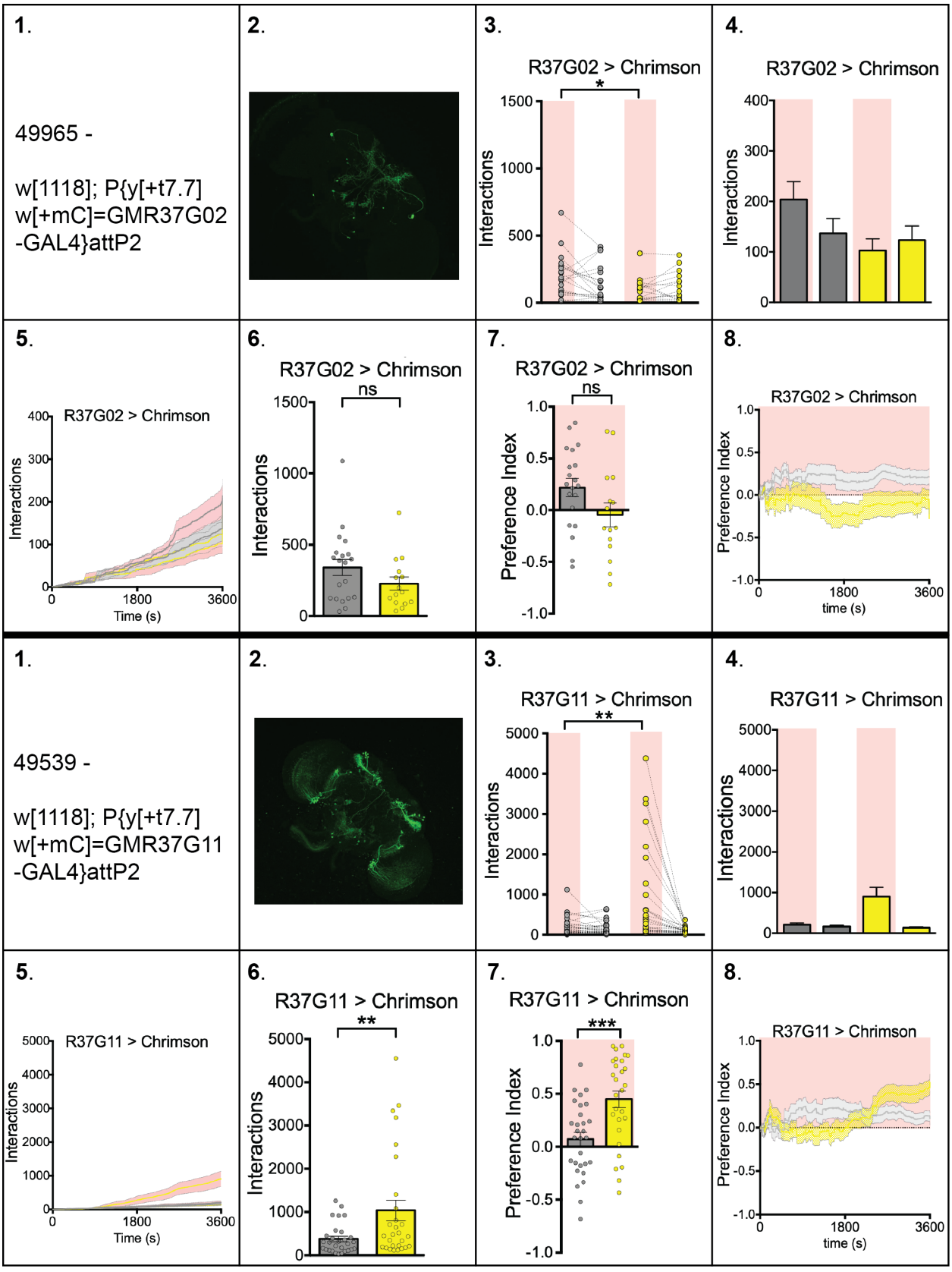
1.
49965 -
w[1118]; P{y[+t7.7] w[+mC]=GMR37G02 -GAL4}attP2
2.
3.
R37G02 > Chrimson
*
Interactions
1500
1000
500
0
4.
R37G02 > Chrimson
Interactions
400
300
200
100
0
5.
R37G02 > Chrimson
Interactions
400
300
200
100
0
0
1800
3600
Time (s)
6.
R37G02 > Chrimson
ns
Interactions
1500
1000
500
0
7.
R37G02 > Chrimson
ns
Preference Index
1.0
0.5
0.0
-0.5
-1.0
8.
R37G02 > Chrimson
Preference Index
1.0
0.5
0.0
-0.5
-1.0
0
1800
3600
time (s)
1.
49539 -
w[1118]; P{y[+t7.7] w[+mC]=GMR37G11 -GAL4}attP2
2.
3.
R37G11 > Chrimson
**
Interactions
5000
4000
3000
2000
1000
0
4.
R37G11 > Chrimson
Interactions
5000
4000
3000
2000
1000
0
5.
R37G11 > Chrimson
Interactions
5000
4000
3000
2000
1000
0
0
1800
3600
Time (s)
6.
R37G11 > Chrimson
**
Interactions
5000
4000
3000
2000
1000
0
7.
R37G11 > Chrimson
***
Preference Index
1.0
0.5
0.0
-0.5
-1.0
8.
R37G11 > Chrimson
Preference Index
1.0
0.5
0.0
-0.5
-1.0
0
1800
3600
time (s)

1.

49987 -

w[1118]; P{y[+t7.7] w[+mC]=GMR38B09 -GAL4}attP2

2.

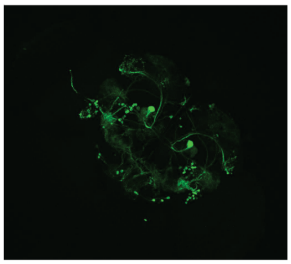

3.

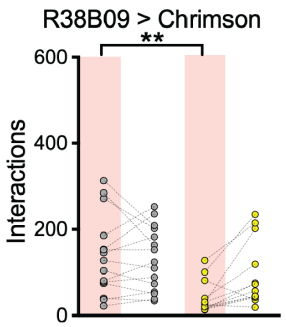

4.

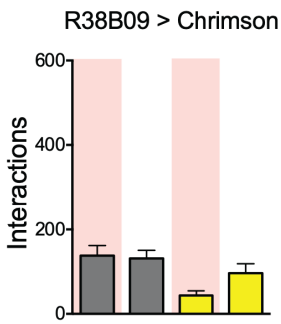

5.

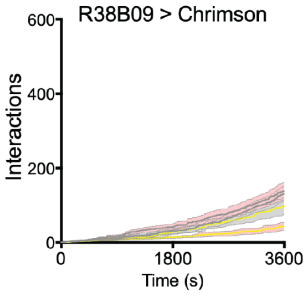

6.

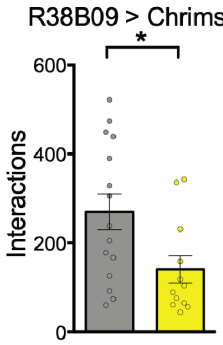

7.

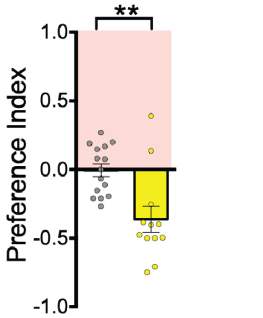

8.

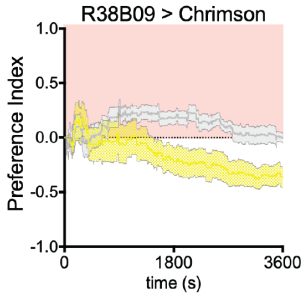

1.

50012 -

w[1118]; P{y[+t7.7] w[+mC]=GMR38F08 -GAL4}attP2

2.

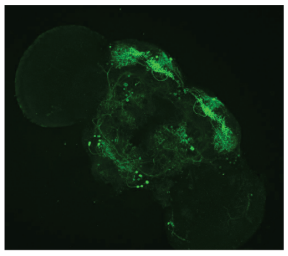

3.

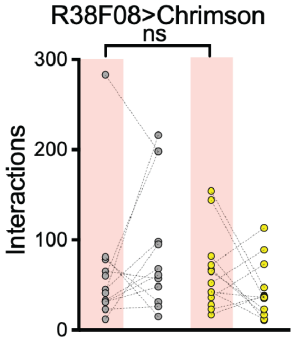

4.

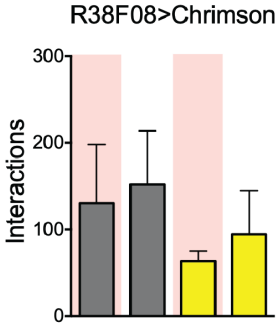

5.

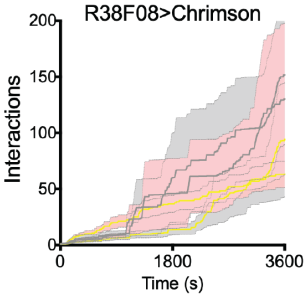

6.

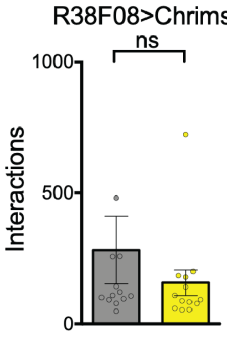

7.

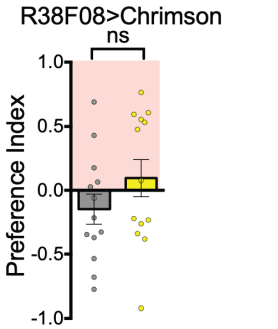

8.

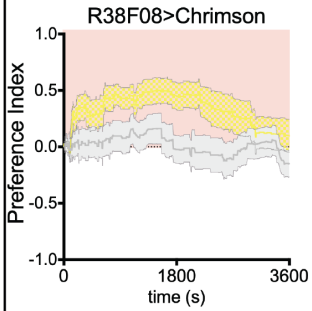

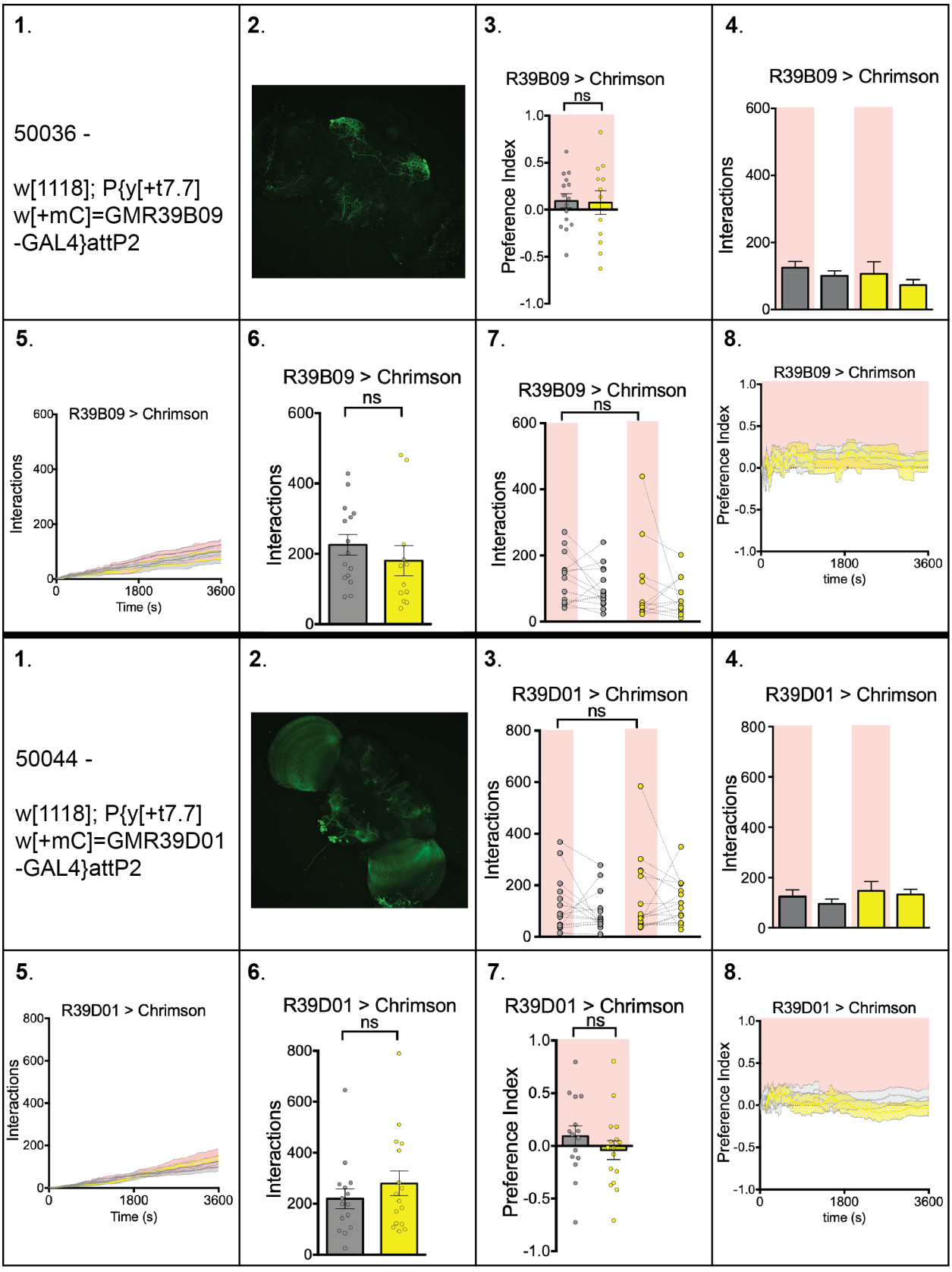
1.
50036 -
w[1118]; P{y[+t7.7] w[+mC]=GMR39B09 -GAL4}attP2
2.
3.
R39B09 > Chrimson
ns
Preference Index
4.
R39B09 > Chrimson
Interactions
5.
R39B09 > Chrimson
Interactions
Time (s)
6.
R39B09 > Chrimson
ns
Interactions
7.
R39B09 > Chrimson
ns
Interactions
8.
R39B09 > Chrimson
Preference Index
time (s)
1.
50044 -
w[1118]; P{y[+t7.7] w[+mC]=GMR39D01 -GAL4}attP2
2.
3.
R39D01 > Chrimson
ns
Interactions
4.
R39D01 > Chrimson
Interactions
5.
R39D01 > Chrimson
Interactions
Time (s)
6.
R39D01 > Chrimson
ns
Interactions
7.
R39D01 > Chrimson
ns
Preference Index
8.
R39D01 > Chrimson
Preference Index
time (s)

1.

50133 -

w[1118]; P{y[+t7.7] w[+mC]=GMR41F05 -GAL4}attP2

2.

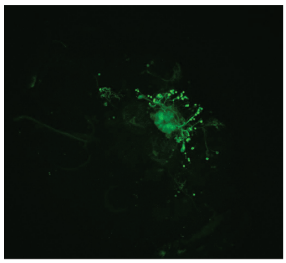

3.

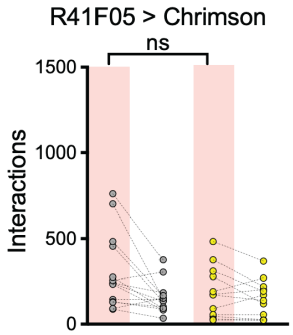

4.

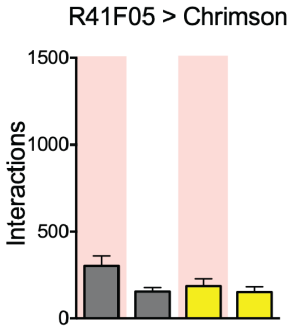

5.

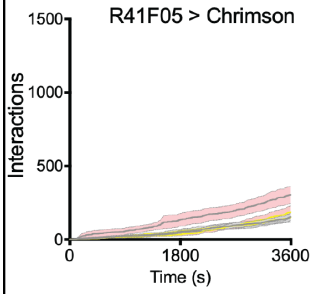

6.

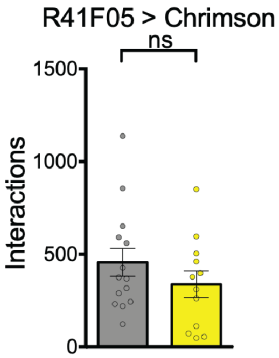

7.

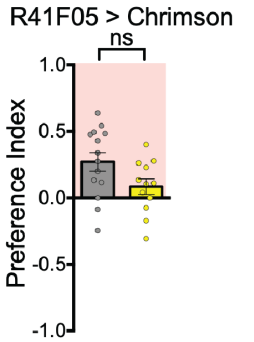

8.

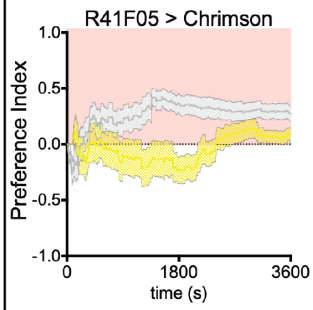

1.

46241 -

w[1118]; P{y[+t7.7] w[+mC]=GMR41H07 -GAL4}attP2

2.

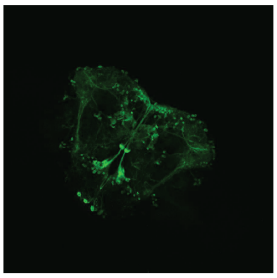

3.

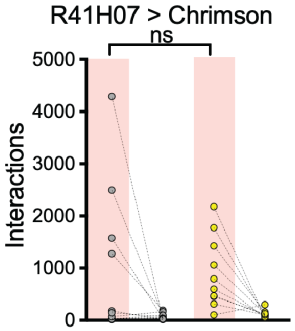

4.

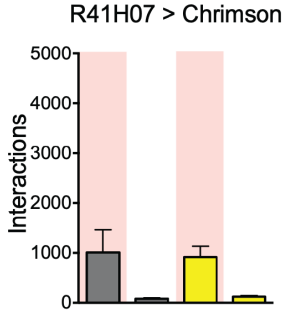

5.

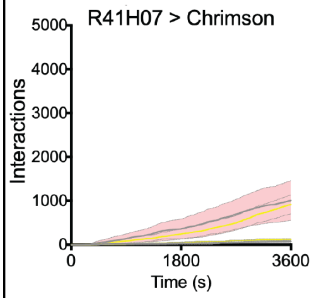

6.

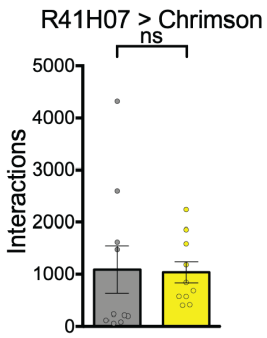

7.

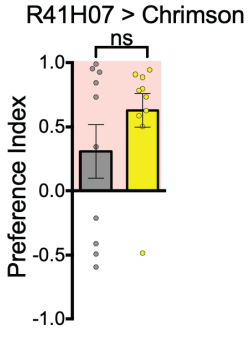

8.

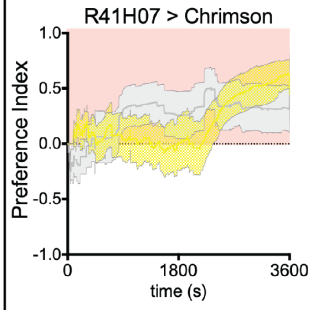

1. 48147 - w[1118]; P{y[+t7.7] w[+mC]=GMR41H09 -GAL4}attP2/TM3, Sb[1]	**2.** 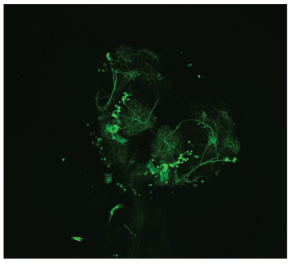	**3.** 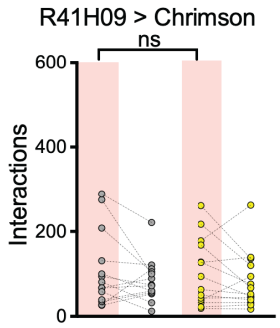	**4.** 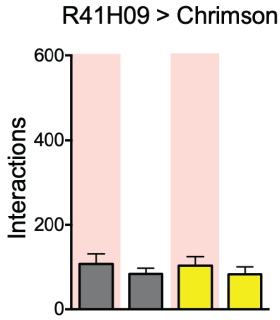
5. 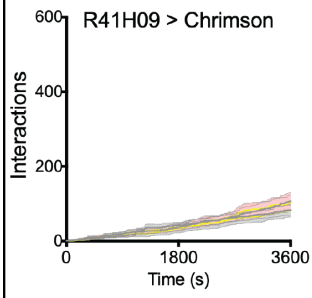	**6.** 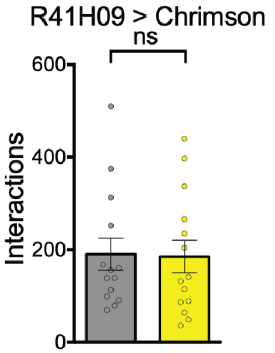	**7.** 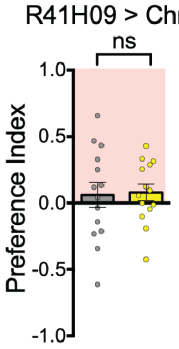	**8.** 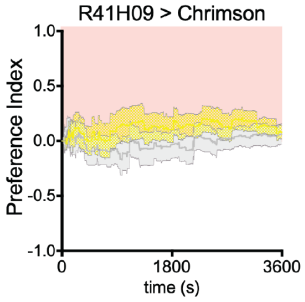
1. 41245 - w[1118]; P{y[+t7.7] w[+mC]=GMR42A06 -GAL4}attP2	**2.** 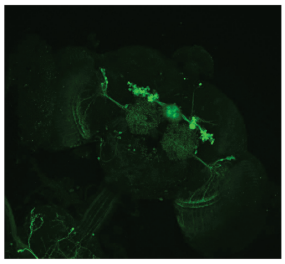	**3.** 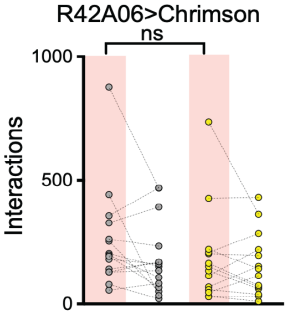	**4.** 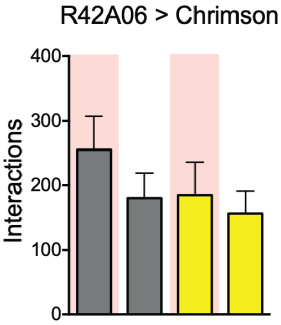
5. 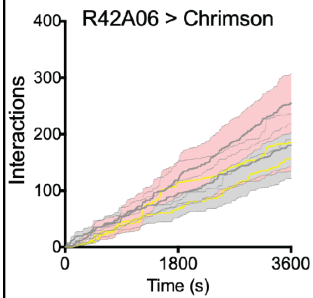	**6.** 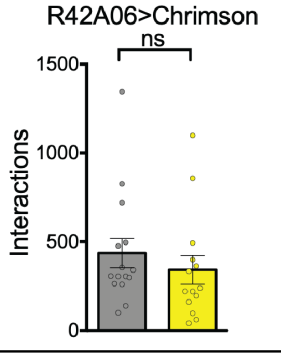	**7.** 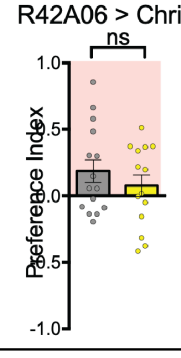	**8.** 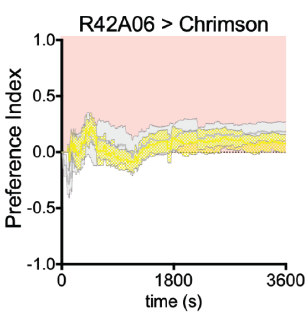

1.

50159 -

w[1118]; P{y[+t7.7] w[+mC]=GMR42E12 -GAL4}attP2

2.

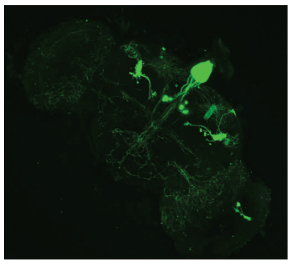

3.

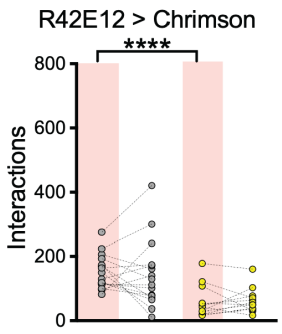

4.

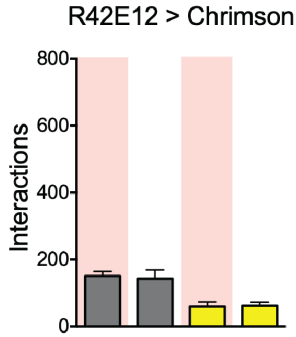

5.

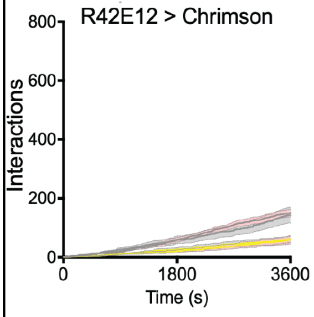

6.

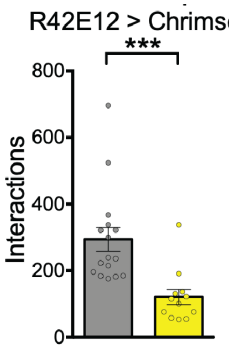

7.

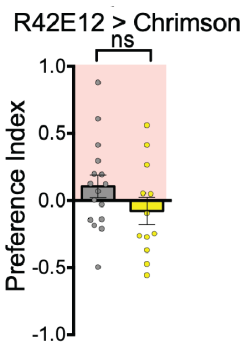

8.

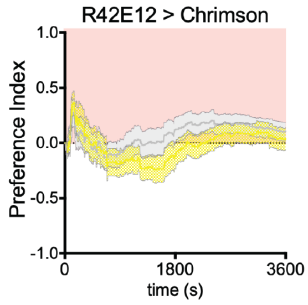

1.

41259 -

w[1118]; P{y[+t7.7] w[+mC]=GMR43D05 -GAL4}attP2

2.

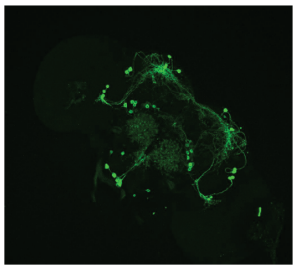

3.

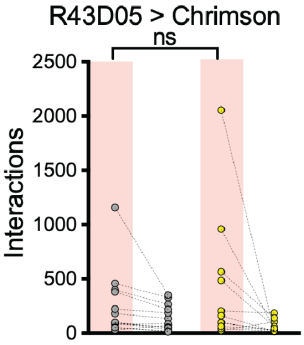

4.

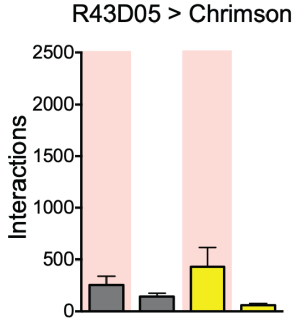

5.

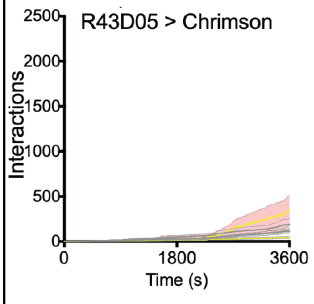

6.

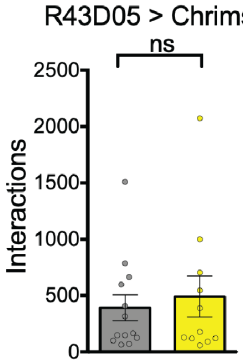

7.

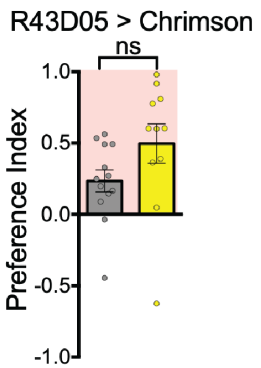

8.

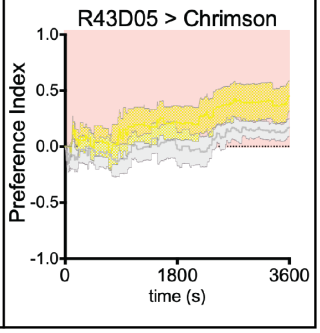

1.

49553 -

w[1118]; P{y[+t7.7] w[+mC]=GMR43D09 -GAL4}attP2

2.

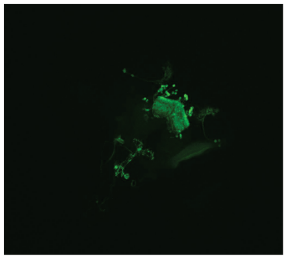

3.

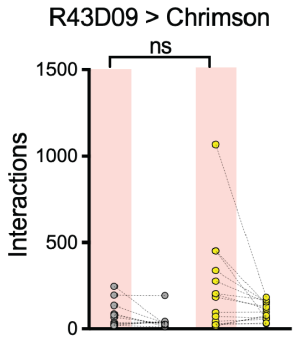

4.

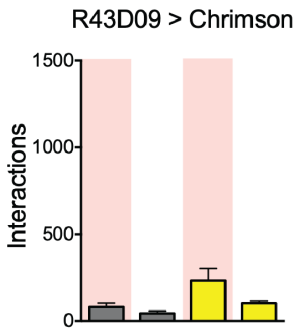

5.

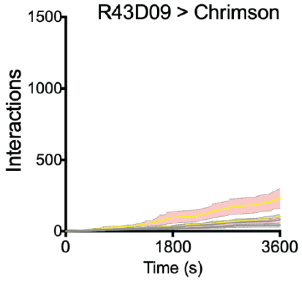

6.

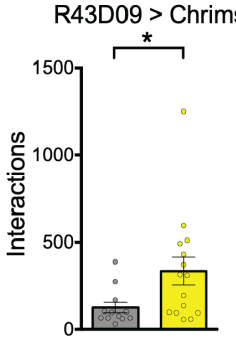

7.

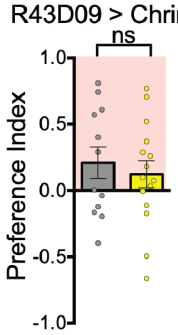

8.

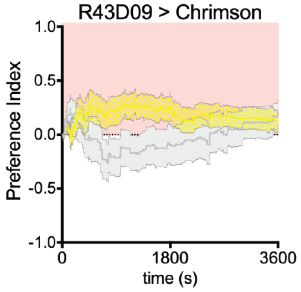

1.

50206 -

w[1118]; P{y[+t7.7] w[+mC]=GMR44D05 -GAL4}attP2

2.

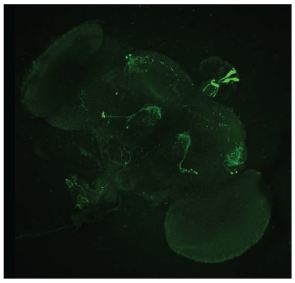

3.

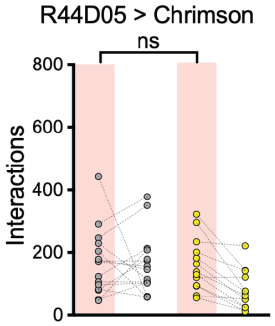

4.

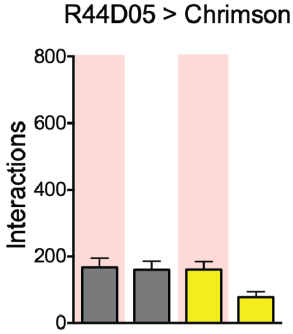

5.

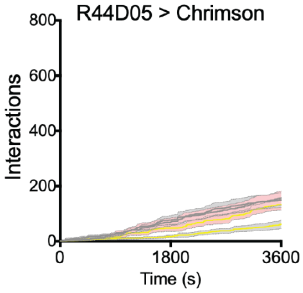

6.

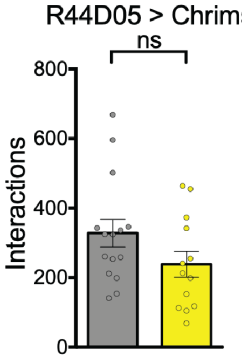

7.

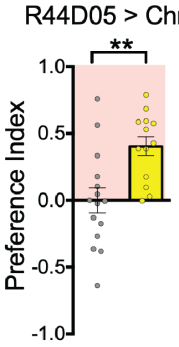

8.

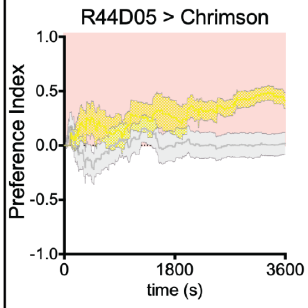

1.

48160 -

w[1118]; P{y[+t7.7] w[+mC]=GMR45D04 -GAL4}attP2/TM3, Sb[1]

2.

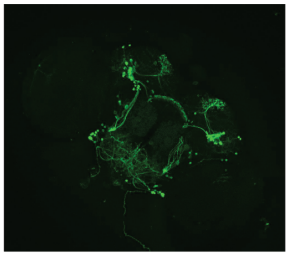

3.

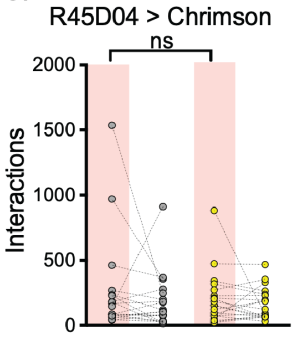

4.

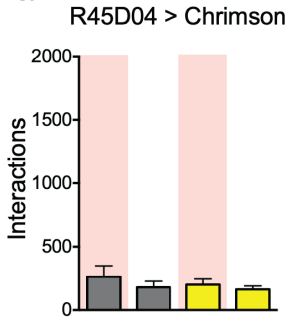

5.

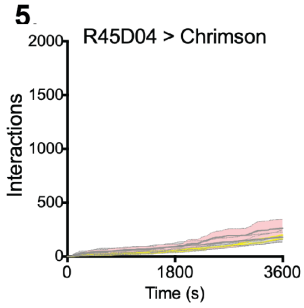

6.

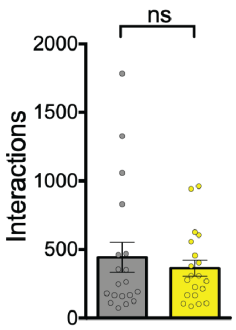

7

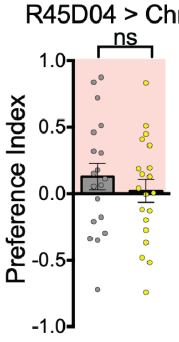

8.

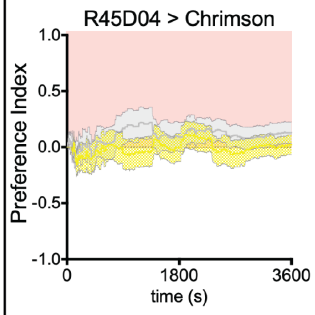

1.

50229 -

w[1118]; P{y[+t7.7] w[+mC]=GMR45E03 -GAL4}attP2

2.

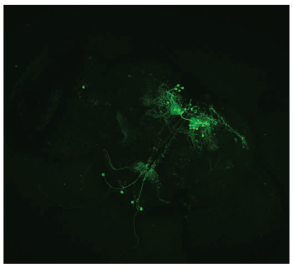

3.

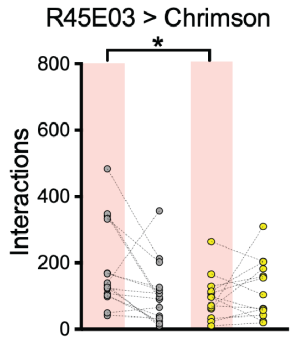

4.

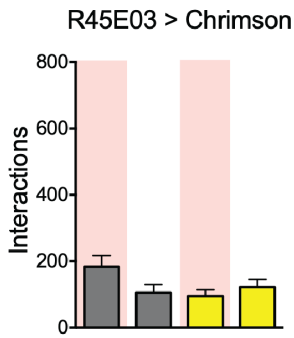

5.

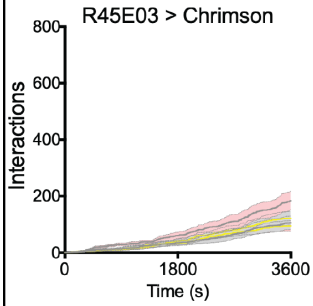

6.

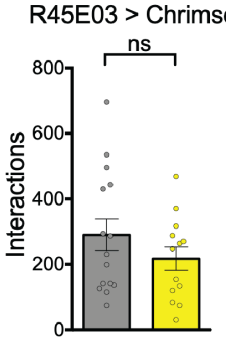

7.

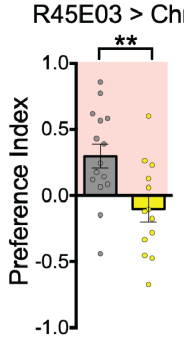

8.

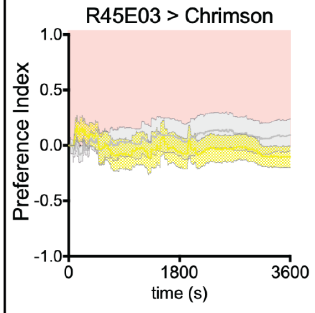

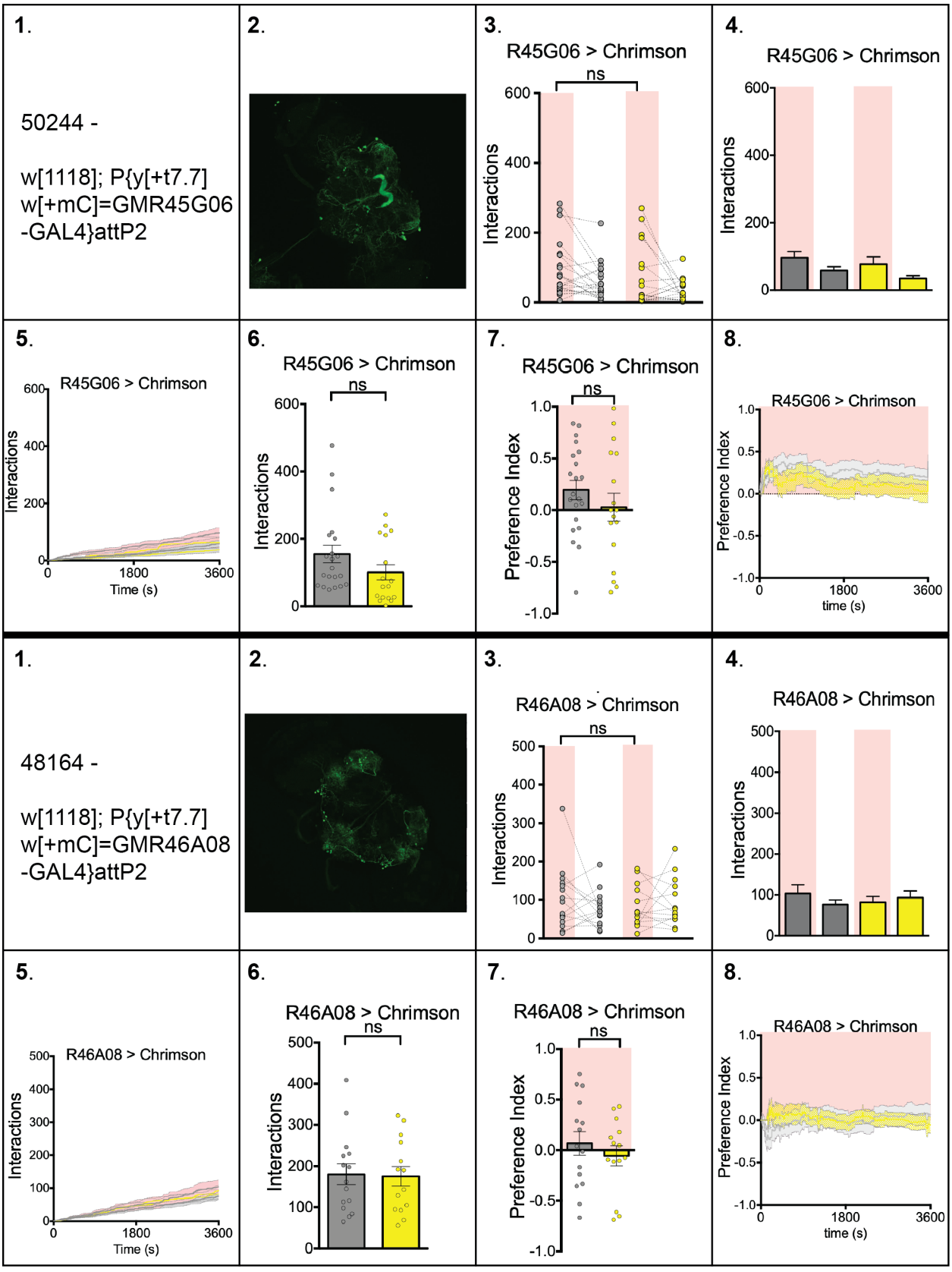
1.
50244 -
w[1118]; P{y[+t7.7] w[+mC]=GMR45G06 -GAL4}attP2
2.
3.
R45G06 > Chrimson
ns
Interactions
4.
R45G06 > Chrimson
Interactions
5.
R45G06 > Chrimson
Interactions
Time (s)
6.
R45G06 > Chrimson
ns
Interactions
7.
R45G06 > Chrimson
ns
Preference Index
8.
R45G06 > Chrimson
Preference Index
time (s)
1.
48164 -
w[1118]; P{y[+t7.7] w[+mC]=GMR46A08 -GAL4}attP2
2.
3.
R46A08 > Chrimson
ns
Interactions
4.
R46A08 > Chrimson
Interactions
5.
R46A08 > Chrimson
Interactions
Time (s)
6.
R46A08 > Chrimson
ns
Interactions
7.
R46A08 > Chrimson
ns
Preference Index
8.
R46A08 > Chrimson
Preference Index
time (s)

1.

47605 -

w[1118]; P{y[+t7.7] w[+mC]=GMR47D05 -GAL4}attP2

2.

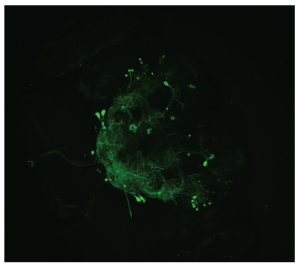

3.

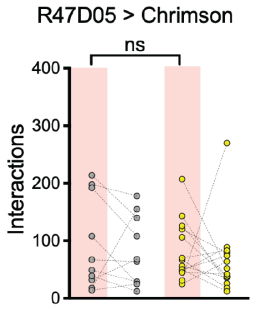

4.

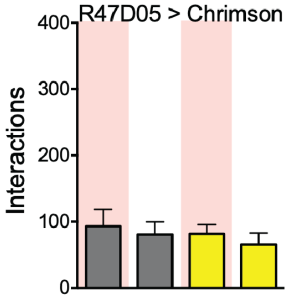

5.

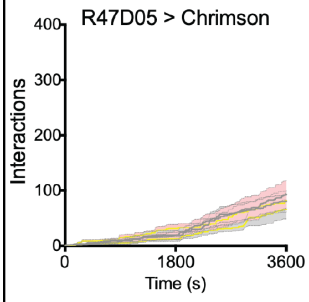

6.

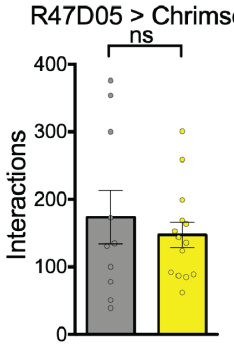

7.

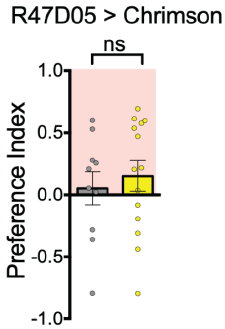

8.

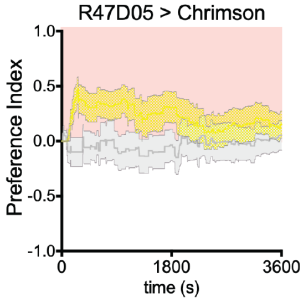

1.

50324 -

w[1118]; P{y[+t7.7] w[+mC]=GMR47F12 -GAL4}attP2

2.

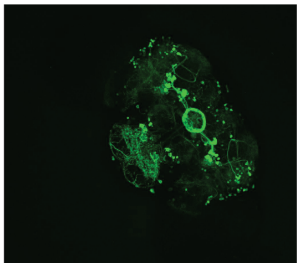

3.

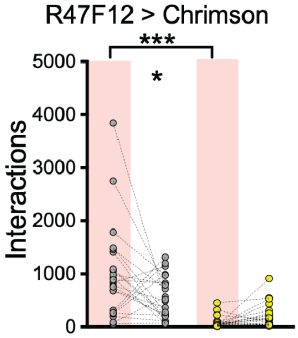

4.

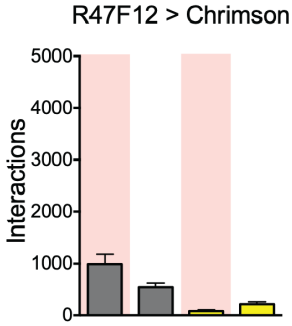

5.

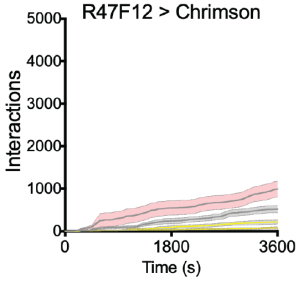

6

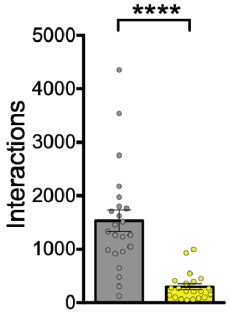

7.

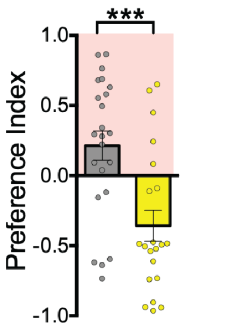

8.

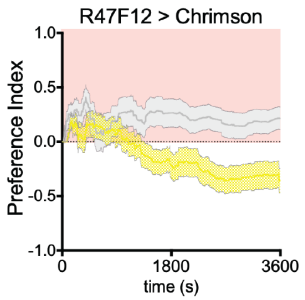

1. 49569 - w[1118]; P{y[+t7.7] w[+mC]=GMR47H07 -GAL4}attP2	**2.** 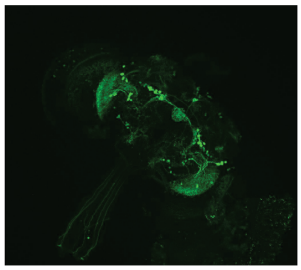	**3.** 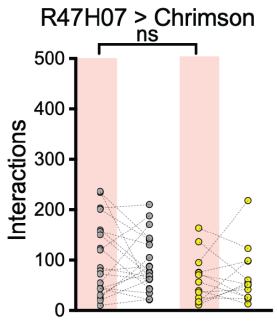	**4.** 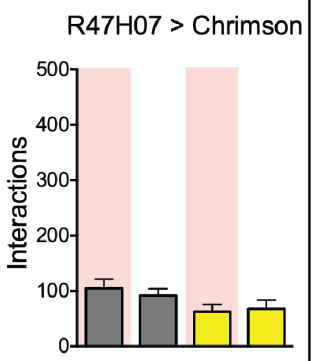
5. 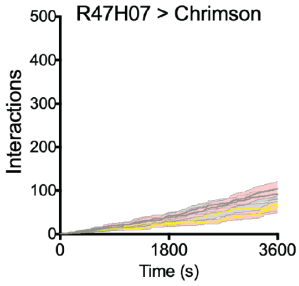	**6.** 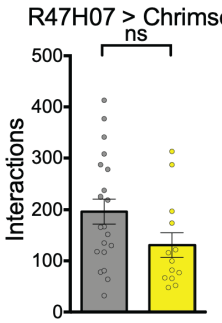	**7.** 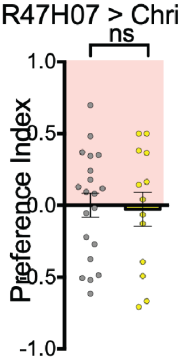	**8.** 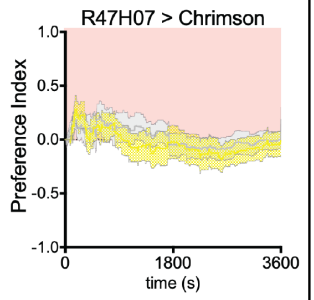
1. 50346 - w[1118]; P{y[+t7.7] w[+mC]=GMR48B03 -GAL4}attP2	**2.** 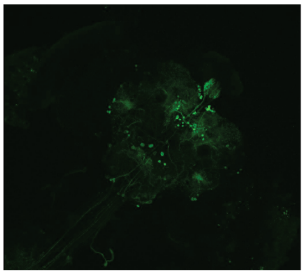	**3.** 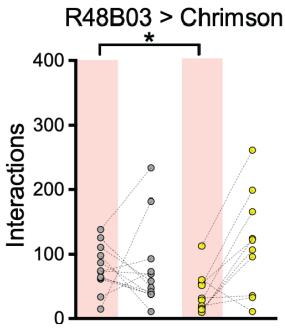	**4.** 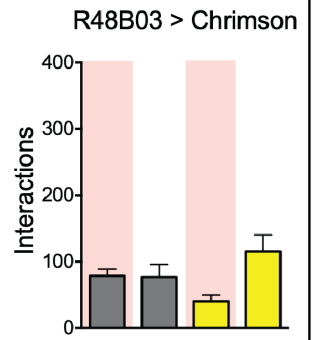
5. 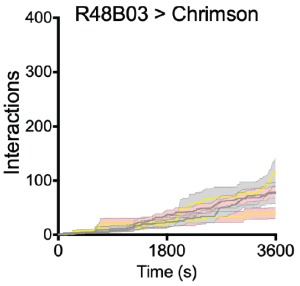	**6.** 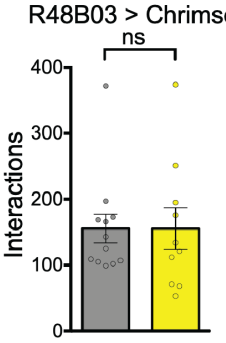	**7.** 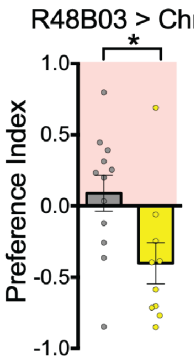	**8.** 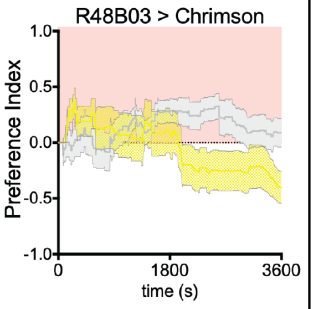

1.

50366 -

w[1118]; P{y[+t7.7] w[+mC]=GMR48E01 -GAL4}attP2

2.

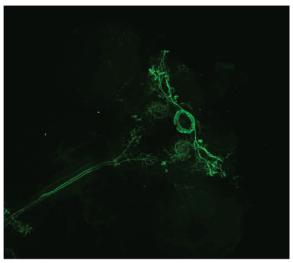

3.

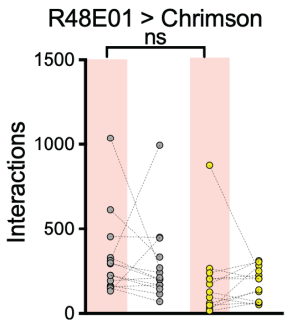

4.

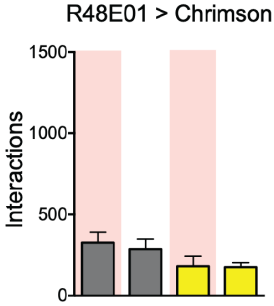

5.

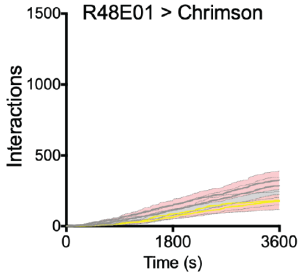

6.

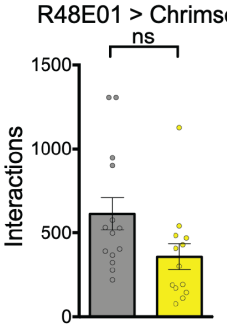

7.

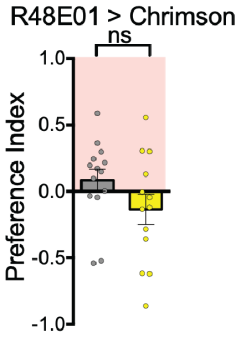

8.

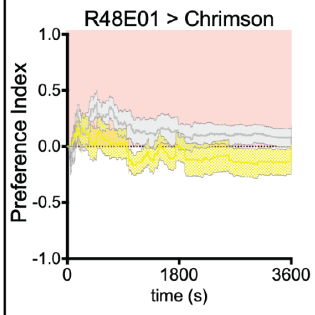

1.

50372 -

w[1118]; P{y[+t7.7] w[+mC]=GMR48E11 -GAL4}attP2

2.

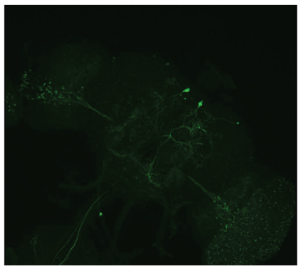

3.

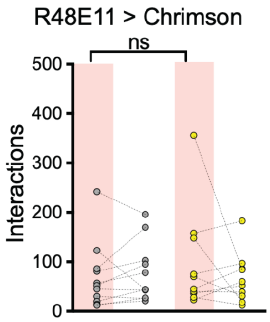

4.

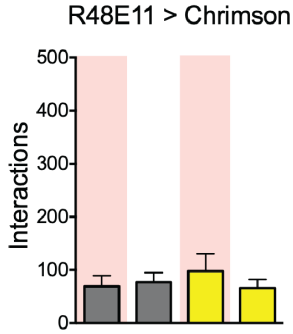

5.

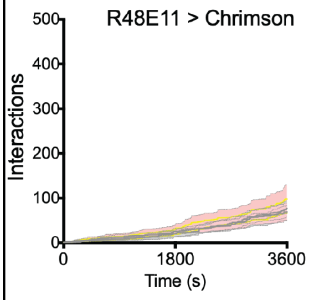

6.

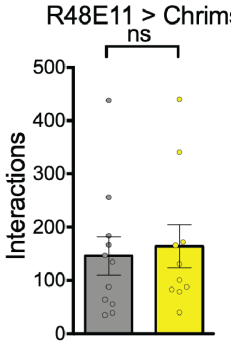

7.

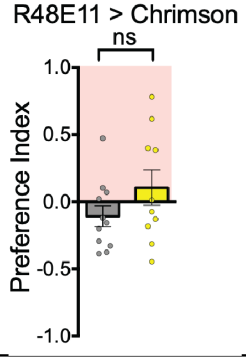

8.

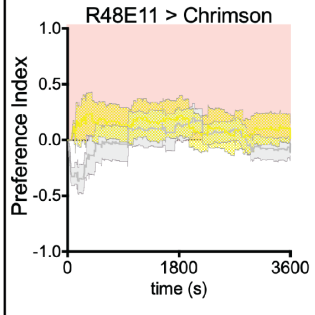

1.

49574 -

w[1118]; P{y[+t7.7] w[+mC]=GMR49A01 -GAL4}attP2

2.

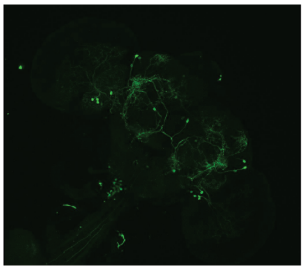

3.

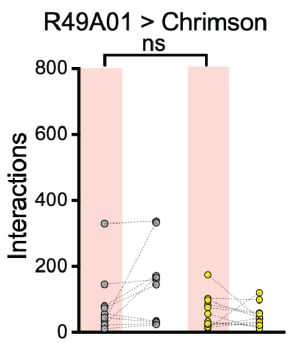

4.

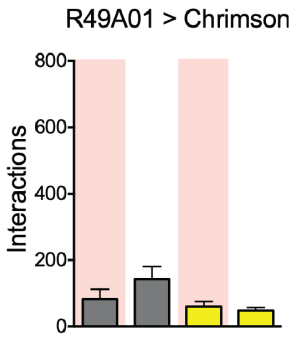

5.

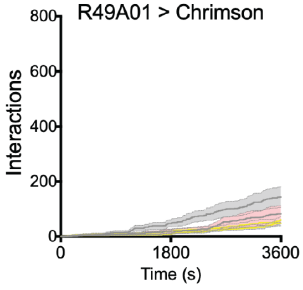

6.

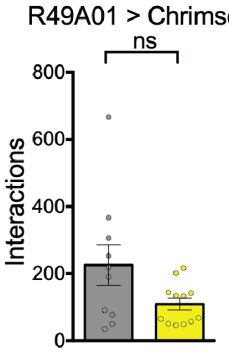

7.

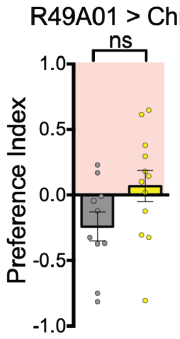

8.

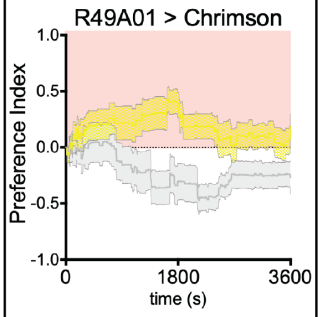

1.

38728 -

w[1118]; P{y[+t7.7] w[+mC]=GMR50B06 -GAL4}attP2

2.

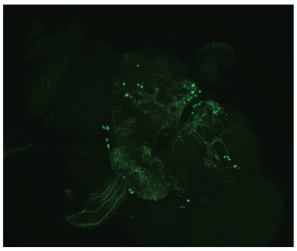

3.

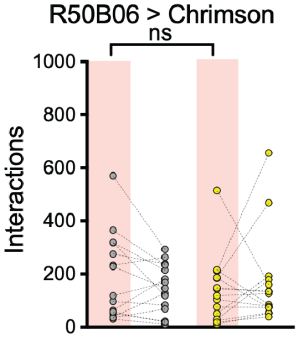

4.

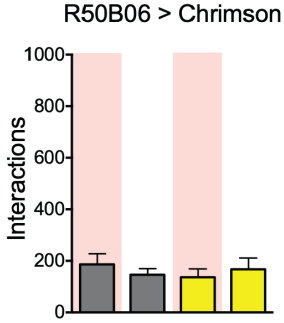

5.

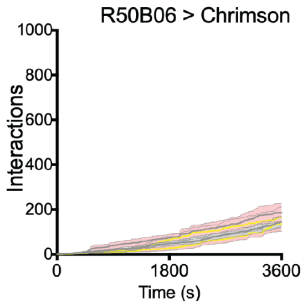

6.

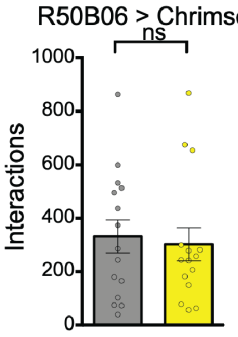

7.

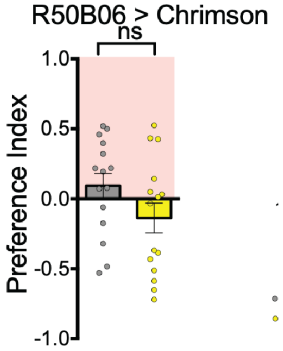

8.

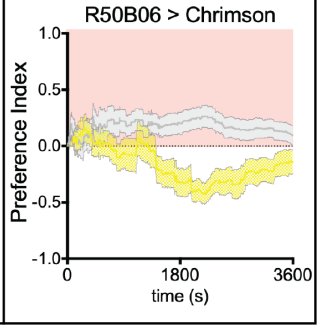

1.

38751 -

w[1118]; P{y[+t7.7] w[+mC]=GMR50E12 -GAL4}attP2

2.

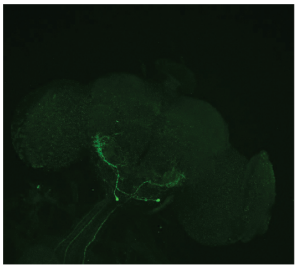

3.

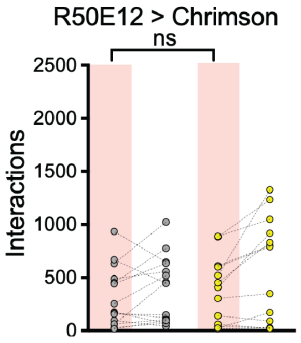

4.

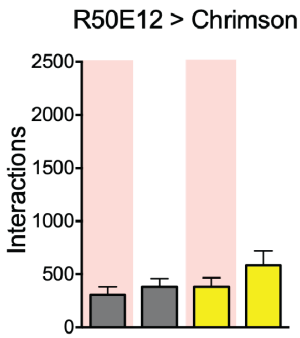

5.

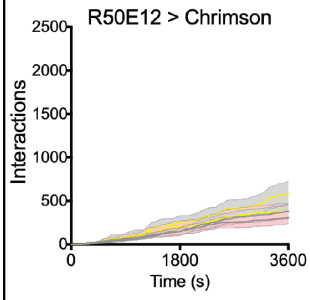

6.

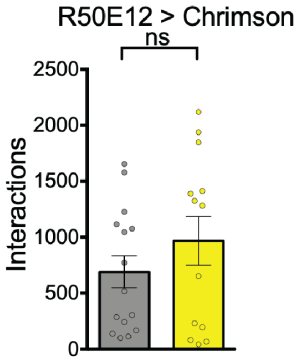

7.

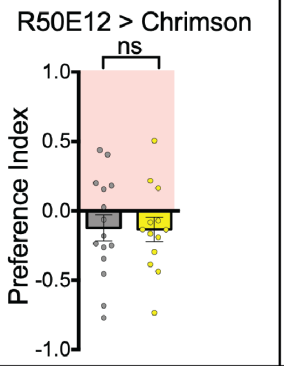

8.

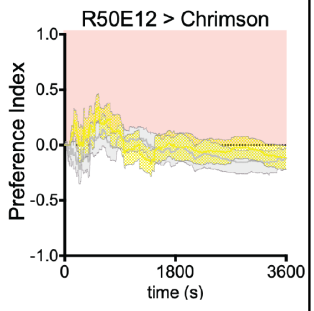

1.

38764 -

w[1118]; P{y[+t7.7] w[+mC]=GMR50H05 -GAL4}attP2

2.

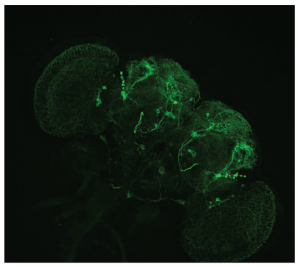

3.

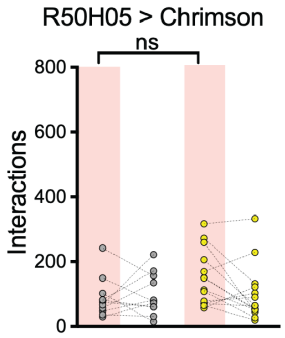

4.

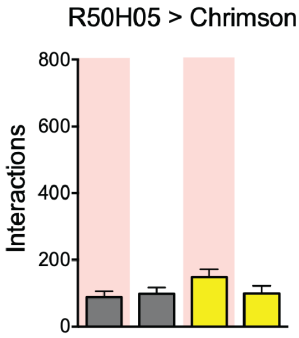

5.

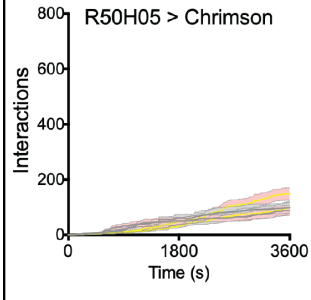

6.

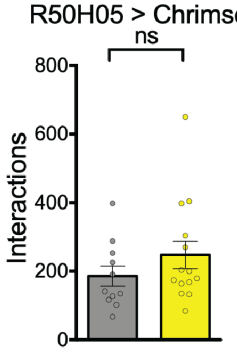

7.

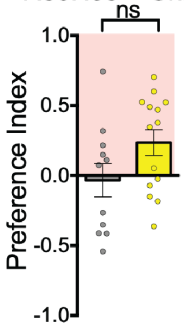

8.

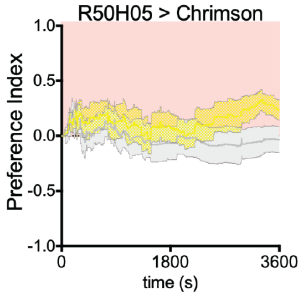

1.

38820 -

w[1118]; P{y[+t7.7] w[+mC]=GMR52B10 -GAL4}attP2

2.

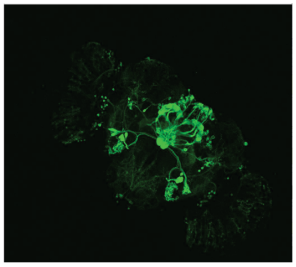

3.

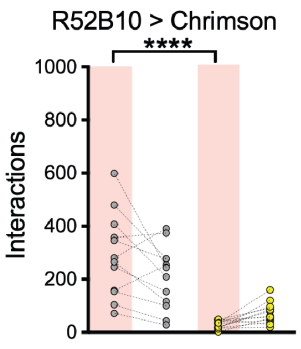

4.

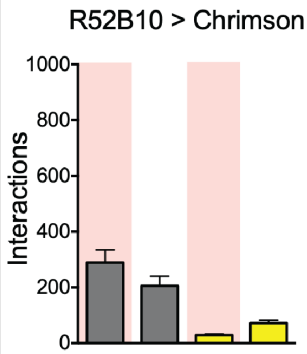

5.

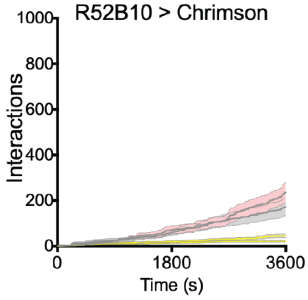

6.

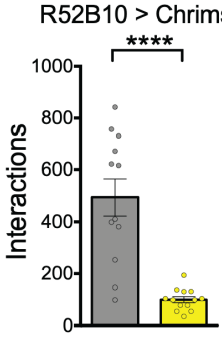

7.

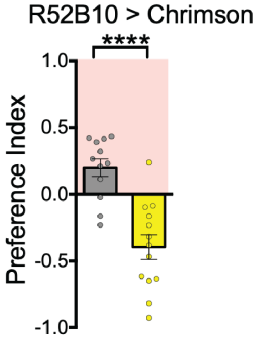

8.

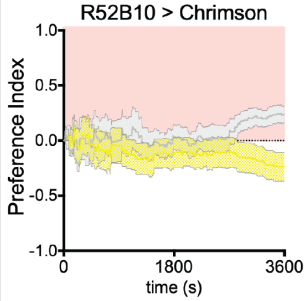

1.

38860 -

w[1118]; P{y[+t7.7] w[+mC]=GMR53A06 -GAL4}attP2

2.

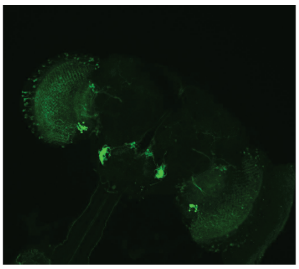

3.

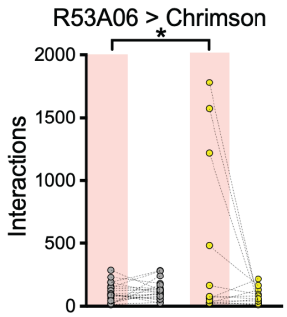

4.

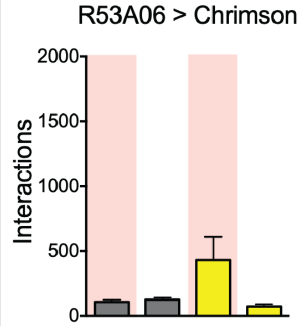

5.

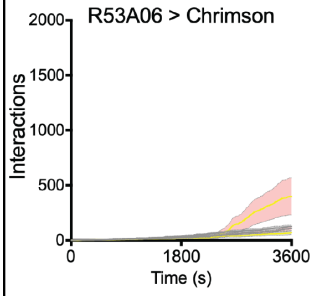

6.

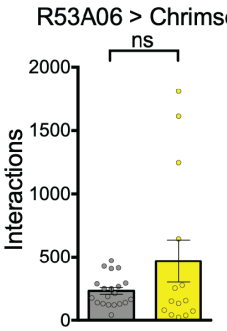

7.

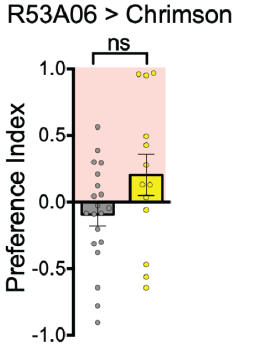

8.

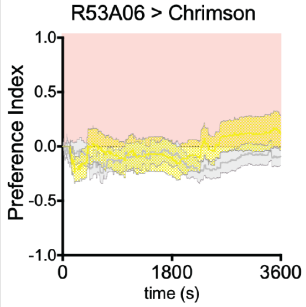

1.

49583 -

w[1118]; P{y[+t7.7] w[+mC]=GMR53B03 -GAL4}attP2

2.

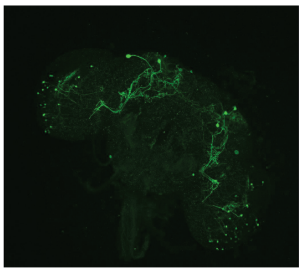

3.

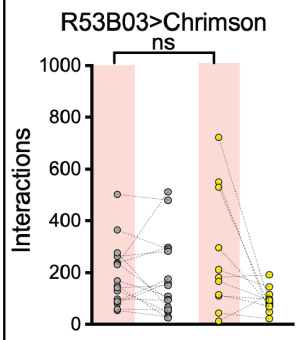

4.

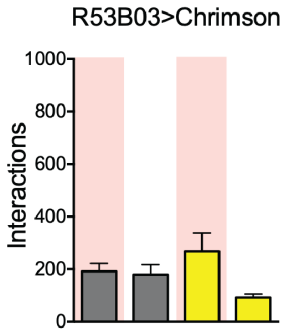

5.

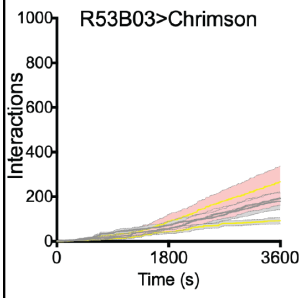

6.

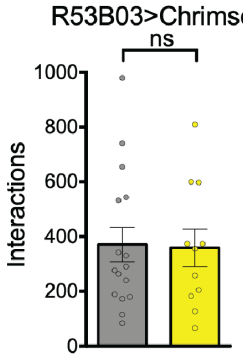

7.

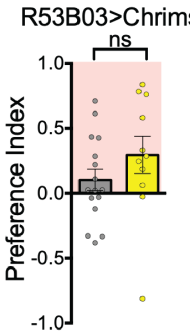

8.

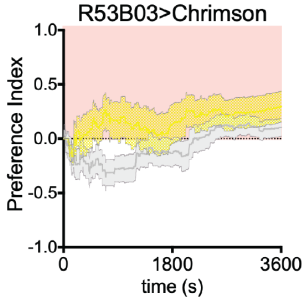

1.

50448 -

w[1118]; P{y[+t7.7] w[+mC]=GMR53G06 -GAL4}attP2

2.

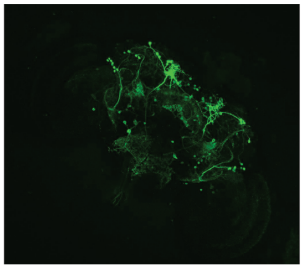

3.

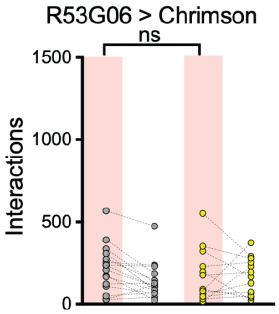

4.

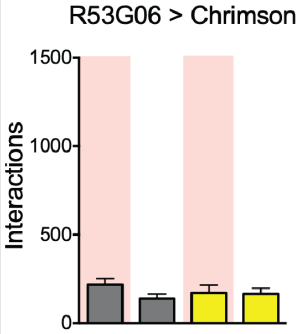

5.

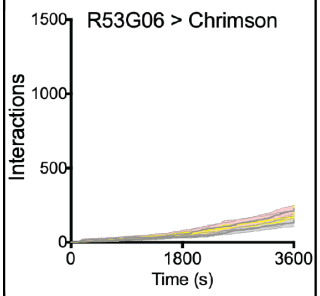

6.

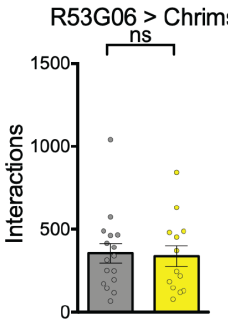

7.

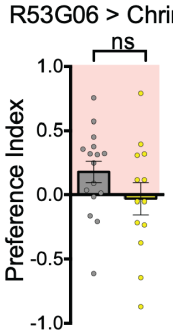

8.

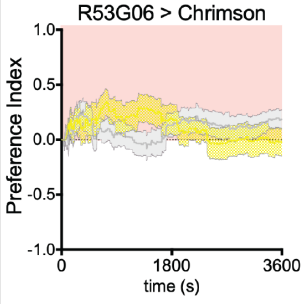

1.

50459 -

w[1118]; P{y[+t7.7] w[+mC]=GMR54A08 -GAL4}attP2

2.

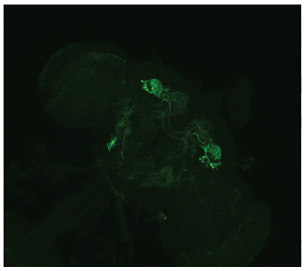

3.

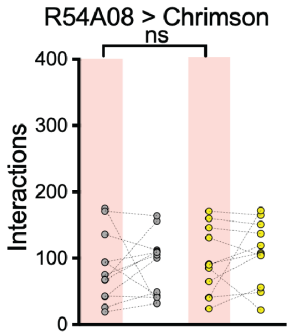

4.

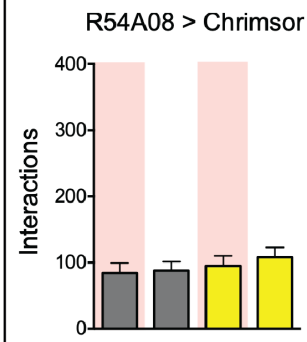

5.

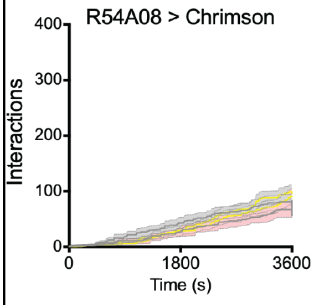

6.

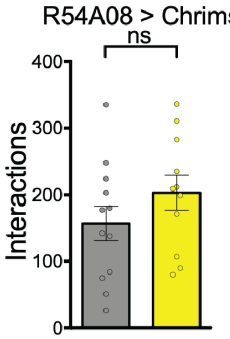

7.

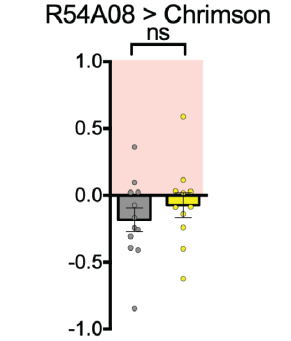

8.

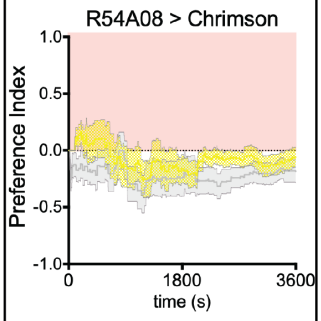

1.

50460 -

w[1118]; P{y[+t7.7] w[+mC]=GMR54A09 -GAL4}attP2

2.

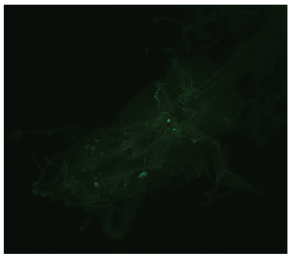

3.

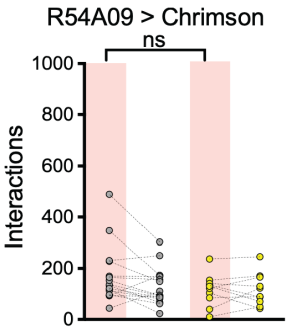

4.

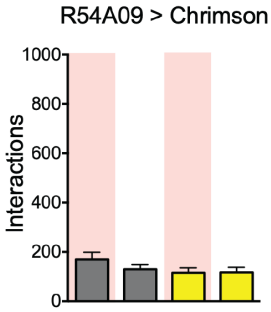

5.

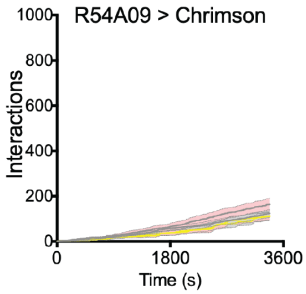

6.

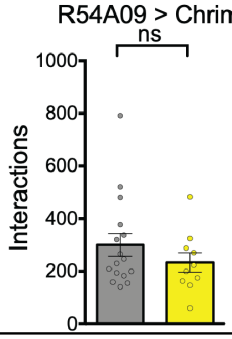

7.

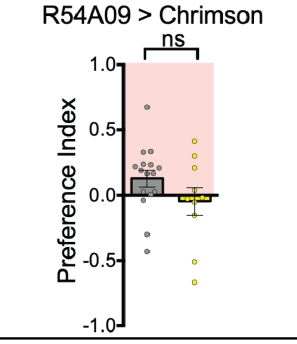

8.

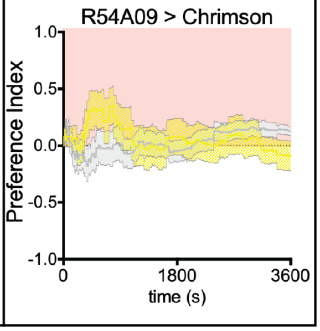

1.

41279 -
w[1118]; P{y[+t7.7]
w[+mC]=GMR54D11
-GAL4}attP2

2.

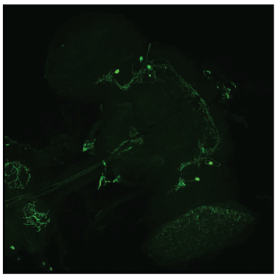

3.

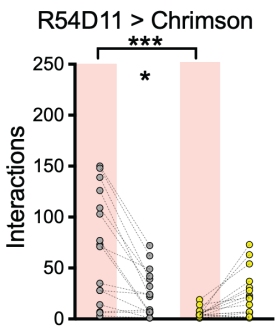

4.

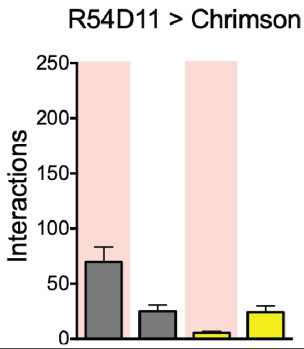

5.

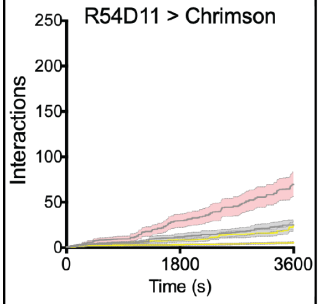

6.

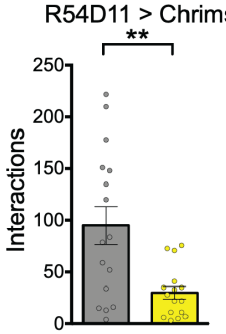

7.

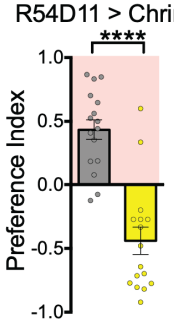

8.

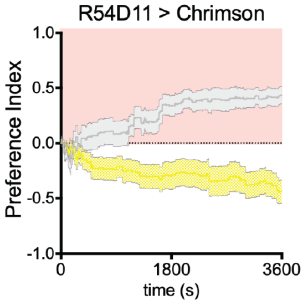

1.

39090 -

w[1118]; P{y[+t7.7]
w[+mC]=GMR54H04
-GAL4}attP2

2.

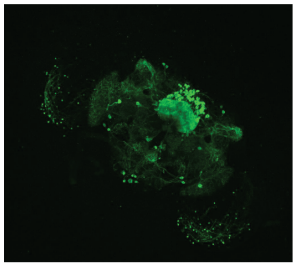

3.

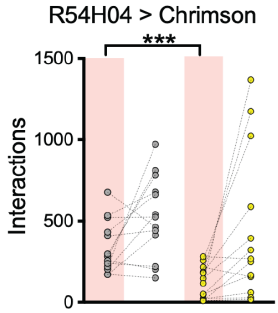

4.

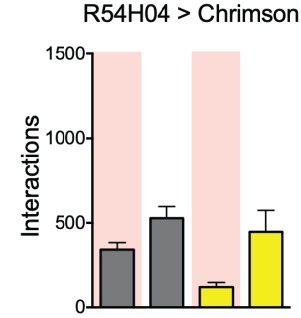

5.

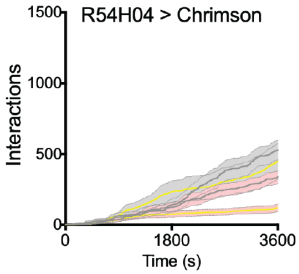

6.

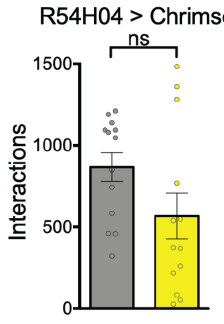

7.

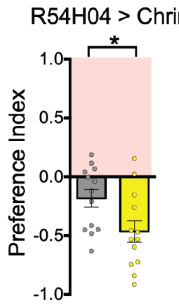

8.

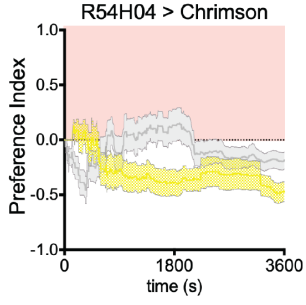

1.

39094 -

w[1118]; P{y[+t7.7] w[+mC]=GMR54H11 -GAL4}attP2

2.

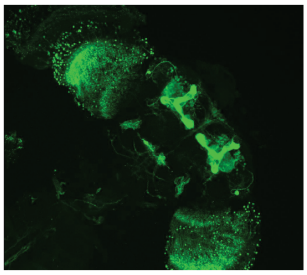

3.

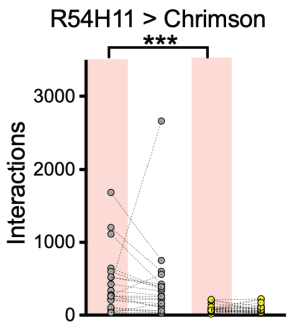

4.

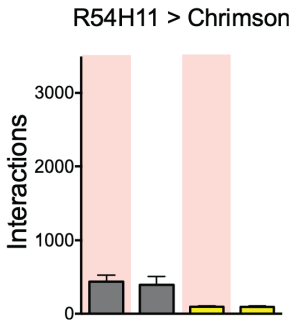

5.

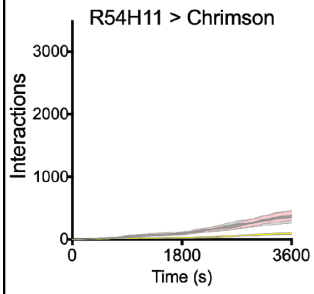

6.

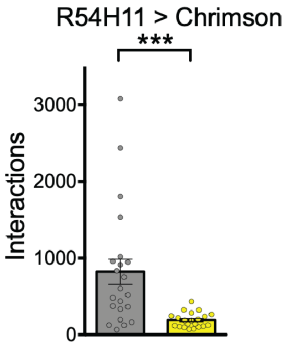

7.

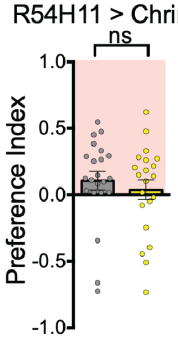

8.

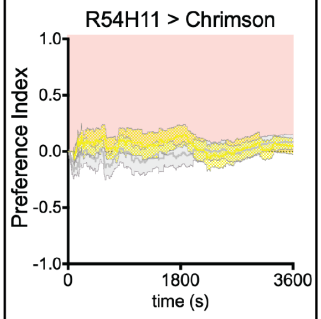

1.

39198 -

w[1118]; P{y[+t7.7] w[+mC]=GMR58H05 -GAL4}attP2

2.

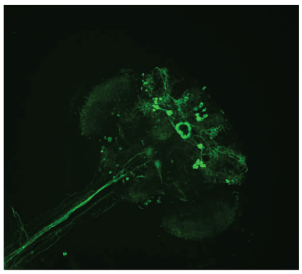

3.

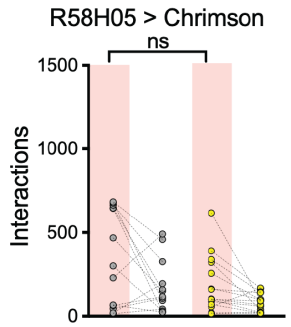

4.

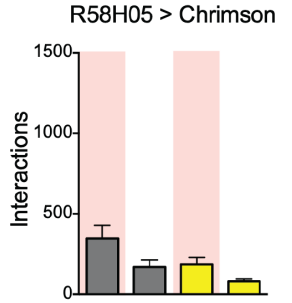

5.

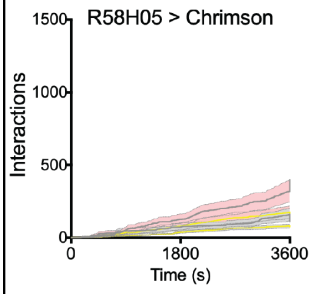

6.

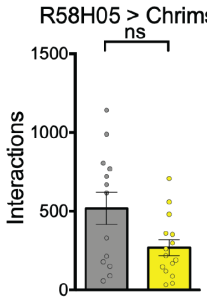

7.

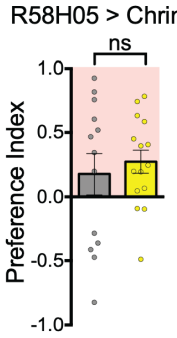

8.

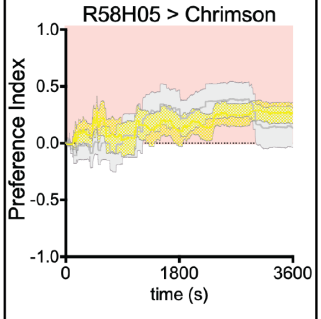

1.

48218 -

w[1118]; P{y[+t7.7] w[+mC]=GMR59C09 -GAL4}attP2/TM3, Sb[1]

2.

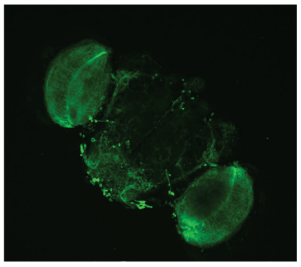

3.

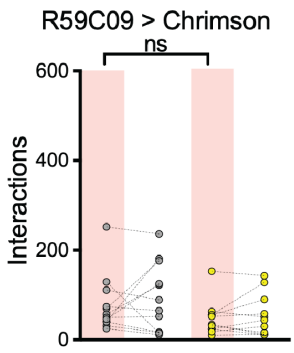

4.

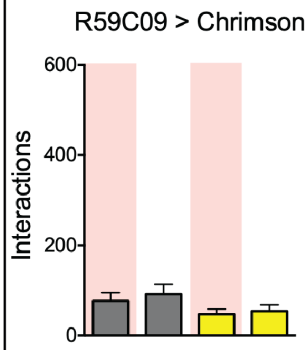

5.

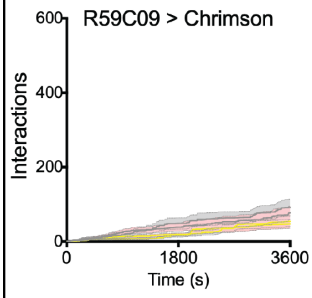

6.

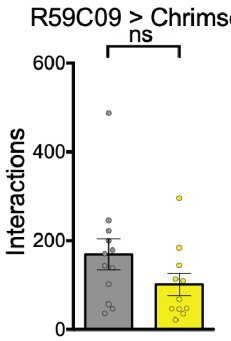

7.

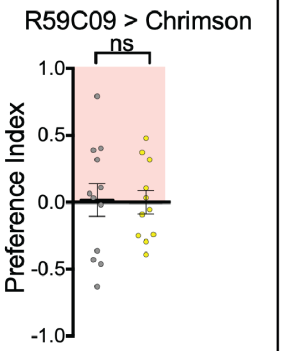

8.

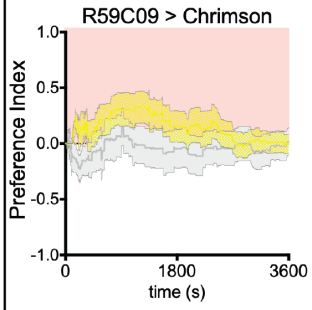

1.

48220 -

w[1118]; P{y[+t7.7] w[+mC]=GMR59D08 -GAL4}attP2/TM3, Sb[1]

2.

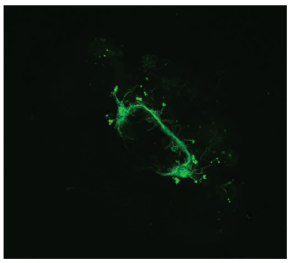

3.

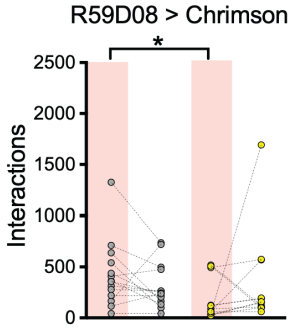

4.

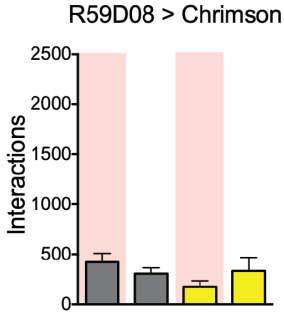

5.

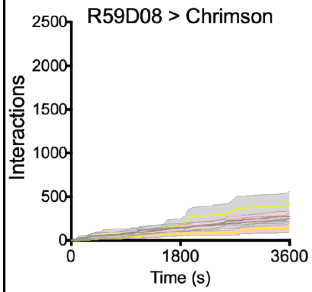

6.

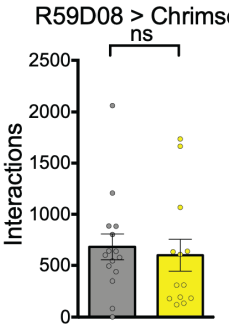

7.

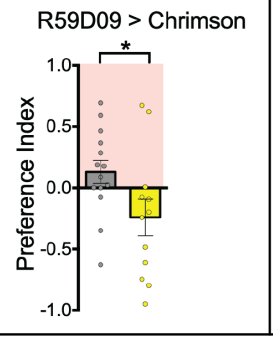

8.

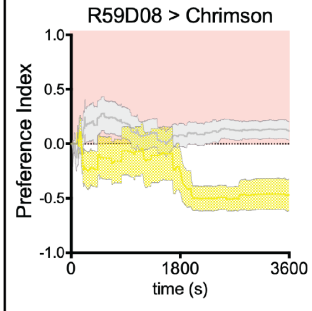

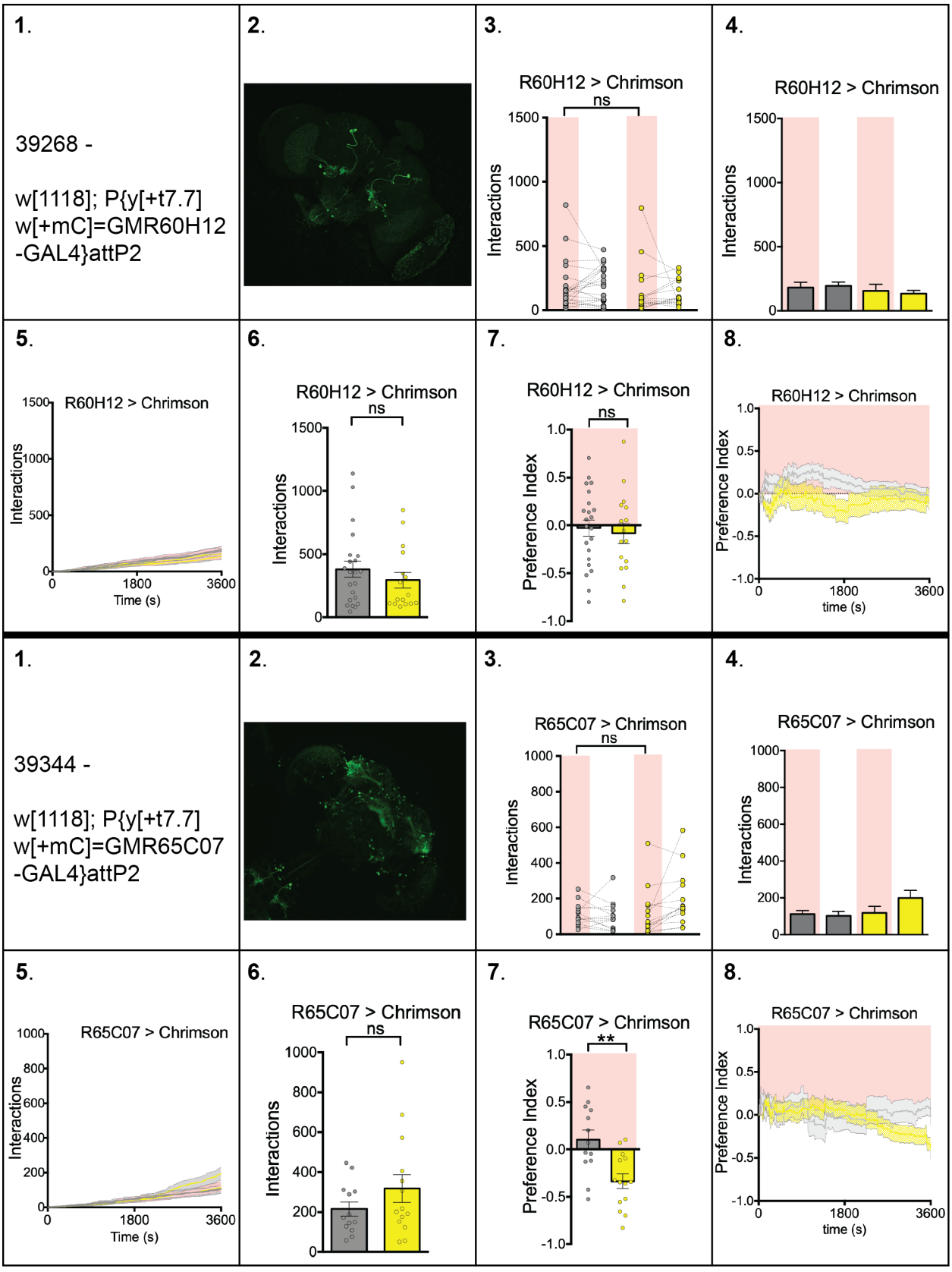
1.
39268 -
w[1118]; P{y[+t7.7] w[+mC]=GMR60H12 -GAL4}attP2
2.
3.
R60H12 > Chrimson
ns
Interactions
4.
R60H12 > Chrimson
Interactions
5.
R60H12 > Chrimson
Interactions
Time (s)
6.
R60H12 > Chrimson
ns
Interactions
7.
R60H12 > Chrimson
ns
Preference Index
8.
R60H12 > Chrimson
Preference Index
time (s)
1.
39344 -
w[1118]; P{y[+t7.7] w[+mC]=GMR65C07 -GAL4}attP2
2.
3.
R65C07 > Chrimson
ns
Interactions
4.
R65C07 > Chrimson
Interactions
5.
R65C07 > Chrimson
Interactions
Time (s)
6.
R65C07 > Chrimson
ns
Interactions
7.
R65C07 > Chrimson
**
Preference Index
8.
R65C07 > Chrimson
Preference Index
time (s)

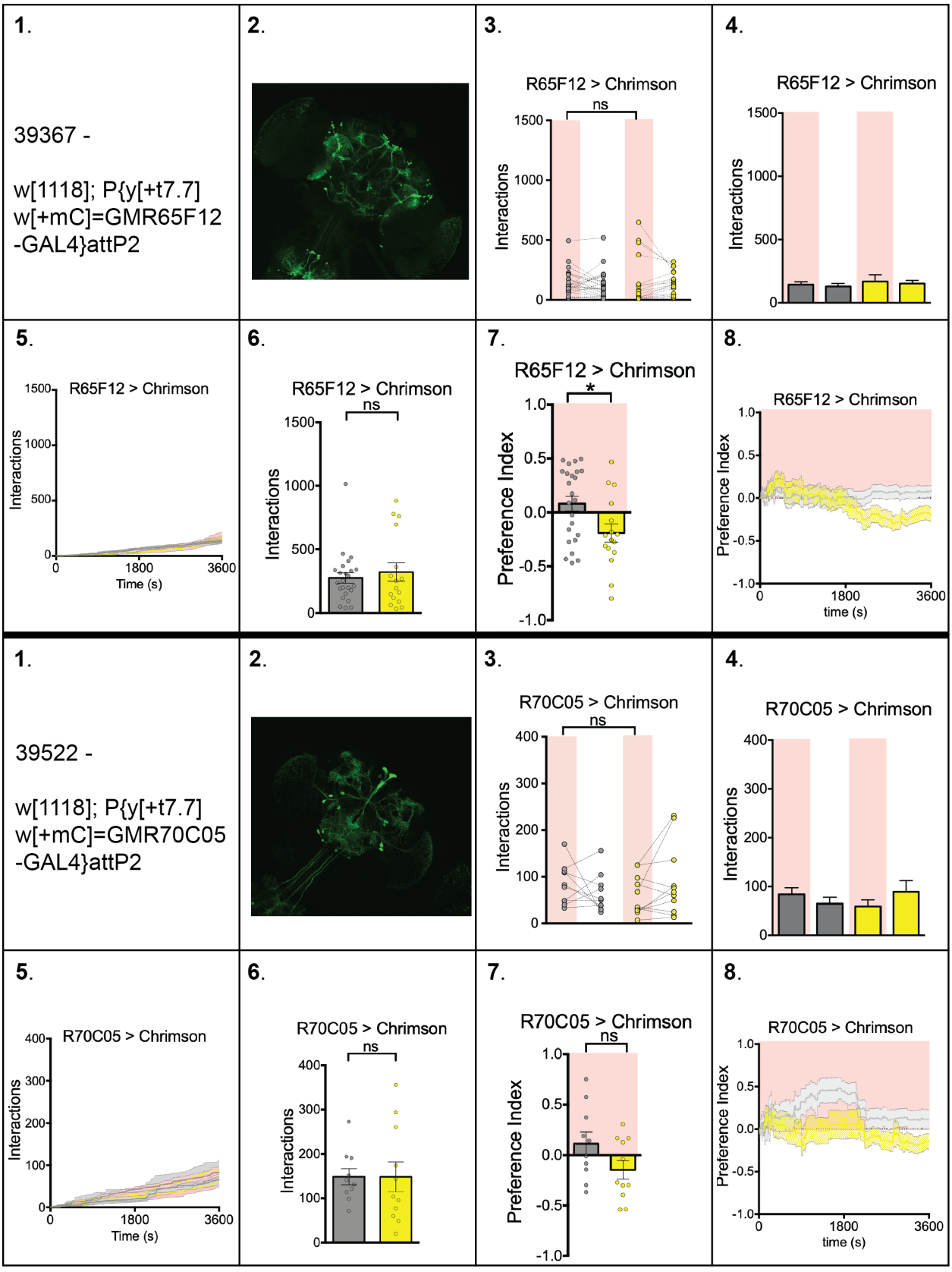
1.
39367 -
w[1118]; P{y[+t7.7] w[+mC]=GMR65F12 -GAL4}attP2
2.
3.
R65F12 > Chrimson
ns
Interactions
1500
1000
500
0
4.
R65F12 > Chrimson
Interactions
5.
R65F12 > Chrimson
Interactions
Time (s)
0
1800
3600
6.
R65F12 > Chrimson
ns
Interactions
7.
R65F12 > Chrimson
*
Preference Index
1.0
0.5
0.0
-0.5
-1.0
8.
R65F12 > Chrimson
Preference Index
time (s)
1.
39522 -
w[1118]; P{y[+t7.7] w[+mC]=GMR70C05 -GAL4}attP2
2.
3.
R70C05 > Chrimson
ns
Interactions
400
300
200
100
0
4.
R70C05 > Chrimson
Interactions
5.
R70C05 > Chrimson
Interactions
Time (s)
0
1800
3600
6.
R70C05 > Chrimson
ns
Interactions
7.
R70C05 > Chrimson
ns
Preference Index
8.
R70C05 > Chrimson
Preference Index
time (s)

1.

39523 -

w[1118]; P{y[+t7.7] w[+mC]=GMR70C07 -GAL4}attP2

2.

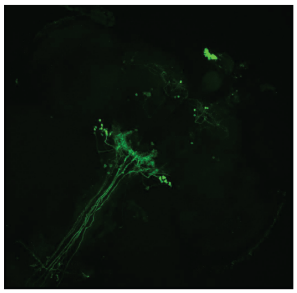

3.

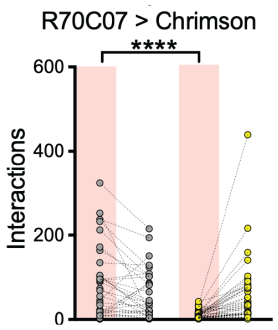

4.

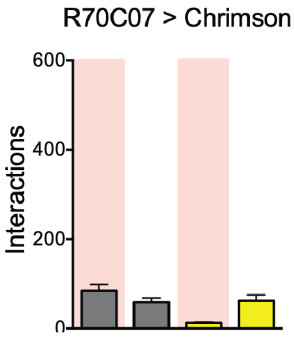

5.

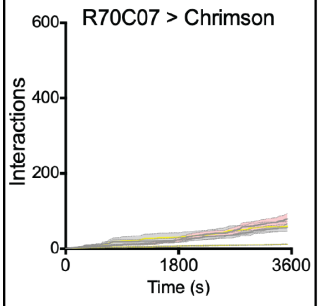

6.

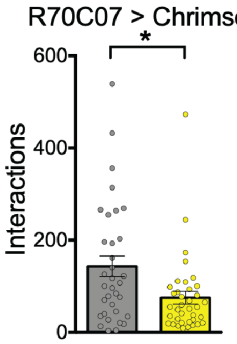

7.

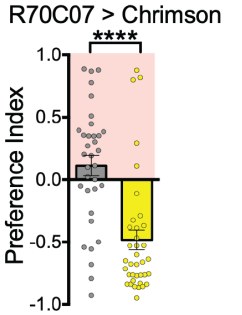

8.

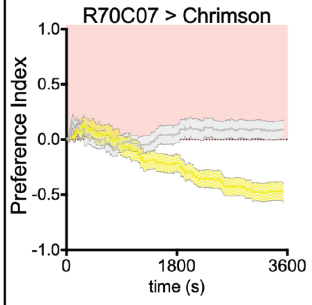

1.

39577 -

w[1118]; P{y[+t7.7] w[+mC]=GMR71C11 -GAL4}attP2

2.

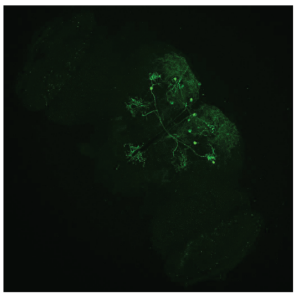

3.

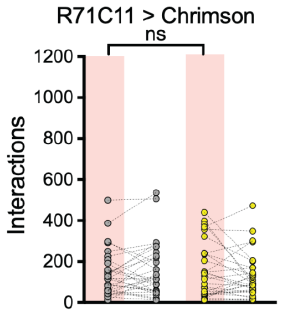

4.

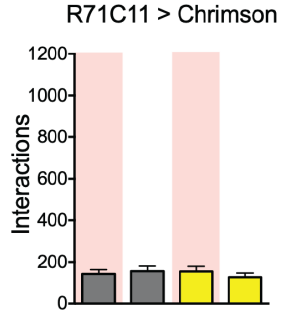

5.

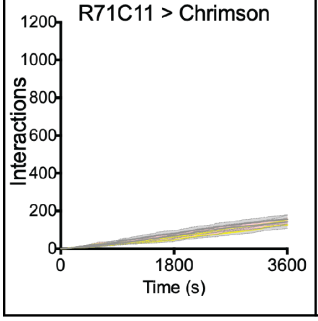

6.

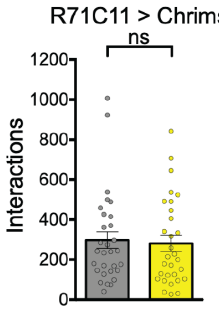

7.

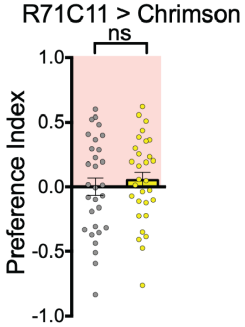

8.

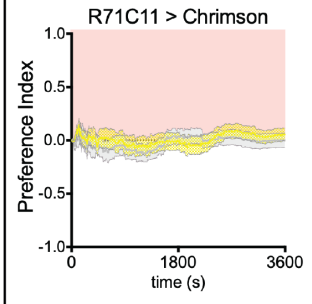

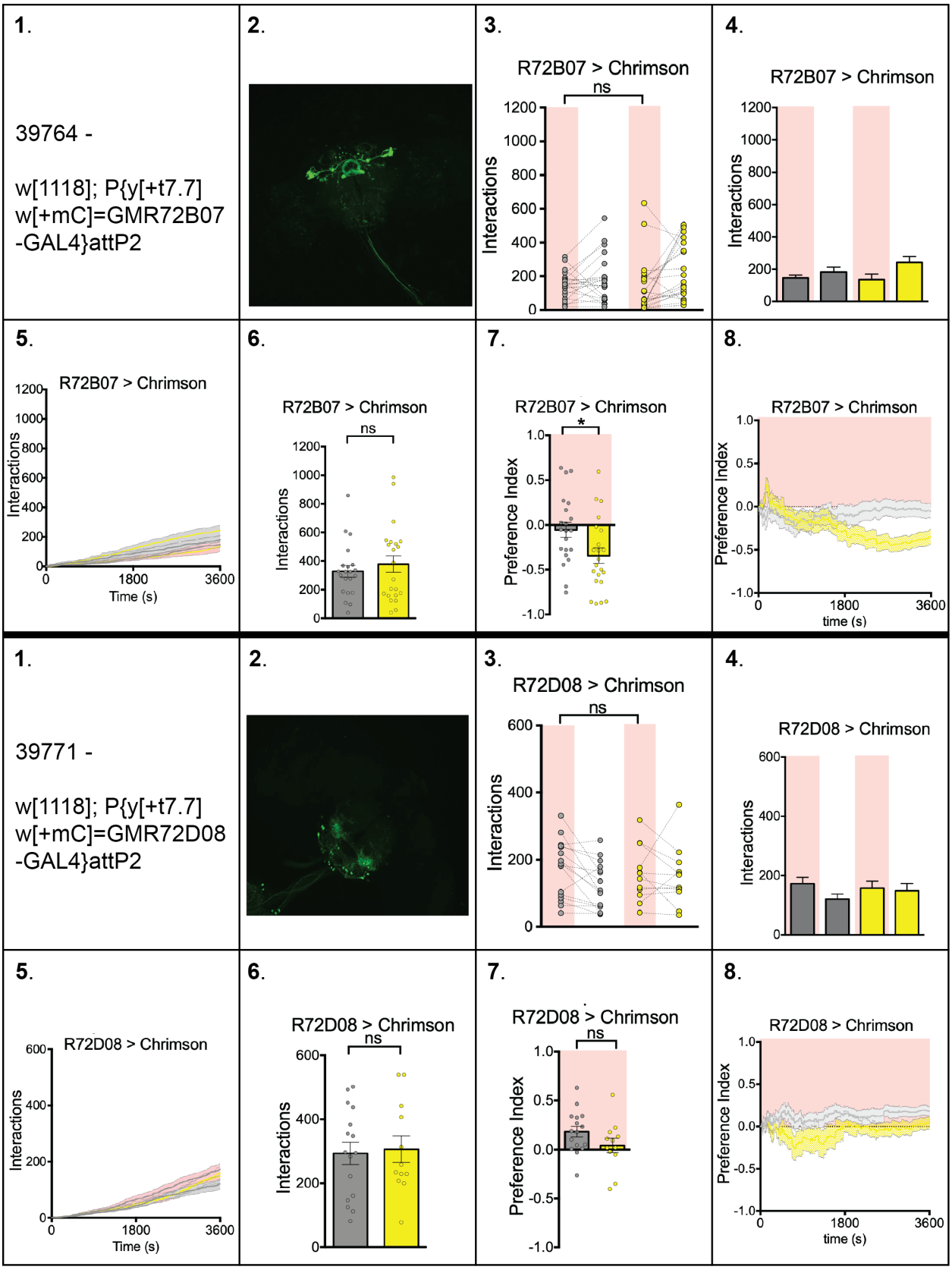
1.
39764 -
w[1118]; P{y[+t7.7] w[+mC]=GMR72B07 -GAL4}attP2
2.
3.
R72B07 > Chrimson
ns
Interactions
4.
R72B07 > Chrimson
Interactions
5.
R72B07 > Chrimson
Interactions
Time (s)
6.
R72B07 > Chrimson
ns
Interactions
7.
R72B07 > Chrimson
*
Preference Index
8.
R72B07 > Chrimson
Preference Index
time (s)
1.
39771 -
w[1118]; P{y[+t7.7] w[+mC]=GMR72D08 -GAL4}attP2
2.
3.
R72D08 > Chrimson
ns
Interactions
4.
R72D08 > Chrimson
Interactions
5.
R72D08 > Chrimson
Interactions
Time (s)
6.
R72D08 > Chrimson
ns
Interactions
7.
R72D08 > Chrimson
ns
Preference Index
8.
R72D08 > Chrimson
Preference Index
time (s)

1.

39796 -

w[1118]; P{y[+t7.7] w[+mC]=GMR72G12 -GAL4}attP2

2.

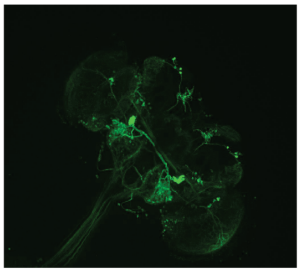

3.

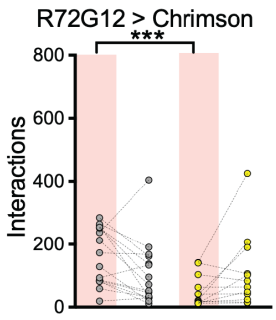

4.

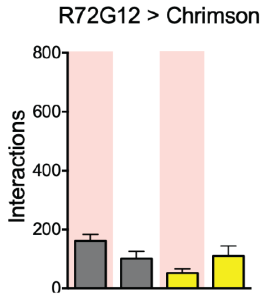

5.

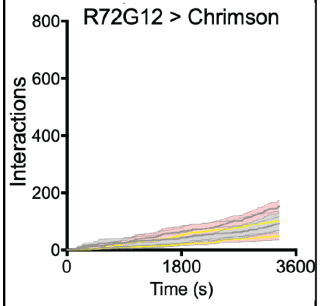

6.

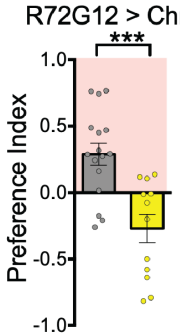

7.

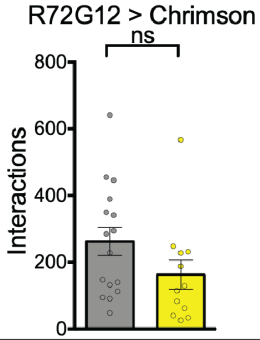

8.

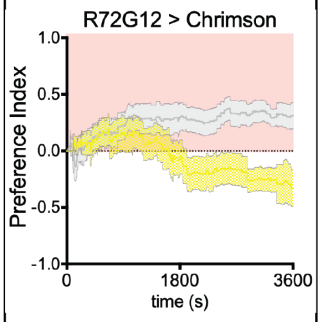

1.

47402 -

w[1118]; P{y[+t7.7] w[+mC]=GMR75C05 -GAL4}attP2

2.

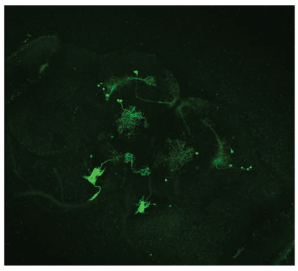

3.

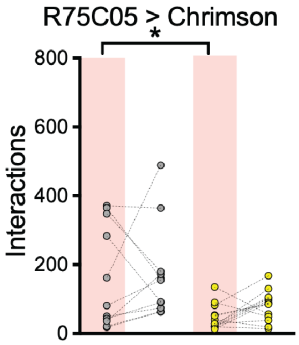

4.

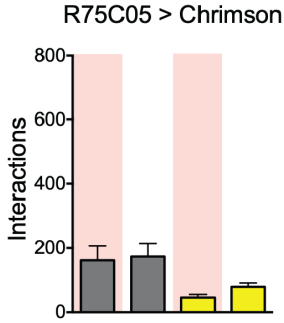

5.

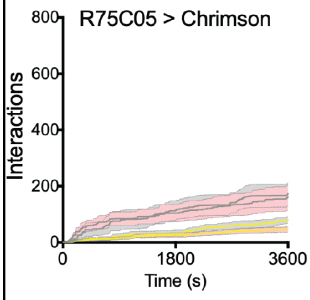

6.

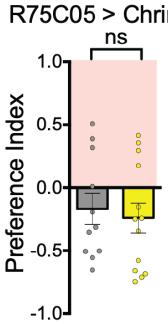

7.

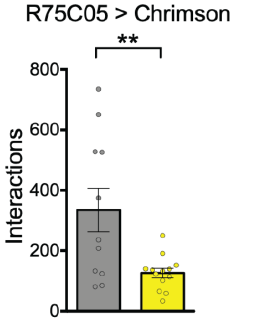

8.

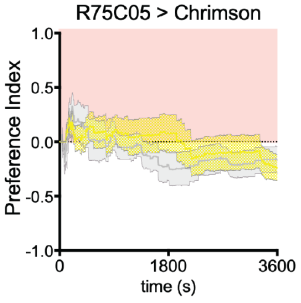

1.

39913 -

w[1118]; P{y[+t7.7] w[+mC]=GMR75H10 -GAL4}attP2

2.

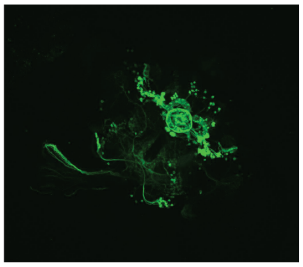

3.

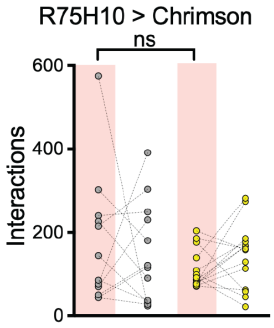

4.

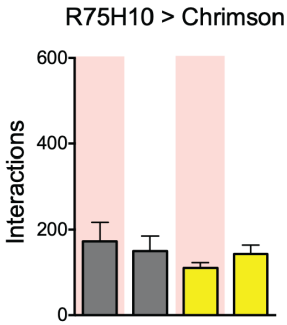

5.

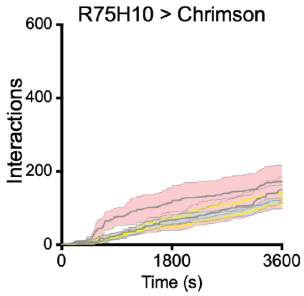

6.

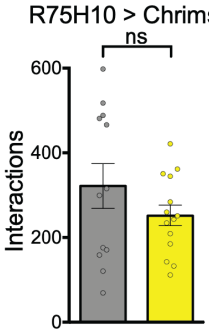

7.

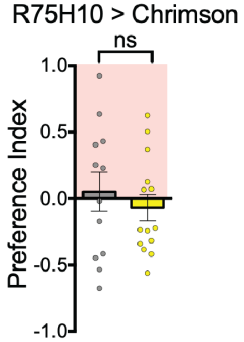

8.

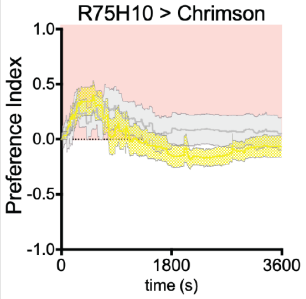

1.

48338 -

w[1118]; P{y[+t7.7] w[+mC]=GMR77E05 -GAL4}attP2

2.

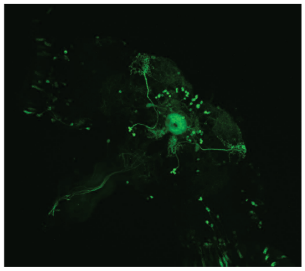

3.

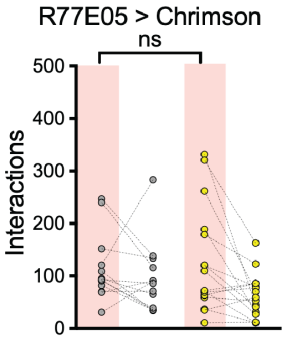

4.

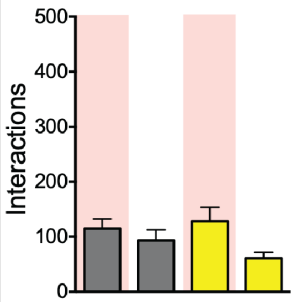

5.

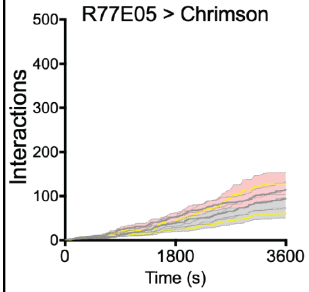

6.

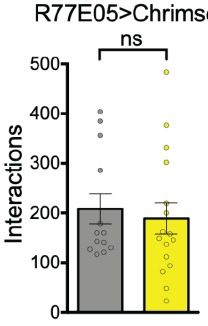

7.

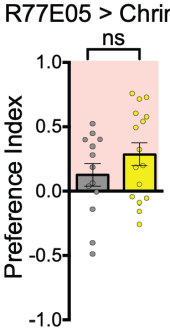

8.

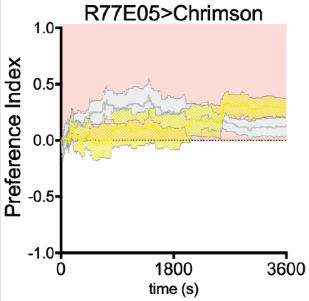

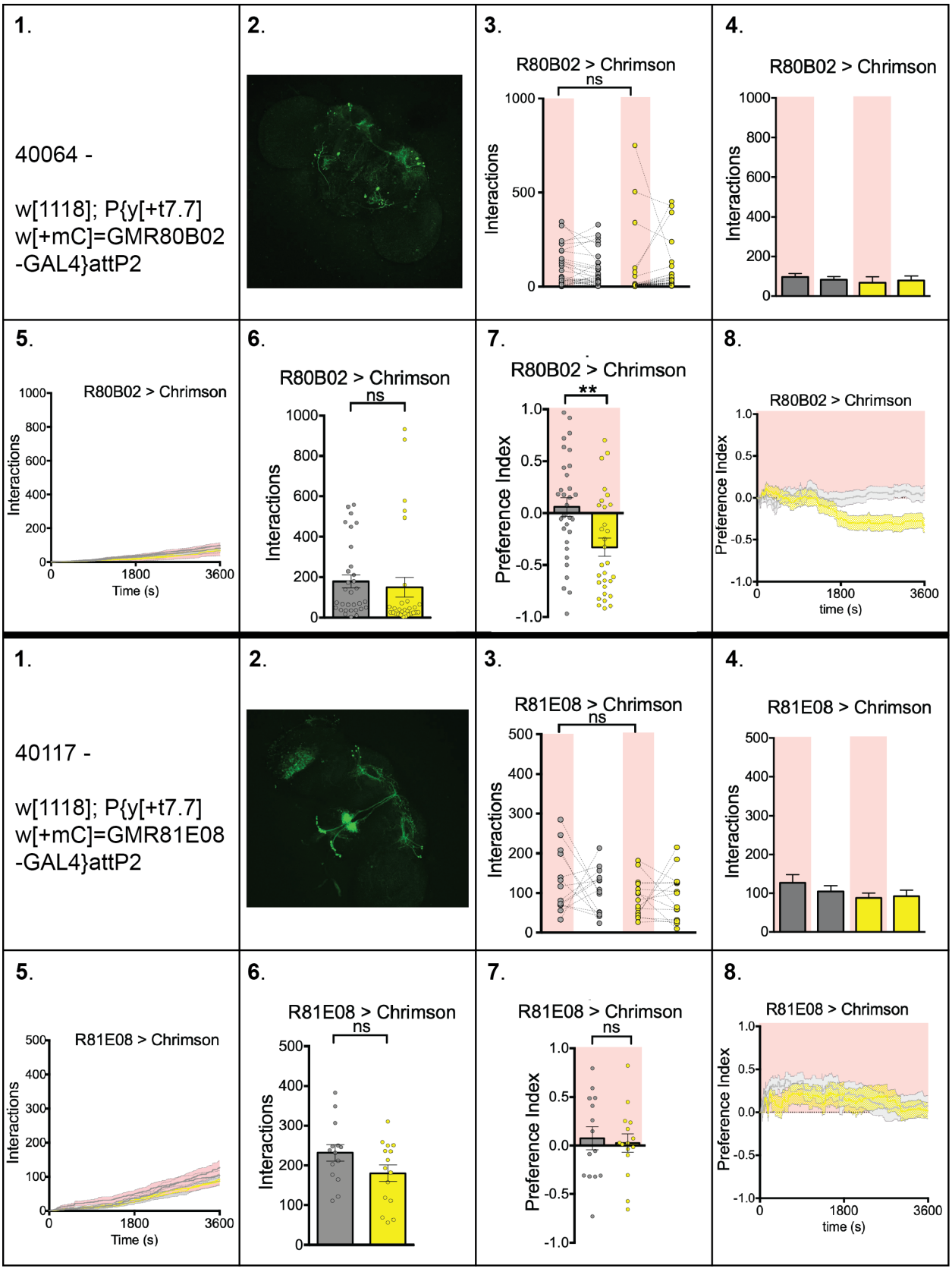
1.
40064 -
w[1118]; P{y[+t7.7] w[+mC]=GMR80B02 -GAL4}attP2
2.
3.
R80B02 > Chrimson
ns
Interactions
4.
R80B02 > Chrimson
Interactions
5.
R80B02 > Chrimson
Interactions
Time (s)
6.
R80B02 > Chrimson
ns
Interactions
7.
R80B02 > Chrimson
**
Preference Index
8.
R80B02 > Chrimson
Preference Index
time (s)
1.
40117 -
w[1118]; P{y[+t7.7] w[+mC]=GMR81E08 -GAL4}attP2
2.
3.
R81E08 > Chrimson
ns
Interactions
4.
R81E08 > Chrimson
Interactions
5.
R81E08 > Chrimson
Interactions
Time (s)
6.
R81E08 > Chrimson
ns
Interactions
7.
R81E08 > Chrimson
ns
Preference Index
8.
R81E08 > Chrimson
Preference Index
time (s)

1.

40147 -

w[1118]; P{y[+t7.7] w[+mC]=GMR82E01 -GAL4}attP2

2.

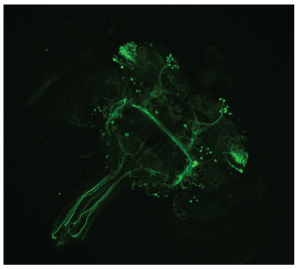

3.

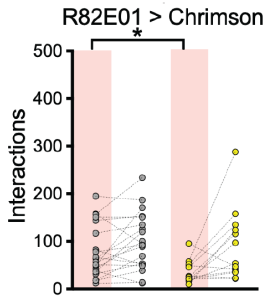

4.

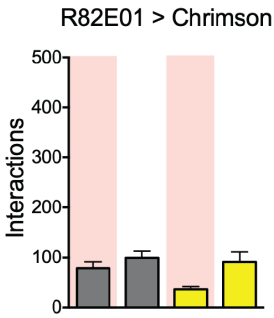

5.

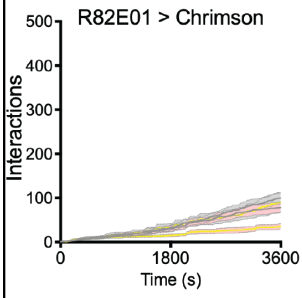

6.

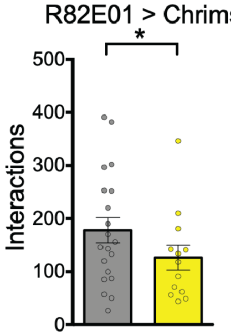

7.

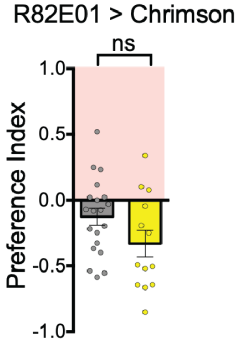

8.

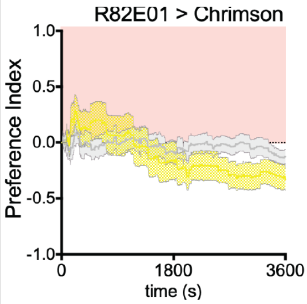

1.

40153 -

w[1118]; P{y[+t7.7] w[+mC]=GMR82E12 -GAL4}attP2

2.

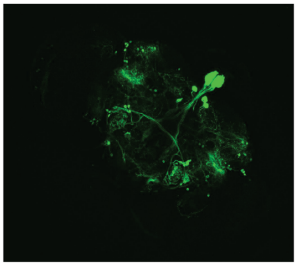

3.

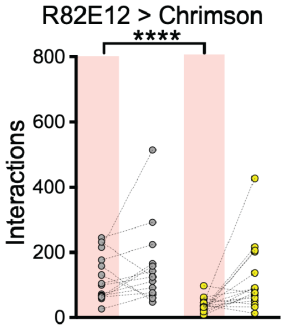

4.

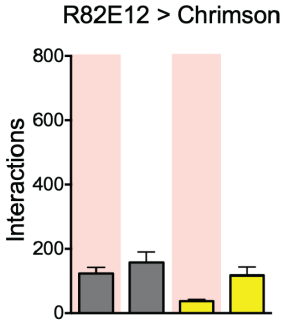

5.

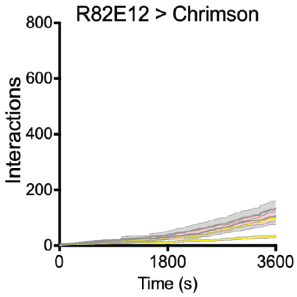

6.

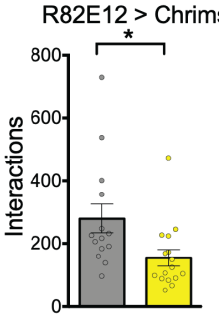

7.

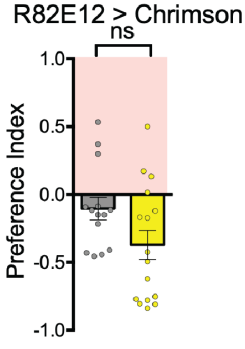

8.

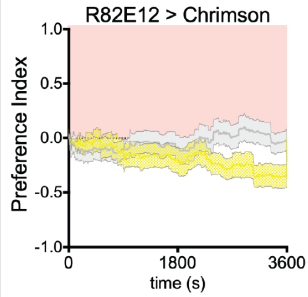

1.

40360 -

w[1118]; P{y[+t7.7] w[+mC]=GMR83D12 -GAL4}attP2

2.

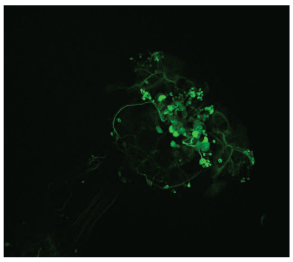

3.

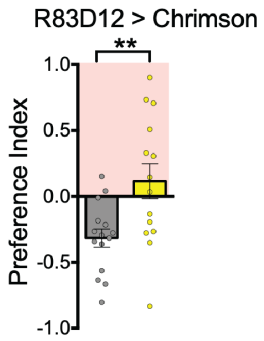

4.

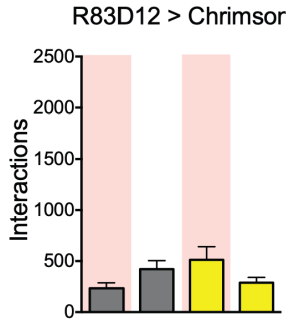

5.

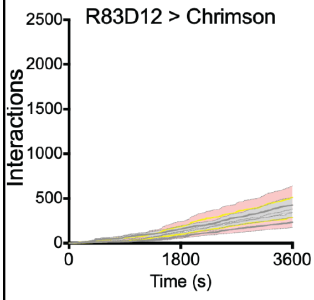

6.

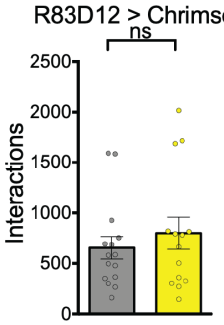

7.

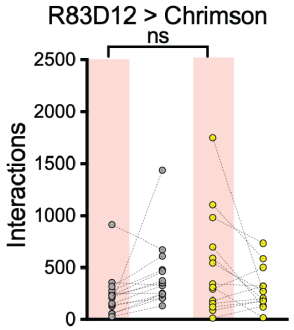

8.

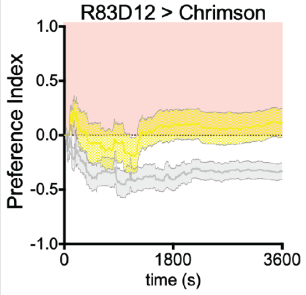

1.

48378 -

w[1118]; P{y[+t7.7] w[+mC]=GMR84C10 -GAL4}attP2/TM3, Sb[1]

2.

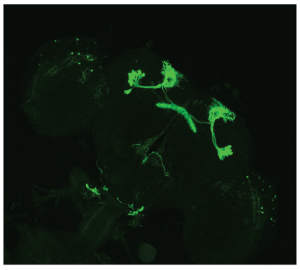

3.

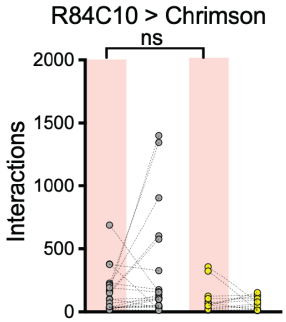

4.

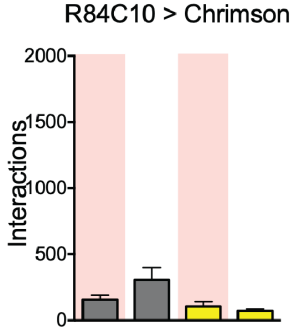

5.

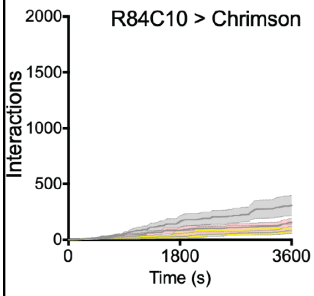

6.

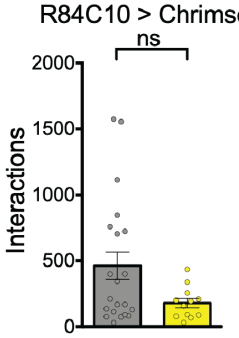

7.

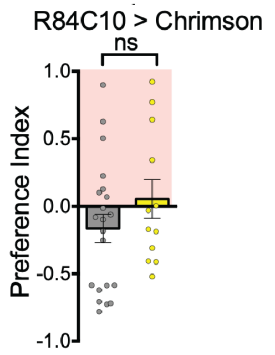

8.

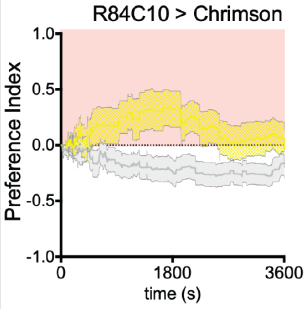

1.

40428 -

w[1118]; P{y[+t7.7] w[+mC]=GMR85D07 -GAL4}attP2

2.

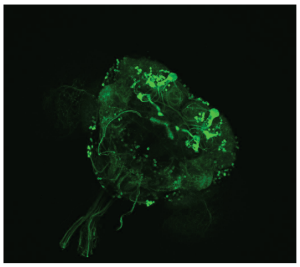

3.

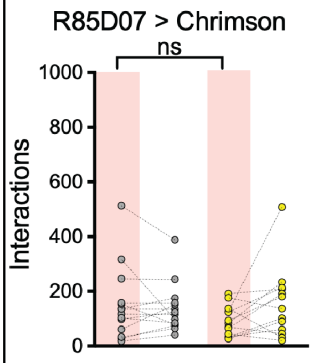

4.

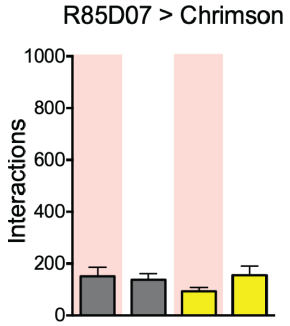

5.

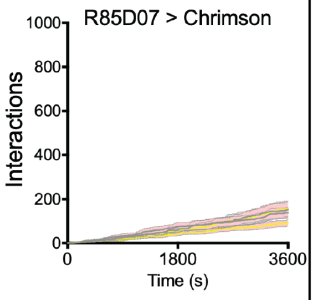

6.

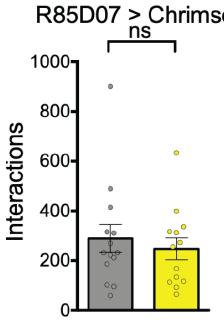

7.

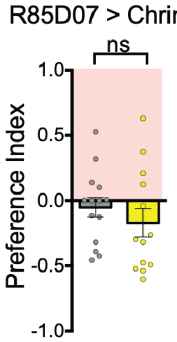

8.

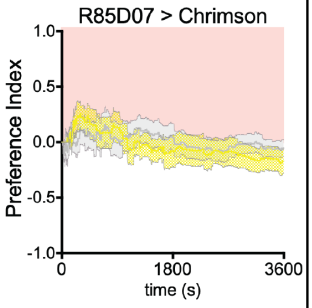

1.

40605 -

w[1118]; P{y[+t7.7] w[+mC]=GMR92B11 -GAL4}attP2

2.

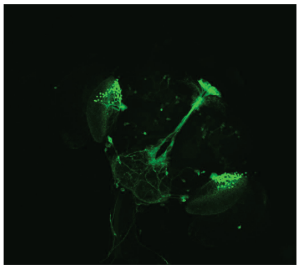

3.

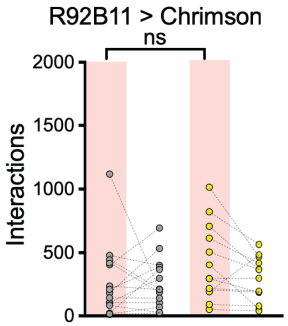

4.

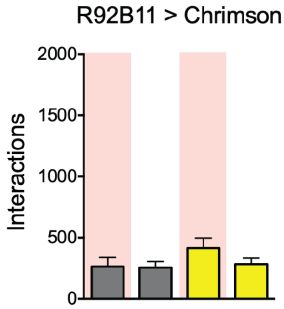

5.

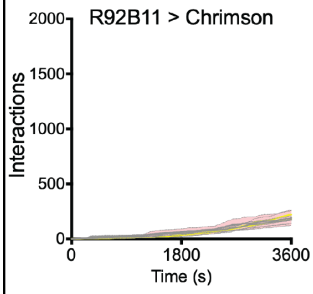

6.

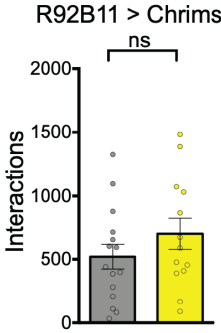

7.

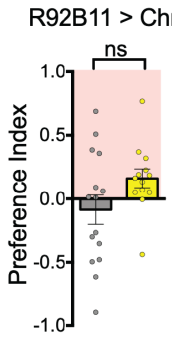

8.

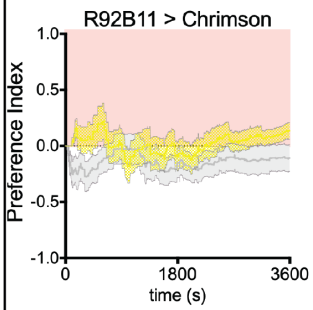

1.

40623 -

w[1118]; P{y[+t7.7] w[+mC]=GMR92E10 -GAL4}attP2

2.

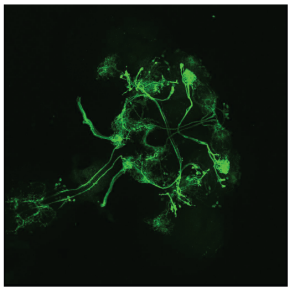

3.

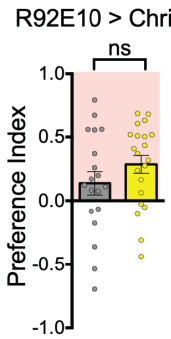

4.

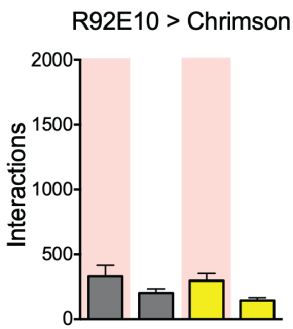

5.

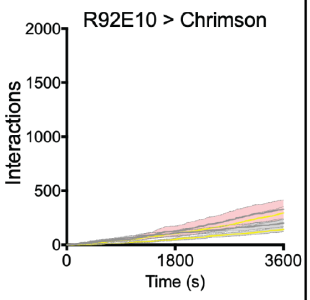

6.

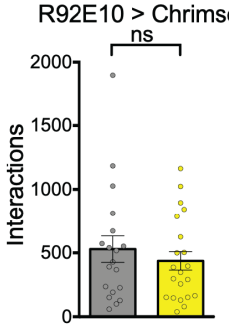

7.

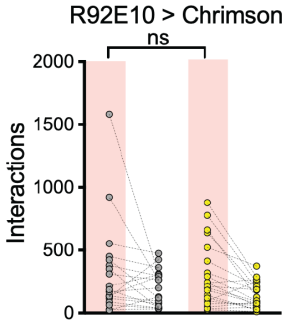

8.

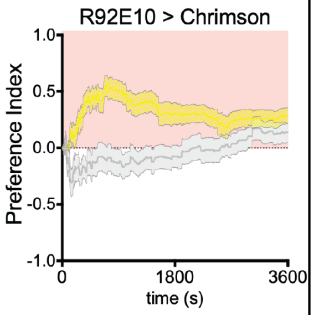

1.

40631 -

w[1118]; P{y[+t7.7] w[+mC]=GMR92H01 -GAL4}attP2

2.

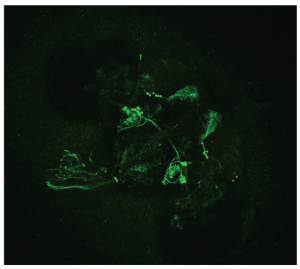

3.

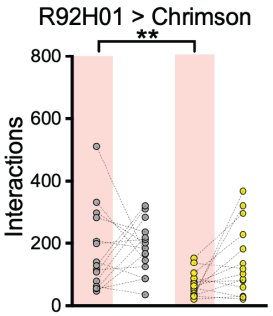

4.

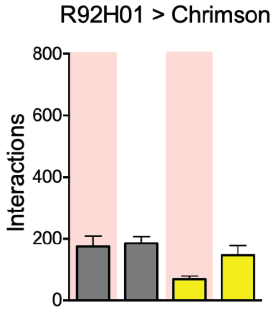

5.

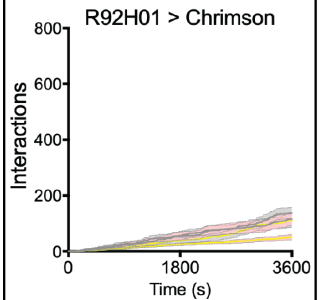

6.

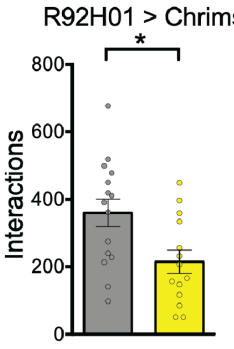

7.

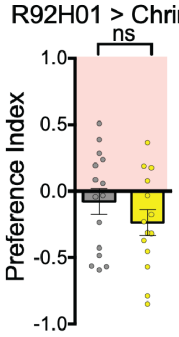

8.

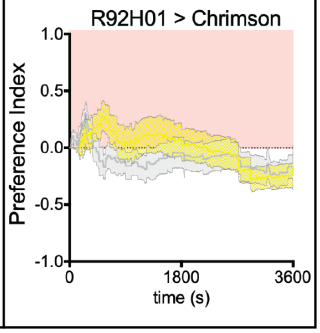

1.

48418 -

w[1118]; P{y[+t7.7] w[+mC]=GMR93D09 -GAL4}attP2/TM3, Sb[1]

2.

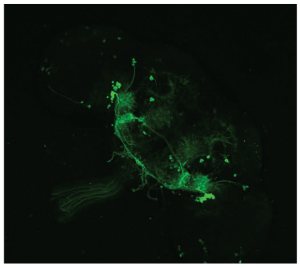

3.

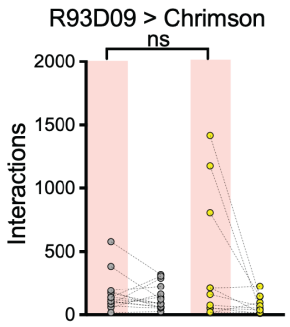

4.

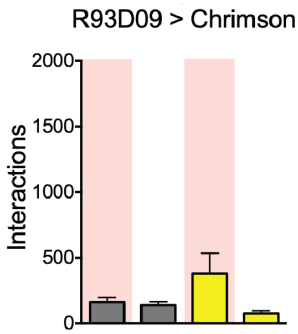

5.

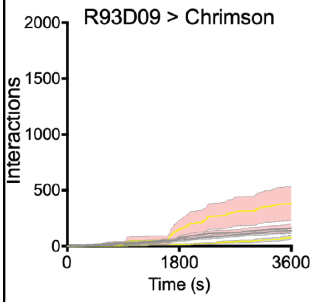

6.

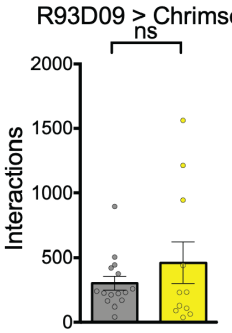

7.

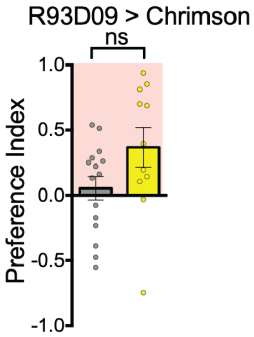

8.